UNIVERSITY OF CALIFORNIA
UNIVERSITY OF CALIFORNIA SANTA CRUZ

THE MONSTER TOWER AND ACTION SELECTORS

A dissertation submitted in partial satisfaction of the
requirements for the degree of

DOCTOR OF PHILOSOPHY

in

MATHEMATICS

by

Wyatt Howard

June 2013

The Dissertation of Wyatt Howard
is approved:

Professor Richard Montgomery, Chair

Professor Viktor Ginzburg

Professor Debra Lewis

Dean Tyrus Miller
Vice Provost and Dean of Graduate Studies

Table of Contents

List of Figures

List of Tables

Abstract

The Monster Tower and Action Selectors

by

Wyatt Howard

This dissertation is a mixture of two different topics from two separate areas of geometry. The first part of the thesis deals focuses on a problem from subriemannian geometry and is motivated by work done by Professors A. Castro, R. Montgomery, M. Zhitomirskii. The second half of this dissertation comes from a problem in symplectic geometry posed by Professor V. Ginzburg.

The first part of the dissertation looks at the classification, up to local diffeomorphism, of a certain type of geometric distribution known as Goursat multi-flags. Montgomery and Zhitomirskii approached this classification problem by working with a structure called the Monster Tower, which is comprised of a sequence of manifolds. Each level of this tower is constructed through a process called Cartan Prolongation. Montgomery and Zhitomirskii pointed out that the problem of classifying the points within each level of the tower is equivalent to the problem of classifying Goursat multi-flags. This work is an extension of the classification work with the $\mathbb{R}^3$ Monster Tower that was initiated by Castro and Montgomery. We will present two different methods for classifying Goursat 2-flags of small critical length within the Monster Tower.

The second half of this research is concerned with symplectic geometry. This research looks at the size of the fixed point set of a Hamiltonian diffeomorphism of a closed symplectic manifold. We look at when the action spectrum is less than or equal to the cuplength of a manifold that is symplectically aspherical. This question examines a partial converse to the Arnold Conjecture. What will be shown is that for some degree greater than zero, the cohomology of the fixed point set must be non-trivial. This implies that there is a non-trivial cycle's worth of fixed points.

Acknowledgments

I would like to thank

Part I

A Monster Tower Approach to Goursat Multi-Flags

Chapter 1

Introduction

The focus of this half of the thesis is the classification of a particular type of geometric distribution known as a Goursat multi-flag. Before discussing this problem in detail, we first focus on the origins of this problem. The motivation for studying Goursat multi-flags arose from a problem in control theory. During the early nineties there was a great deal of research being done on a control system known as the *Car with n Trailers*. This is a control system in $\mathbb{R}^2$ with a car towing n trailers. This systems has 2 controls (inputs) and $n+2$ degrees of freedom. One control is the velocity of the car. The other is the steering.

The car with n trailers was originally formulated and studied by J.P. Laumond, R. Murray, and S. Sastry ([Lau93] and [MS93]). Then in 1996 F. Jean started to examine the relationship between the various trailer configurations and a rank 2 distribution associated to the kinematic equations of the system ([Jea96]). The car with n trailers system is parametrized by $q = (x, y, \theta_0, \cdots, \theta_n)$, where (x, y) are the coordinates of the last trailers, θ_n is the orientation angle of the car with respect to the positive X-Axis, and θ_i, for $i = 0, \cdots, n-1$, is the orientation angle of the $(n-i)$-th trailer with respect to the the positive X-Axis. The two inputs (or controls) are the angular velocity ω_n (the steering wheel) and the tangential velocity v_n (the accelerator). In summary, the configuration space for the n trailer system is $\mathbb{R}^2 \times (S^1)^{n+1}$.

The kinematics of the car with two degrees of freedom pulling n trailers is

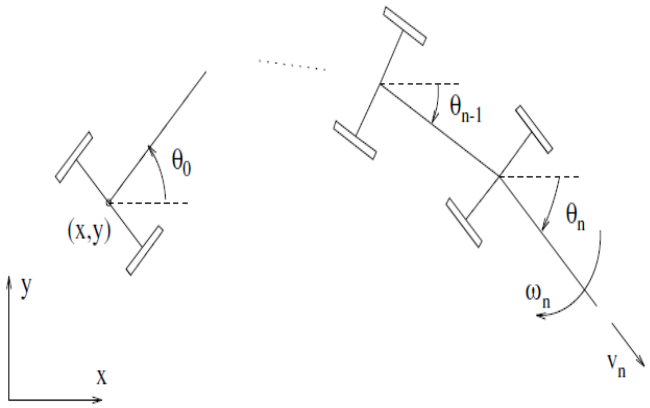

Figure 1.1: The Car with n Trailers

given by

$$\dot{x} = cos(\theta_0)v_0$$

$$\dot{y} = sin(\theta_0)v_0$$

$$\dot{\theta}_i = sin(\theta_{i+1} - \theta_i)v_{i+1} \text{ with } v_{i+1} = \prod_{j=i+1}^{n} cos(\theta_j - \theta_{j-1})v_n \text{ for } i = 0, \cdots, n-1$$

$$\dot{\theta}_n = \omega_n$$

The above relationships are not obvious. We have derived them in an appendix to the thesis.

These relations tell us that the motion of the system is characterized by the equation

$$\dot{q} = \omega_n X_1^n(q) + v_n X_2^n(q)$$

$$\text{with } \begin{cases} X_1^n & = \frac{\partial}{\partial \theta_n} \\ X_2^n & = cos(\theta_0) f_0^n \frac{\partial}{\partial x} + sin(\theta_0) f_0^n \frac{\partial}{\partial y} \\ & \quad + sin(\theta_1 - \theta_0) f_1^n \frac{\partial}{\partial \theta_0} + \cdots + sin(\theta_n - \theta_{n-1}) \frac{\partial}{\partial \theta_{n-1}} \end{cases}$$

and $f_i^n = \prod_{j=i+1}^{n} cos(\theta_j - \theta_{j-1})$, for $i = 0, \cdots, n-1$. Jean was particularly interested in understanding the connection between the various trailer configurations and the degree of nonholonomy of the rank 2 distribution generated by X_1^n and X_2^n. One important property of this distribution is that it is an example of a type of geometric distribution known as a *Goursat* 1-*flag*.

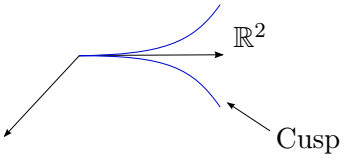

(a) The curve $\gamma(t) = (t^2, t^3)$.

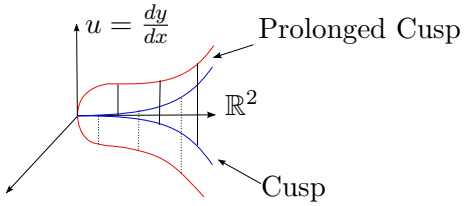

(b) Prolongation of the curve.

A Goursat flag is a nonholonomic distribution D with *slow growth*. By slow growth we mean that the rank of the associated flag of distributions

$$D \quad \subset \quad D + [D, D] \quad \subset \quad D + [D, D] + [[D, D], [D, D]] \ldots,$$

grows by one at each bracketing step. The condition of nonholonomy guarantees that after sufficiently many steps we will obtain the entire tangent bundle of the ambient manifold. By an abuse of notation, D in this context also denotes the sheaf of vector fields spanning D.

A little over ten years ago, R. Montgomery and M. Zhitomirskii took up the task of classifying Goursat 1-flags up to local diffeomorphism equivalence. In order to accomplish this they worked with an iterated sequence of manifolds know as the *Monster Tower*. Each level of the tower is a manifold along with an associated distribution. The first level of the tower is generally taken to be $\mathbb{R}^n$ with the tangent bundle as the associated distribution. Then each consecutive level of the tower is created from the level one below it through a process known as *Cartan prolongation*. In [MZ01] Montgomery and Zhitomirskii were able to create a dictionary between the Goursat 1-flags that arise from the various trailer configurations and points within the Monster Tower with $\mathbb{R}^2$ as the base of the tower. As a result, this meant that if the points within the Monster Tower were classified within each level of the tower up to local diffeomorphism equivalence, then all of the equivalent configuration of these trailers would be classified as well. By 2010 Montgomery and Zhitomriskii had an essentially complete classification of the points within the $\mathbb{R}^2$ Monster Tower. The main idea behind their classification of the tower was to partition the points at any given level of the tower using an invariant that they called the RVT coding system. In addition to this, they used analytic singular curves and applied Cartan prolongation to these curves and looked at when these singularities were resolved. This idea is illustrated in Figures 1.2*a* and 1.2*b* below.

Generalizations of Goursat flags have been proposed in the literature. One such

notion is that of a *Goursat multi-flag.* A Goursat n-flag of length k is a distribution of rank $(n+1)$ sitting in a $(n+1)+kn$ dimensional ambient manifold, where the rank of the associated flag increases by n at each bracketing step. For clarity, we have included the exact definition in the appendix to the thesis. A well-known example of a Goursat multi-flag is the Cartan distribution C of the jet space $J^k(\mathbb{R}, \mathbb{R}^n)$. Iterated bracketing this time produces a flag of distributions

$$C \quad \subset \quad C + [C, C] \quad \subset \quad C + [C, C] + [[C, C], [C, C]] \ldots,$$

where the rank jumps by n at each step.

To our knowledge the general theory behind Goursat multi-flags made their first appearance in the works of A. Kumpera and J. L. Rubin ([KR82]). P. Mormul has also been very active in breaking new ground ([Mor04]), and developed new combinatorial tools to investigate the normal forms of these distributions. This work is founded on an article ([SY09]) by Yamaguchi and Shibuya that demonstrates a universality result which essentially states that any Goursat multi-flag arises as a type of lifting of the tangent bundle of $\mathbb{R}^n$.

Now, as mentioned above, the Monster Tower can be constructed with a base manifold of $\mathbb{R}^n$ for any $n \geq 2$. This leads to the following question:

> *Is there any dynamical system that serves as motivation for studying the* $\mathbb{R}^n$ *Monster Tower for* $n \geq 3$*?*

The *Articulated Arm of Length* k *in* $\mathbb{R}^n$ for $n \geq 3$ is one concrete example. The Articulated Arm of Length k, as seen in Figure 1.2, is a series of k segments $[M_i, M_{i+1}]$, for $i = 0, \cdots, k-1$, with each arm having a constant length of 1 between M_i and M_{i+1}, and each M_i is a point in $\mathbb{R}^n$. There is also the kinematic restraint that the velocity of each joint M_i is collinear with the segment $[M_i, M_{i+1}]$. As of 2011 F. Pelletier established a direct connection between the articulated system and the Monster Tower ([Pel11] and [PS12]). A starting point for the basic properties and control theory results concerning this dynamical system can be found in [LR11].

In this thesis we concentrate on the problem of classifying Goursat multi-flags of small length. Specifically, we will consider Goursat 2-flags of length up to 4. Goursat 2-flags exhibit many new geometric features that Goursat 1-flags did not possess ([MZ10]).

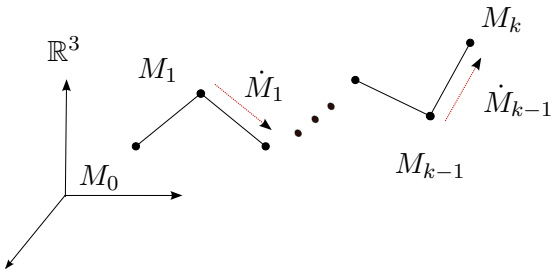

Figure 1.2: The Articulated Arm in $\mathbb{R}^3$.

> *Our main result states that there are* 34 *inequivalent Goursat* 2*-flags of length* 4 *and we provide the exact number of Goursat* 2*-flags for each length* $k \leq 3$ *as well.*

Our approach is constructive. Due to space limitations we will write down only a few instructive examples.

In [SY09] Shibuya and Yamaguchi they establish that every Goursat 2-flag germ appears somewhere within the following tower of fiber bundles:

$$\cdots \to \mathcal{P}^4(2) \to \mathcal{P}^3(2) \to \mathcal{P}^2(2) \to \mathcal{P}^1(2) \to \mathcal{P}^0(2) = \mathbb{R}^3, \tag{1.0.1}$$

and the fiber of the projection map from $\mathcal{P}^k(2)$ to $\mathcal{P}^{k-1}(2)$ is a real projective plane, and adding the dimensions one obtains the dimension formula $\dim(\mathcal{P}^k(2)) = 3 + 2k$. In Chapter 3 of the thesis we show how this tower is constructed.

Each manifold $\mathcal{P}^k(2)$ is equipped with a rank 3 nonholonomic distribution Δ_k, and there is a simple geometric relation between the distributions pertaining to neighboring levels. The construction of Δ_k is recursive, and depends upon the geometric data at the base level $\mathcal{P}^0$.

The distributions Δ_k in $\mathcal{P}^k(2)$ are themselves Goursat 2-flags of length k. Moreover, two Goursat 2-flags are equivalent if and only if the corresponding points of the Monster Tower are mapped one to the other by a *symmetry* of the tower at level k. The paper [SY09] also establishes that all such symmetries are prolongations of diffeomorphisms of $\mathbb{R}^3$. The above observations tell us that

> *the classification problem for Goursat 2-flags is equivalent to the classification of points within the Monster Tower up to symmetry.*

In order to solve this latter problem we use a combination of two methods, namely the singular curve method as in [MZ01] and a new method that we call the *isotropy method.*

A variant of the isotropy method was already used in [MZ01], and it is somewhat inspired by É. Cartan's *moving frame* method ([Fav57]).

We would like to mention that P. Mormul and Pelletier ([MP10]) have proposed an alternative solution to the classification problem. In their classification work, they employed Mormul's results and tools that came from his work with Goursat n-flags. In [Mor09], Mormul discusses two coding systems for special 2-flags and showed that the two coding systems are the same. One system is the *extended Kumpera Ruiz system,* which is a coding system used to describe 2-flags. The other is called *singularity class coding,* which is an intrinsic coding system that describes the sandwich diagram ([MZ01]) associated to 2-flags. In the appendix to the thesis we have included an outline on how these coding systems relate to the RVT coding system. Then, building upon Mormul's work in [Mor03], Mormul and Pelletier used the idea of strong nilpotency of special multi-flags, along with the properties of his two coding systems, to classify these distributions up to length 4. Our 34 orbits agrees with theirs.

In Chapter 2 we acquaint ourselves with the main definitions necessary for the statements of our main results, the statement of the main results, and a few explanatory remarks. Chapter 3 consists of the preliminary material. In this chapter we discuss the basic tools and ideas that will be needed to prove our various results. Chapter 4 is devoted to the proofs of the main results. Finally, in Chapter 5, we provide an appendix to the thesis where one can find supplementary information. In particular, we have listed the definition of a Goursat n-flag, a derivation of the kinematic equations for the car with n trailers, and some lengthy computations along with other useful tools and examples to help the reader with the theory.

Chapter 2

Settings and Main Results

In this portion of the thesis we present the classification of the points within the Monster Tower with critical length at most 4. A large amount of the work will be the classification of the points within the first 4 levels of the Monster Tower. In order to do this we use a singular curve approach and another technique that we call the isotropy method.

2.1 The Setting and Main Results

Theorem 2.1.1 (Orbit counting per level) *In the $n = 2$ (or spatial) Monster Tower the number of orbits within each of the first four levels of the tower are as follows:*

Level 1:	*Level 2:*	*Level 3:*	*Level 4:*
1	2	7	34

The main idea behind determining the number of orbits in the first four levels of the tower is to use a blend of the singular curve methods as introduced in [MZ10] and a technique we call the isotropy method (adapted from [MZ01]). The curve method alone suffices to yield Theorem 2.1.1 up to level 3. In order to get to level 4 we must use the isotropy method in combination with a classification of special directions which generalizes the RVT coding of [MZ10]. This classification, or *coding* is described in Section 3.3.3. Our main result, in detail, is the following theorem, of which Theorem 2.1.1 is an immediate corollary.

Table 2.1: Number of orbits within the first three levels of the Monster Tower.

Level of tower	RVT code	Number of orbits	Normal forms
1	R	1	$(t, 0, 0)$
2	RR	1	$(t, 0, 0)$
	RV	1	$(t^2, t^3, 0)$
3	RRR	1	$(t, 0, 0)$
	RRV	1	$(t^2, t^5, 0)$
	RVR	1	$(t^2, t^3, 0)$
	RVV	1	(t^3, t^5, t^7), $(t^3, t^5, 0)$
	RVT	2	(t^3, t^4, t^5), $(t^3, t^4, 0)$
	RVL	1	(t^4, t^6, t^7)

Theorem 2.1.2 (Listing of orbits within each RVT code) *Table 2.1 is a breakdown of the number of orbits that appear within each RVT class within the first three levels.*
For level 4 there is a total of 23 possible RVT classes. Of the 23 possibilities 14 of them consist of a single orbit. The classes $RRVT$, $RVRV$, $RVVR$, $RVVV$, $RVVT$, $RVTR$, $RVTV$, $RVTL$ consist of 2 orbits, and the class $RVTT$ consists of 4 orbits.

Remark 2.1.3 *There are a few words that should be said to explain the normal forms column in Table 2.1. Let $p_k \in \mathcal{P}^k$, for $k = 1, 2, 3$, have RVT code ω, meaning ω is a word from the second column of the table. Let $\gamma \in Germ(p_k)$, then γ is RL equivalent to one of the curves listed in the normal forms column for the RVT class ω. Now, for the class RVV we notice that there are two inequivalent curves sitting in the normal forms column, but that there is only one orbit within that class. This is because the two normal forms are equal to each other, at $t = 0$, after three prolongations. However, after four prolongations they represent different points at the fourth level. This corresponds to the fact that at the fourth level class $RVVR$ breaks up into two orbits.*

The following theorems are in [CM12] and helped to reduce the number calculations in our orbit classification process.

Definition 2.1.1 *A point $p_k \in \mathcal{P}^k$ is called a Cartan point if its RVT code is R^k, where $R^k = \underbrace{R \cdots R}_{k \text{ times}}$.*

Theorem 2.1.4 *The RVT class R^k forms a single orbit at any level within the Monster Tower $\mathcal{P}^k(n)$ for $k \geq 1$ and $n \geq 1$. Every point at level 1 is a Cartan point. For $k > 1$ the set R^k is an open dense subset of $\mathcal{P}^k(n)$.*

Definition 2.1.2 *A parametrized curve belongs to the A_{2k} class, $k \geq 1$, if it is RL equivalent to the curve*

$$(t^2, t^{2k+1}, 0)$$

Theorem 2.1.5 *Let $p_k \in \mathcal{P}^k$ with $k = j + m + 1$, with $m \geq 0, k \geq 1$ non-negative integers, and $p_k \in R^j C R^m$. Then $Germ(p_k)$ contains a curve germ equivalent to the A_{2k} singularity, which implies that the RVT class $R^j C R^m$ consists of a single orbit.*

Remark 2.1.6 *The letter C, as well as any other letter other than the letter R, in the above stands for a critical point. This notation will be explained in more detail in Section* 3.3.1.

Theorem 2.1.7 *Let ω be an RVT class comprised of k-orbits.*
Then the addition of R's to the beginning of the code ω, meaning $R \cdots R\omega$, will be an RVT class with k-orbits.

Theorem 2.1.7 allows one to reduce the number of calculations needed to compute the number of orbits within an RVT class found within higher levels of the Monster Tower. For example, the class $RRRRRRVV$ will have exactly the same number of orbits as RVV. This theorem helped in the classification of points within the fourth level of the tower by reducing the number of calculations we needed to do with the isotropy method. It also tells us how many orbits there are within any RVT class that starts with a sequence of R's and has at most 3 critical adjacent letters.

Remark 2.1.8 Monster Tower is a fiber compactification of jet spaces. *The space of k-jets of functions $f : \mathbb{R} \to \mathbb{R}^2$, usually denoted by $J^k(\mathbb{R}, \mathbb{R}^2)$ is an open dense subset of $\mathcal{P}^k$. It is in this sense that a point $p \in \mathcal{P}^k$ is roughly speaking the k-jet of a curve in $\mathbb{R}^3$. Sections of the bundle*

$$J^k(\mathbb{R}, \mathbb{R}^2) \to \mathbb{R} \times \mathbb{R}^2$$

are k-jet extensions of functions. Explicitly, given a vector-valued function $t \mapsto f(t) = (x(t), y(t))$ its k-jet extension is defined as

$$(t, f(t)) \mapsto (t, x(t), y(t), x'(t), y'(t), \ldots, x^{(k)}(t), y^{(k)}(t)).$$

Superscripts here denotes the order of the derivative. It is an instructive exercise to show that for certain choices of fiber affine coordinates in $\mathcal{P}^k$, not involving critical directions, that our local charts will look like a copy of $J^k(\mathbb{R}, \mathbb{R}^2)$.

Another reason to look at curves is that it gives us a better picture of the overall behavior of an RVT class. If one knows all the possible curve normal forms for a particular RVT class, say ω, then not only does one know how many orbits are within the class ω, but one also knows how many orbits are within the regular prolongation of ω. By regular prolongation of an RVT class ω we mean the addition of only R's to the end of the word ω, i.e. the regular prolongation of ω is $\omega R \cdots R$. This method of using curves to classify RVT classes was used in [MZ10].

Chapter 3

Preliminaries

This chapter will provide all of the necessary background for the Monster Tower and its various properties.

3.1 Cartan Prolongation

Cartan Prolongation is Before we being, we want to say that a *geometric distribution* hereafter denotes a linear subbundle of the tangent bundle with fibers of constant dimension.

3.1.1 Prolongation

Let the pair (Z, Δ) denote a manifold Z of dimension d equipped with a distribution Δ of rank r. We denote by $\mathbb{P}(\Delta)$ the *projectivization* of Δ. As a manifold,

$$\mathbb{P}(\Delta) \equiv Z^1,$$

has dimension $d + (r - 1)$.

Example 3.1.1 *Take $Z = \mathbb{R}^3$, $\Delta = TR^3$ viewed as a rank 3 distribution. Then Z^1 is simply the trivial bundle $\mathbb{R}^3 \times \mathbb{P}^2$, where the factor on the right denotes the projetive plane.*

Various geometric objects in Z can be canonically prolonged (lifted) to the new manifold Z^1. In what follows prolongations of curves and transformations are quintessential.

Table 3.1: Some geometric objects and their Cartan prolongations.

curve $c : (I, 0) \to (Z, q)$	curve $c^1 : (I, 0) \to (Z^1, q)$, $c^1(t) = (\text{point,moving line}) = (c(t), \text{span}\{\frac{dc}{dt}(t)\})$
diffeomorphism $\Phi : Z \circlearrowleft$	diffeomorphism $\Phi^1 : Z^1 \circlearrowleft$, $\Phi^1(p, \ell) = (\Phi(p), d\Phi_p(\ell))$
rank r linear subbundle $\Delta \subset TZ$	rank r linear subbundle $\Delta_{1(p,\ell)} = d\pi^{-1}_{(p,\ell)}(\ell) \subset TZ^1$, $\pi : Z^1 \to Z$ is the canonical projection.

Given an analytic curve $c : (I, 0) \to (Z, q)$, where I is some open interval in $\mathbb{R}$ containing the origin and $c(0) = q$, we can naturally define a new curve

$$c^1 : (I, 0) \to (Z^1, (q, \ell))$$

with image in Z^1 and where $\ell = \text{span}\{\frac{dc}{dt}(0)\}$. This new curve, $c^1(t)$, is called the *prolongation* of $c(t)$. If $t = t_0$ is not a regular point, then we define $c^1(t_0)$ to be the limit $\lim_{t\to t_0} c^1(t)$ where the limit varies over the regular points $t \to t_0$. An important fact to note, proved in [MZ01], is that the analyticity of Z and c implies that the limit is well defined and that the prolonged curve $c^1(t)$ is analytic as well. Since this process can be iterated, we will write $c^k(t)$ to denote the k-fold prolongation of the curve $c(t)$.

The manifold Z^1 also comes equipped with a distribution Δ_1 called the *Cartan prolongation of* Δ ([BH93]) which is defined as follows. Let $\pi : Z^1 \to Z$ be the projection map $(p, \ell) \mapsto p$. Then

$$\Delta_1(p, \ell) = d\pi^{-1}_{(p,\ell)}(\ell),$$

i.e. *it is the subspace of* $T_{(p,\ell)}Z^1$ *consisting of all tangents to curves which are prolongations of curves in* Z *that pass through* p *with a velocity vector contained in* ℓ. It is easy to check using linear algebra that Δ_1 is also a distribution of rank r.

By a *symmetry* of the pair (Z, Δ) we mean a local diffeomorphism Φ of Z that preserves the subbundle Δ.

The symmetries of (Z, Δ) can also be prolonged to symmetries Φ^1 of (Z^1, Δ_1) as follows. Define

$$\Phi^1(p, \ell) := (\Phi(p), d\Phi_p(\ell)).$$

Since[1] $d\Phi_p$ is invertible and $d\Phi_p$ is linear the second component is well defined as a projective map. This new transformation in (Z^1, Δ_1) is the *prolongation* of Φ. Objects

[1]We also use the notation Φ_* for the pushforward or tangent map $d\Phi$.

of interest and their Cartan prolongations are summarized in Table 3.1. We note that the word prolongation will always be synonymous with Cartan prolongation.

Example 3.1.2 (Prolongation of a cusp) *Let* $c(t) = (t^2, t^3, 0)$ *be the cusp in* $\mathbb{R}^3$. *Then* $c^1(t) = (x(t), y(t), z(t), [dx : dy : dz]) = (t^2, t^3, 0, [2t : 3t^2 : 0])$. *After we introduce fiber affine coordinates* $u = \frac{dy}{dx}$ *and* $v = \frac{dz}{dx}$ *around the point* $(0, 0, 0, [1 : 0 : 0])$ *we obtain the immersed curve*

$$c^1(t) = (t^2, t^3, 0, \frac{3}{2}t, 0)$$

3.2 The Monster Tower

3.2.1 Constructing the Monster Tower.

We start with $\mathbb{R}^{n+1}$ as our base manifold Z and take $\Delta_0 = T\mathbb{R}^{n+1}$. Prolonging Δ_0 we get $\mathcal{P}^1(n) = \mathbb{P}(\Delta_0)$ equipped with the distribution Δ_1 of rank n. By iterating this process we end up with the manifold $\mathcal{P}^k(n)$ which is endowed with the rank n distribution $\Delta_k = (\Delta_{k-1})^1$ and fibered over $\mathcal{P}^{k-1}(n)$. In this thesis we will be studying the case $n = 2$.

Definition 3.2.1 *The Monster Tower is a sequence of manifolds with distributions,* $(\mathcal{P}^k, \Delta_k)$, *together with fibrations*

$$\cdots \to \mathcal{P}^k(n) \to \mathcal{P}^{k-1}(n) \to \cdots \to \mathcal{P}^1(n) \to \mathcal{P}^0(n) = \mathbb{R}^{n+1}$$

and we write $\pi_{k,i} : \mathcal{P}^k(n) \to \mathcal{P}^i(n)$ *for the respective bundle projections.*

This explains how the tower shown in equation (1.0.1) is obtained by iterated Cartan prolongation of the pair $(\mathbb{R}^3, \Delta_0)$.

Definition 3.2.2 Diff(3) *is taken to be the pseudogroup of diffeomorphism germs of* $\mathbb{R}^3$.

Remark 3.2.1 The pseudogroup *Diff*(3). *Saying that* Diff(3) *is a pseudogroup roughly means that for any open set* $U \subseteq \mathbb{R}^3$, *the identity restricted to this set is an element of* Diff(3), *and for any local diffeomorphism in* Diff(3) *defined on* U *its inverse, defined on* $\Phi(U)$ *is in* Diff(3) *as well. Also, for any* $\Phi_1, \Phi_2 \in$ Diff(3) *where* $\Phi_1 : U_1 \to V_1$ *and* $\Phi_2 : U_2 \to V_2$, *for* U_i *and* V_i *open subsets of* $\mathbb{R}^3$ *with* $V_1 \cap U_2 \neq \emptyset$, *then the composition* $\Phi_2 \circ \Phi_1^{-1} : \Phi_1^{-1}(V_1 \cap U_2) \to \Phi_2(V_1 \cap U_2)$ *is an element of* Diff(3). *A more detailed discussion about pseudogroups can be found in [KN96].*

The following result found in a paper by Shibuya and Yamaguchi will be important for our classification of points within the Monster Tower.

Theorem 3.2.2 *For $n > 1$ and $k > 0$ any local diffeomorphism of $\mathcal{P}^k(n)$ preserving the distribution Δ_k is the restriction of the k-th prolongation of a local diffeomorphism $\Phi \in \mathrm{Diff}(n)$.*

Proof: See ([SY09], pg. 795). □

Shibuya and Yamaguchi also point out that this is a result due to A. Bäcklund [Bäc75].

Remark 3.2.3 *The importance of the above result cannot be stressed enough. This theorem is the theoretical foundation for the isotropy method, discussed in Section 5 of the thesis. It will be crucial for classifying orbits within the Monster Tower.*

Remark 3.2.4 *Since we will be working almost exclusively with the $n = 2$ Monster Tower in this thesis, we will just write $\mathcal{P}^k$ for $\mathcal{P}^k(2)$.*

Definition 3.2.3 *Two points p, q in $\mathcal{P}^k$ are said to be equivalent, written $p \sim q$, if there is a $\Phi \in \mathrm{Diff}(3)$ such that $\Phi^k(p) = q$.*

Definition 3.2.4 *Let $p \in \mathcal{P}^k$ then we denote $\mathcal{O}(p)$ to be the orbit of the point p under the action by elements of* Diff(3) *to the k-th level of the Monster Tower, where a point q is an element in $\mathcal{O}(p)$ if q is equivalent to the point p.*

3.2.2 Orbits.

Theorem 3.2.2 tells us that any symmetry of $\mathcal{P}^k$ comes from prolonging a diffeomorphism of a real affine three-space k times. Let us denote by $\mathcal{O}(p)$ the orbit of the point p under the action of *Diff*(3).

In trying to calculate the various orbits within the Monster Tower we found it convenient to fix the base points from which they originated from in $\mathbb{R}^3$. In particular, if p_k is a point in $\mathcal{P}^k$ and $p_0 = \pi_{k,0}(p_k)$ is the base point in $\mathbb{R}^3$, then by a change of coordinates we can take the point p_0 to be the origin in $\mathbb{R}^3$. This means that we can replace the pseudogroup *Diff*(3), diffeomorphism germs of $\mathbb{R}^3$, by the group $\mathit{Diff}_0(3)$ of diffeomorphism germs that map the origin back to the origin in $\mathbb{R}^3$.

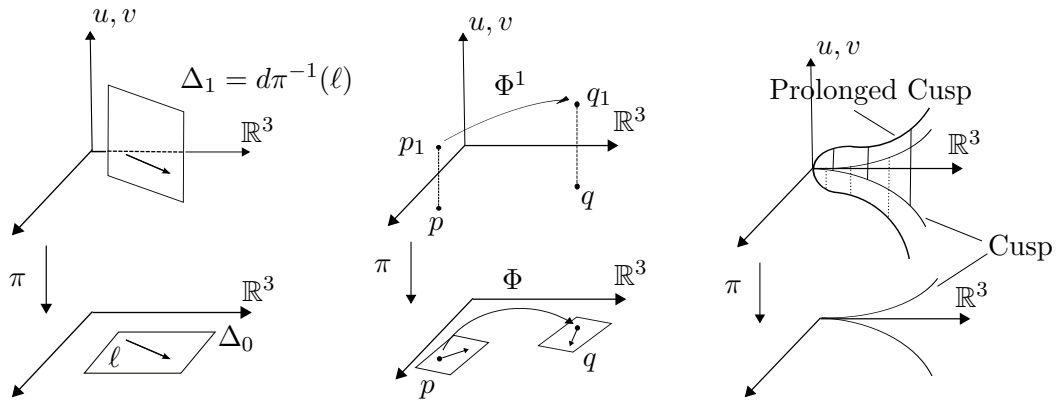

(a) Prolongation of a distribution (b) Prolongation of a diffeomorphism (c) Prolongation of a curve

Figure 3.1: Prolongations

Definition 3.2.5 *We say that a curve or curve germ $\gamma : (\mathbb{R}, 0) \to (\mathbb{R}^3, \boldsymbol{0})$ realizes the point $p_k \in \mathcal{P}^k$ if $\gamma^k(0) = p_k$, where $p_0 = \pi_{k,0}(p_k) \equiv \boldsymbol{0}$.*

> It is important to note at this point that prolongation and projection commute. This fact is discussed in detail in [MZ10] and in [CM12].

Definition 3.2.6 *A direction $\ell \subset \Delta_k(p_k)$, $k \geq 1$ is called a critical direction if there exists an immersed curve at level k that is tangent to the direction ℓ, and whose projection to level zero, meaning the base manifold, is a constant curve. If no such curve exists, then we call ℓ a regular direction. Note that while ℓ is technically a line we will by an abuse of terminology refer to it as a direction.*

Definition 3.2.7 *Let $p \in \mathcal{P}^k$. The set of curves*

$$\mathrm{Germ}(p) \quad := \quad \{c : (\mathbb{R}, 0) \to (\mathbb{R}^3, \boldsymbol{0}) | c^k(0) = p \text{ and } \frac{dc^k}{dt}|_{t=0} \neq 0 \text{ is a regular direction}\},$$

is called the germ associated to the point p.

Definition 3.2.8 *Two curves γ, σ in $\mathbb{R}^3$ are RL equivalent, written $\gamma \sim \sigma$ if there exists a diffeomorphism germ $\Phi \in \mathrm{Diff}(3)$ and a reparametrization $\tau \in \mathrm{Diff}_0(1)$ such that $\sigma = \Phi \circ \gamma \circ \tau$.*

We can then define $\mathrm{Germ}(p) \sim \mathrm{Germ}(q)$ to mean that every curve in $\mathrm{Germ}(p)$ is RL equivalent to some curve in $\mathrm{Germ}(q)$ and conversely, every curve in $\mathrm{Germ}(q)$ is RL equivalent to some curve in $\mathrm{Germ}(p)$.

3.3 RVT Coding

The RVT coding system was first used in [MZ10]. Then in [CM12] they extended this coding system from the $\mathbb{R}^2$ Monster Tower to the $\mathbb{R}^3$ Monster Tower. As is also pointed out by Castro and Montgomery, this coding system holds if we take the base manifold to be $\mathbb{C}^3$, too. The RVT coding system partitions the points at any given level of the tower where we attach a sequence of R's, V's, T's, and L's, along with various decorations to the T's and L's, One important feature of this coding is that the various symmetries at any given level of the tower preserve the RVT code. This means that if we take the collection of points within a fixed RVT class and apply a symmetry to them, then those points stay within that RVT class.

We first introduce the RC coding system and from there refine our coding system to produce the RVT coding system.

3.3.1 RC Coding of Points.

Definition 3.3.1 *A point $p_k \in \mathcal{P}^k$, where $p_k = (p_{k-1}, \ell)$ is called a regular or critical point if the line ℓ is a regular direction or a critical direction.*

Definition 3.3.2 *For $p_k \in \mathcal{P}^k$, $k \geq 1$ and $p_i = \pi_{k,i}(p_k)$, we write $\omega_i(p_k) = R$ if p_i is a regular point and $\omega_i(p_k) = C$ if p_i is a critical point. Then the word $\omega(p_k) = \omega_1(p_k) \cdots \omega_k(p_k)$ is called the RC code for the point p_k. The number of letters within the RC code for p_k equals the level of the tower that the point lives in. Note that $\omega_1(p_k)$ is always equal to R by Theorem 2.1.4.*

So far we have not discussed how critical directions sit inside of Δ_k. The following section will show that there is more than one kind of critical direction that can appear within the distribution Δ_k.

3.3.2 Baby Monsters.

One can apply prolongation to any analytic n-dimensional manifold F in place of $\mathbb{R}^n$. Start out with $\mathcal{P}^0(F) = F$ and take $\Delta_0^F = TF$. Then the prolongation of the

pair (F, Δ_0^F) is $\mathcal{P}^1(F) = \mathbb{P}TF$ equipped with the rank m distribution $\Delta_1^F \equiv (\Delta_0^F)^1$. By iterating this process k times we end up with new the pair $(\mathcal{P}^k(F), \Delta_k^F)$, which is analytically diffeomorphic to $(\mathcal{P}^k(n-1), \Delta_k)$ ([CM12]).

Now, apply this process to the fiber $F_i(p_i) = \pi_{i,i-1}^{-1}(p_{i-1}) \subset \mathcal{P}^i$ through the point p_i at level i. The fiber is an $(n-1)$-dimensional integral submanifold for Δ_i. Prolonging, we see that $\mathcal{P}^1(F_i(p_i)) \subset \mathcal{P}^{i+1}$, and $\mathcal{P}^1(F_i(p_i))$ has the associated distribution $\delta_i^1 \equiv \Delta_1^{F_i(p_i)}$; that is,

$$\delta_i^1(q) = \Delta_{i+1}(q) \cap T_q(\mathcal{P}^1(F_i(p_i)))$$

which is a hyperplane within $\Delta_{i+1}(q)$, for $q \in \mathcal{P}^1(F_i(p_i))$. When this prolongation process is iterated, we end up with the submanifolds

$$\mathcal{P}^j(F_i(p_i)) \subset \mathcal{P}^{i+j}$$

with the hyperplane subdistribution $\delta_i^j(q) \subset \Delta_{i+j}(q)$ for $q \in \mathcal{P}^j(F_i(p_i))$.

Definition 3.3.3 *A Baby Monster born at level i is a sub-tower $(\mathcal{P}^j(F_i(p_i)), \delta_i^j)$, for $j \geq 0$ within the ambient Monster Tower. If $q \in \mathcal{P}^j(F_i(p_i))$ then we will say that a Baby Monster born at level i passes through q and that $\delta_i^j(q)$ is a critical hyperplane passing through q, which was born at level i.*

Definition 3.3.4 *The vertical plane $V_k(q)$ is the critical hyperplane $\delta_k^0(q)$. We note that it is always one of the critical hyperplanes passing through q.*

The following statement elucidates the geometric properties of critical directions.

Theorem 3.3.1 *A direction $\ell \subset \Delta_k$ is critical if and only if ℓ is contained in a critical hyperplane.*

3.3.3 Arrangements of critical hyperplanes for $n = 2$.

Over any point p_k, at the k-th level of the Monster Tower, there is a total of three different hyperplane configurations for Δ_k. These three configurations are shown in Figures 3.2a, 3.2b, and 3.2c.

Figure 3.2*a* is the picture for $\Delta_k(p_k)$ when the k-th letter in the RVT code for p_k is the letter R. This means that the vertical hyperplane, labeled with a V, is the

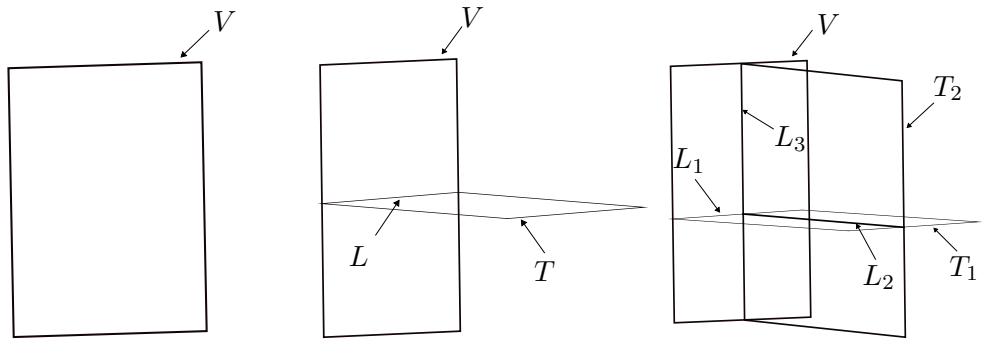

(a) Above a regular point. (b) Above a vertical or tangency point. (c) Above an L point.

Figure 3.2: Arrangement of critical hyperplanes.

only critical hyperplane sitting inside of $\Delta_k(p_k)$. Figure 3.2*b* is the picture for $\Delta_k(p_k)$ when the k-th letter in the RVT code is either the letter V or the letter T. This gives a total of two critical hyperplanes sitting inside of $\Delta_k(p_k)$ and one distinguished critical direction: one is the vertical hyperplane and the other is the tangency hyperplane, labeled by the letter T. The intersection of vertical and tangency hyperplane gives a distinguished critical direction, which is labeled by the letter L. Now, Figure 3.2*c* describes the picture for $\Delta_k(p_k)$ when the k-th letter in the RVT code of p_k is the letter L. Figure 3.2*c* depicts this situation where there is now a total of three critical hyperplanes: one is the vertical hyperplane, and two tangency hyperplanes, labeled as T_1 and T_2. Now, because of the presence of these three critical hyperplanes we need to refine our notion of an L direction and add two more distinct L directions. These three directions are labeled as L_1, L_2, and L_3. More details concerning the properties of these critical hyperplanes and their various configurations can be found in [CM12].

With the above picture in mind, we can now refine our RC coding and define the RVT code for points within the Monster Tower. Take $p_k \in \mathcal{P}^k$ and if $\omega_i(p_k) = C$ then we look at the point $p_i = \pi_{k,i}(p_k)$, where $p_i = (p_{i-1}, \ell_{i-1})$. Then depending on which critical hyperplane, or distinguished direction, contains ℓ_{i-1}, we replace the letter C by the letter V, T, L, T_i for $i = 1, 2$, or L_j for $j = 1, 2, 3$. One can see from the above geometric considerations that these critical letters must follow three simple *grammar rules*.

(i) The first one states that the initial letter in any RVT code string must be the

letter R. This is a consequence of Theorem 2.1.4.

(ii) The second is that the letters T or L, along with T_i for $i = 1, 2$ and L_j for $j = 1, 2, 3$, cannot immediately follow the letter R.

(iii) The last one is that the letters T_2 and L_j for $j = 1, 2, 3$ can only appear immediately after the letter $L = (L_1)$.

For the case of length 4 the letters T_2 and L_j for $j = 2, 3$ can only appear immediately after the letter $L = (L_1)$. However, for a point of length larger than 4 we believe that this rule still holds. This fact will be investigated in a future work by one of the authors.

Example 3.3.2 (Examples of RVT codes) *The following are examples of RVT codes: $R \cdots R$, $RVVT$, $RVLT_2R$, and $RVLL_2$. The code RTL is not allowed because the letter T is preceded by the letter R and the code RLT_3 is not allowed because the letter L comes immediately after the letter R.*

As a result, we see that each of the first four levels of the Monster Tower is made up of the following RVT classes:

- Level 1:

$$R$$

- Level 2:

$$RR, RV$$

- Level 3:

$$RRR, RRV, RVR, RVV, RVT, RVL$$

- Level 4:

$$RRRR, RRRV$$

$$RRVR, RRVV, RRVT, RRVL$$

$$RVRR, RVRV, RVVR, RVVV, RVVT, RVVL$$

$$RVTR, RVTV, RVTT, RVTL$$

$$RVLR, RVLV, RVLT_1, RVLT_2, RVLL_1, RVLL_2, RVLL_3$$

Remark 3.3.3 *As it was pointed out in [CM12] the symmetries, at any level in the Monster Tower preserve the critical hyperplanes. In other words, if Φ^k is a symmetry at level k in the Monster Tower and δ_i^j is a critical hyperplane within Δ_k then $\Phi_*^k(\delta_i^j) = \delta_i^j$. As a result, the RVT classes creates a partition of the various points within any level of the Monster Tower,i.e., the RVT classes are invariant under the* Diff(3) *action. More details about the properties of the various critical hyperplanes and distinguished critical directions can be found in [CM12].*

Now, from the above configurations of critical hyperplanes section one might ask the following question: how does one "see" the two tangency hyperplanes that appear over an "L" point and where do they come from? This question was an important one to ask when trying to classify the number of orbits within the fourth level of the Monster Tower and to better understand the geometry of the tower. We will provide an example to answer this question, but before we do so we must discuss some details about a particular coordinate system called Kumpera-Rubin coordinates to help us do various computations within the Monster Tower.

3.4 Kumpera-Rubin Coordinates

When doing local computations in the tower (1.0.1), one needs to work with suitable coordinates. A good choice of coordinates was suggested by Kumpera and Ruiz ([KR82]) in the Goursat case, and later generalized by Kumpera and Rubin ([KR82]) for multi-flags. A detailed description of the inductive construction of Kumpera-Rubin coordinates was given in [CM12] and we have included this general construction in an appendix to the thesis (Section 5.4). For the sake of clarity, we will just highlight the coordinates' attributes through an example in this section.

Example 3.4.1 (Constructing fiber affine coordinates in $\mathcal{P}^2$)

Level One:

Consider the pair $(\mathbb{R}^3, T\mathbb{R}^3)$ and let (x, y, z) be local coordinates on $\mathbb{R}^3$. The triple of 1-forms $\{dx, dy, dz\}$ form a coframe of $T\mathbb{R}^3$. Any line ℓ_0 in the tangent space at $p_0 \in \mathbb{R}^3$ has projective coordinates $[dx|_{\ell_0} : dy|_{\ell_0} : dz|_{\ell_0}]$. Since the affine group of

$\mathbb{R}^3$, which is contained in *Diff*(3), acts transitively on $\mathbb{P}(T\mathbb{R}^3)$, we can fix $p_0 = (0,0,0)$ $(= \mathbf{0})$ and $\ell_0 = \text{span}\left\{\frac{\partial}{\partial x}\right\}$. Thus $dx|_{\ell_0} \neq 0$ and we introduce fiber affine coordinates $[1 : dy/dx : dz/dx]$ where,

$$u = \frac{dy}{dx}, v = \frac{dz}{dx}.$$

The Pfaffian system describing the prolonged distribution Δ_1 on $\mathcal{P}^1 = \mathbb{R}^3 \times \mathbb{P}^2$ is

$$\{dy - udx = 0, dz - vdx = 0\} = \Delta_1 \subset T\mathcal{P}^1.$$

At the point $p_1 = (p_0, \ell_0) = (x, y, z, u, v) = (0, 0, 0, 0, 0)$ the distribution is the linear subspace

$$\Delta_{1\,(0,0,0,0,0)} = \{dy = 0, dz = 0\}.$$

The triple of 1-forms $\{dx, du, dv\}$ form a local coframe for Δ_1 near $p_1 = (p_0, \ell_0)$. The fiber, $F_1(p_1) = \pi_{1,0}^{-1}(p_0)$, is given by $x = y = z = 0$. The 2-plane of critical directions ("bad-directions") is thus spanned by $\frac{\partial}{\partial u}, \frac{\partial}{\partial v}$.

The reader may have noticed that we could have instead chosen any regular direction at level 1 instead, e.g. $\frac{\partial}{\partial x} + a\frac{\partial}{\partial u} + b\frac{\partial}{\partial v}$ and centered our chart at it. Again, this is because all regular directions at level one are pairwise equivalent by a symmetry transformation.

Remark 3.4.2 *Let us remind the reader that $\mathcal{P}^1$ is diffeomorphic to $\mathbb{R}^3 \times \mathbb{P}^2$ but $\mathcal{P}^k$ is not a trivial bundle over $\mathbb{R}^3$ if $k \geq 2$ (cf. [CM12], section 2).*

Level Two (RV points):

Any line $\ell_1 \subset \Delta_1(p_1')$, for p_1' near p_1, will have projective coordinates

$$[dx|_{\ell_1} : du|_{\ell_1} : dv|_{\ell_1}].$$

If we choose a critical direction, say $\ell_1 = span\{\frac{\partial}{\partial u}\}$, then $du(\frac{\partial}{\partial u}) = 1$ and we can center our chart at the direction ℓ_1 and the chart is given by the projective coordinates $[\frac{dx}{du} : 1 : \frac{dv}{du}]$. *We will show below that any two critical directions are equivalent and therefore such a choice does not result in any loss of generality.* We introduce new fiber affine coordinates

$$u_2 = \frac{dx}{du}, v_2 = \frac{dy}{du},$$

and the distribution Δ_2 will be described in this chart as

$$\begin{aligned}\Delta_2 = \{&dy - udx = 0, dz - vdx = 0,\\ &dx - u_2du = 0, dv - v_2du = 0\} \subset T\mathcal{P}^2.\end{aligned}$$

Level Three (The Tangency Hyperplanes over an L point):

We take $p_3 = (p_2, \ell_2) \in RVL$ with p_2 as in the level two discussion. We now look at a local affine coordinates near the point p_2. We will show that inside of this chart that the tangency hyperplane T_1 in $\Delta_3(p_3)$ is the critical hyperplane $\delta_2^1(p_3) = span\{\frac{\partial}{\partial v_2}, \frac{\partial}{\partial v_3}\}$ and the tangency hyperplane T_2 is the critical hyperplane $\delta_1^2(p_3) = span\{\frac{\partial}{\partial v_2}, \frac{\partial}{\partial u_3}\}$.

We begin with the local coordinates near p_3. Let us first recall that the distribution Δ_2 is coframed by $\{du, du_2, dv_2\}$ in this case. Within Δ_2 the vertical hyperplane is given by $du = 0$ and the tangency hyperplane by $du_2 = 0$. The point $p_3 = (p_2, \ell)$ with ℓ being an L direction means that both $du|_\ell = 0$ and $du_2|_\ell = 0$. This means that the only choice for local coordinates near p_3 is given by $[\frac{du}{dv_2} : \frac{du_2}{dv_2} : 1]$. As a result, the fiber coordinates at level 3 are

$$u_3 = \frac{du}{dv_2}, v_3 = \frac{du_2}{dv_2}$$

and the distribution Δ_3 will be described in this chart as

$$\begin{aligned}\Delta_3 = \{&dy - udx = 0, dz - vdx = 0,\\ &dx - u_2du = 0, dv - v_2du = 0,\\ &du - u_3dv_2 = 0, du_2 - v_3dv_2 = 0\} \subset T\mathcal{P}^3.\end{aligned}$$

With this in mind, we are ready to determine how the two tangency hyperplanes are situated within Δ_3.

- **Showing T_1 is equal to $\delta_2^1(p_3)$:** First we note that $p_3 = (x, y, z, u, v, u_2, v_2, u_3, v_3) = (0, 0, 0, 0, 0, 0, 0, 0, 0)$ with $u = \frac{dy}{dx}$, $v = \frac{dz}{dx}$, $u_2 = \frac{dx}{du}$, $v_2 = \frac{dv}{du}$, $u_3 = \frac{du}{dv_2}$, $v_3 = \frac{du_2}{dv_2}$. With this in mind, we start by looking at the vertical hyperplane $V_2(p_2) \subset \Delta_2(p_2)$ and prolong the fiber $F_2(p_2)$ associated to $V_2(p_2)$ and see that

$$\mathcal{P}^1(F_2(p_2)) = \mathbb{P}V_2 = (p_1, u_2, v_2, [du : du_2 : dv_2]) = (p_1, u_2, v_2, [0 : a : b])$$

$$= (p_1, u_2, v_2, [0 : \tfrac{a}{b} : 1]) = (p_1, u_2, v_2, 0, v_3)$$

where $a, b \in \mathbb{R}$ with $b \neq 0$. One sees that Δ_3, in a neighborhood of p_3, is given by

$$\Delta_3 = span\left\{u_3 X^{(2)} + v_3\frac{\partial}{\partial u_2} + \frac{\partial}{\partial v_2}, \frac{\partial}{\partial u_3}, \frac{\partial}{\partial v_3}\right\}$$

with $X^{(2)} = u_2 X_1^{(1)} + \frac{\partial}{\partial u} + v_2\frac{\partial}{\partial v}$ and $X^{(1)} = u\frac{\partial}{\partial y} + v\frac{\partial}{\partial z} + \frac{\partial}{\partial x}$ and that $T_{p_3}(\mathcal{P}^1(F_2(p_2))) = span\{\frac{\partial}{\partial u_2}, \frac{\partial}{\partial v_2}, \frac{\partial}{\partial v_3}\}$. From the definition of δ_i^j we have that

$$\delta_2^1(p_3) = \Delta_3(p_3) \cap T_{p_3}(\mathcal{P}^1(F_2(p_2)))$$

which gives that

$$\delta_2^1(p_3) = span\left\{\frac{\partial}{\partial v_2}, \frac{\partial}{\partial v_3}\right\}.$$

Now, since $V_3(p_3) \subset \Delta_3(p_3)$ is given by $V_3(p_3) = span\{\frac{\partial}{\partial u_3}, \frac{\partial}{\partial v_3}\}$ we see, based upon Figure 3.2*c*, that $T_1 = \delta_2^1(p_3)$.

- **Showing T_2 is equal to $\delta_1^2(p_3)$:** We begin by looking at $V_1(p_1) \subset \Delta_1(p_1)$ and at the fiber $F_1(p_1)$ associated to $V_1(p_1)$. When we prolong the fiber space we see that

$$\mathcal{P}^1(F_1(p_1)) = \mathbb{P}V_1 = (0, 0, 0, u, v, [dx : du : dv]) = (0, 0, 0, u, v, [0 : a : b])$$

$$= (0, 0, 0, u, v, [0 : 1 : \tfrac{b}{a}]) = (0, 0, 0, u, v, 0, v_2)$$

where $a, b \in \mathbb{R}$ with $a \neq 0$. Now Δ_2, in a neighborhood of p_2, is given by

$$\Delta_2 = span\left\{u_2 X^{(1)} + \frac{\partial}{\partial u} + v_2\frac{\partial}{\partial v}, \frac{\partial}{\partial u_2}, \frac{\partial}{\partial v_2}\right\}$$

and at the same time $T_{p_2}(\mathcal{P}^1(F_1(p_1))) = span\{\frac{\partial}{\partial u}, \frac{\partial}{\partial v}, \frac{\partial}{\partial v_2}\}$. This gives

$$\delta_1^1(p_2) = \Delta_2(p_2) \cap T_{p_2}(\mathcal{P}^1(F_1(p_1)))$$

and we have in a neighborhood of p_2 that

$$\delta_1^1 = span\left\{u_2 X^{(1)} + \frac{\partial}{\partial u} + v_2\frac{\partial}{\partial v}, \frac{\partial}{\partial v_2}\right\}.$$

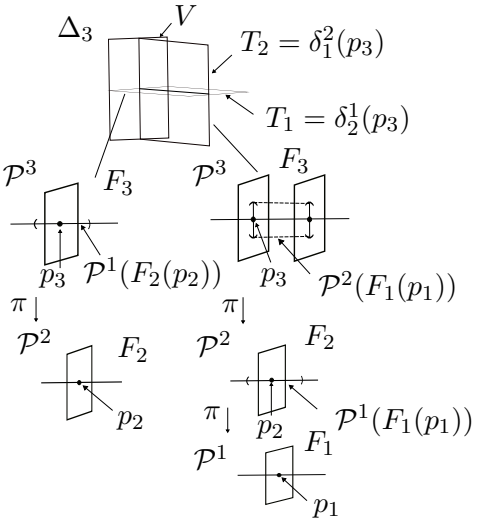

Figure 3.3: Critical hyperplane configuration over $p_3 \in RVL$.

Now, in order to figure out what $\delta_1^2(p_3)$ is we need to prolong the fiber $F_1(p_1)$ twice and then look at the tangent space at the point p_3. We see that

$$\begin{aligned}\mathcal{P}^2(F_1(p_1)) = \mathbb{P}\delta_1^1 &= (0,0,0,u,v,0,v_2,[du : du_2 : dv_2]) \\ &= (0,0,0,u,v,0,v_2,[a:0:b]) \\ &= (0,0,0,u,v,0,v_2,[\tfrac{a}{b}:0:1]) \\ &= (0,0,0,u,v,0,v_2,u_3,0)\end{aligned}$$

then since

$$\delta_1^2(p_3) = \Delta_3(p_3) \cap T_{p_3}(\mathcal{P}^2(F_1(p_1)))$$

with $\Delta_3(p_3) = span\{\frac{\partial}{\partial v_2}, \frac{\partial}{\partial u_3}, \frac{\partial}{\partial v_3}\}$ and $T_{p_3}(\mathcal{P}^2(F_1(p_1))) = span\{\frac{\partial}{\partial u}, \frac{\partial}{\partial v}, \frac{\partial}{\partial v_2}, \frac{\partial}{\partial u_3}\}$ then

$$\delta_1^2(p_3) = span\left\{\frac{\partial}{\partial v_2}, \frac{\partial}{\partial u_3}\right\}$$

and from looking at Figure 3.2*c* one can see that $T_2 = \delta_1^2(p_3)$.

Remark 3.4.3 *The above example, along with Figure 3.3, gives some reasoning for why a critical hyperplane, which is not the vertical one, is called a tangency hyperplane. Also, in Figure 3.3 we have drawn the submanifolds $\mathcal{P}^1(F_2(p_2))$ and $\mathcal{P}^1(F_1(p_1))$ to reflect*

the fact that they have some component which is tangent to the manifolds $\mathcal{P}^3$ and $\mathcal{P}^2$ respectively and that their other component is tangent to the vertical space. At the same time, they are drawn to show the fact that $\mathcal{P}^2(F_1(p_1))$ is tangent to the $\frac{\partial}{\partial u_3}$ direction while $\mathcal{P}^1(F_2(p_2))$ is tangent to the $\frac{\partial}{\partial v_3}$ direction. Another reason for why we use this terminology is because it was first introduced in the context of the $n = 1$ Monster Tower to distinguish those critical directions that were not vertical, and that were actually contained in the tangent bundle of $\mathcal{P}^k(1)$ ([MZ10]).

3.5 Semigroup of a Curve

An important piece of information that we need to present is some terminology relating to curves. Some of the following properties about curve germs are presented in greater detail in [CM12].

Definition 3.5.1 *The order of an analytic curve germ $f(t) = \sum_{i\geq 0} a_i t^i$ is the smallest integer i such that $a_i \neq 0$. We write $ord(f)$ for this (nonegative) integer. The multiplicity of a curve germ $\gamma : (\mathbb{R}, 0) \to (\mathbb{R}^n, 0)$, denoted $mult(\gamma)$, is the minimum of the orders of its coordinate functions $\gamma_i(t)$ relative to any coordinate system vanishing at p.*

Definition 3.5.2 *A curve germ is said to be well parameterized if γ cannot be written in the form $\gamma = \sigma \circ \tau$ where $\tau : (\mathbb{R}, 0) \to (\mathbb{R}, 0)$ with $\tau'(0) = 0$ ([Wal04]).*

Definition 3.5.3 *If $\gamma : (\mathbb{R}, 0) \to (\mathbb{R}^n, 0)$ is a well-parameterized curve germ, then its* semigroup *is the collection of positive integers $ord(P(\gamma(t)))$ as P varies over analytic functions of n variables vanishing at 0.*

Because $\text{ord}(PQ(\gamma(t))) = \text{ord}(P(\gamma(t))) + \text{ord}(Q(\gamma(t)))$ the curve semigroup is indeed an algebraic semigroup, i.e. a subset of $\mathbb{N}$ closed under addition. The semigroup of a well-parameterized curve is a basic diffeomorphism invariant of the curve.

Definition 3.5.4 *(Following Arnol'd from [Arn99], end of introduction) A curve germ γ in $\mathbb{R}^3$ has symbol $[m, n]$, $[m, n, p]$, or $[m, (n, p)]$ if it is equivalent to a curve germ of the form $(t^m, t^n, 0) + O(t^{n+1})$, $(t^m, t^n, t^p) + O(t^{p+1})$, or $(t^m, t^n + t^p, 0) + O(t^{p+1})$ respectively, with $m < n < p$ being positive integers.*

We also impose some restrictions on the symbols in order to insure that the curve is well-parameterized. One restriction is that the integers m, n or m, n, p are relatively prime. The other is that for the length 3 symbols that the final integer p is not in the semigroup generated by m and n.

Remark 3.5.1 *Arnol'd pointed out in [Arn99] that one can use the semigroup of a curve germ as a tool to see if it is RL equivalent to a simpler curve germ. Details and examples about semigroup calculations can be found within [Arn99] as well as in [Wal04]. We do though provide the following short example to help the reader.*

Example 3.5.2 *Let $\gamma_1(t) = (t^3, t^5, t^7)$ and $\gamma_2(t) = (t^3, t^5+t^6+t^8, t^7+t^9)$ be curve germs defined for t in an open interval about zero. Both of the curves γ_1 and γ_2 generate the same semigroup. In this case the semigroup is the set $S = \{3, [4], 5, 6, 7, \cdots\}$ where the binary operation is addition. The numbers 3, 5, 6, and so on are elements of this semigroup while the bracket around the number 4 means that it is not an element of S. When we write "$\cdots$" after the number 7 it means that every positive integer after 7 is an element in our semigroup. Arnol'd points out that the terms in the semigroup tells us which powers of t we can eliminate from the curve. This means that every term, t^i for $i \geq 7$, can be eliminated, except for the t^7 term in the last component function, from the above power series expansion for the component functions $x(t)$, $y(t)$, and $z(t)$ by a change of variables given by $(x, y, z) \mapsto (x + f(x, y, z), y + g(x, y, z), z + h(x, y, z))$. Since the numbers 6, 8, and 9 are included in the semigroup it means that we can use a combination of RL equivalences to kill the t^6 and t^8 terms in the y component and the t^9 term in the z component of γ_2. This means that the curve germs γ_1 and γ_2 are in fact RL equivalent.*

3.5.1 The points-to-curves and back philosophy

The idea is to translate the problem of classifying orbits in the tower (1.0.1) into an equivalent classification problem for finite jets of space curves. Here we are going to mention some highlights of this approach, we will refer the diligent reader to [CM12] check the technical details.

For any $p \in \mathcal{P}^k(n)$ we associate the set $Germ(p)$ and look at the operation of k-fold prolongation applied to curve germs in $Germ(p)$. This yields immersed curves at level k in the Monster Tower, and tangent to some line ℓ having nonconstant projection onto

the base manifold $\mathbb{R}^3$. Such set of *good directions* were christened *regular* in [CM12], and within each subspace Δ_k they form an open dense set. A *bad direction* ℓ_*, or *critical direction* in the terminology of [CM12], are those directions which will project down to a point under the differential of the bundle projection map. The set of critical directions within each Δ_k is a finite union of planes. Symmetries of $\mathcal{P}^k$ do preserve the different types of directions.

In [CM12] it was proved that that $Germ(p)$ is always non-empty. Consider now the set valued map $p \mapsto Germ(p)$. One can prove that $p \sim q$ iff $Germ(p) \sim Germ(q)$. An immediate and yet useful consequence of this fact is the following:

Lemma 3.5.3 (Fundamental lemma of points-to-curves approach) *Let Ω be a subset of $\mathcal{P}^k(n)$ and suppose for each $p \in \Omega$ that* Germ(p) *contains only a finite number of equivalence classes of curve germs. Then the set Ω is comprised of only a finite number of orbits.*

3.6 The Isotropy Method

The last piece of information that we need to present before we begin the proofs section is the isotropy method. This technique is used to classify points at the fourth level of the Monster Tower. This is because the curve approach failed to provide us with nice and clean normal forms for the various RVT classes at the fourth level of the tower. We provide a specific example of how the curve approach breaks down at level 4 in the proofs section. Suppose we want to look at a particular RVT class, at the k-th level, given by ω (a word of length k) and we want to see how many orbits there are. Suppose as well that we understand its projection $\pi_{k,k-1}(\omega)$ one level down, which decomposes into N orbits. Choose representative points p_i, $i = 1, \cdots, N$ for the N orbits in $\pi_{k,k-1}(\omega)$, and consider the group $G_{k-1}(p_i)$ of level $k-1$ symmetries that fix p_i. This group is called the *isotropy group of* p_i. Since elements Φ^{k-1} of the isotropy group fix p_i, their prolongations $\Phi^k = (\Phi^{k-1}, \Phi^{k-1}_*)$ act on the fiber over p_i. Under the action of the isotropy group the fiber decomposes into some number $n_i \geq 1$ (possibly infinite) of orbits. Summing up, we find that ω decomposes into $\sum_{i=1}^{N} n_i \geq N$ orbits. This will tell us how many orbits there are for the class ω.

This is the idea behind the approach (see Figure

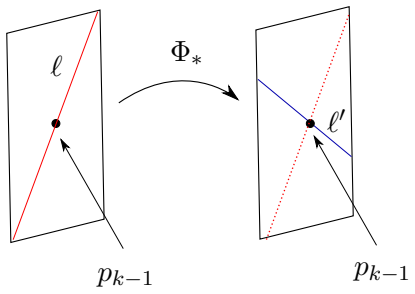

Figure 3.4: The Isotropy Method

This is the theory. Now we need to explain how one actually prolongs diffeomorphisms in practice. Since the manifold $\mathcal{P}^k$ is a type of fiber compactification of $J^k(\mathbb{R}, \mathbb{R}^2)$, it is reasonable to expect that the prolongation of diffeomorphisms from the base $\mathbb{R}^3$ should be similar to what one does when prolonging point symmetries from the theory of jet spaces. See specifically [DZ04] and [Olv93].

Given a point $p_k \in \mathcal{P}^k$ and a map $\Phi \in \mathit{Diff}(3)$ we would like to write explicit formulas for $\Phi^k(p_k)$. Coordinates of p_k can be made explicit. Now take any curve $\gamma(t) \in \mathit{Germ}(p_k)$, and consider the prolongation of $\Phi \circ \gamma(t)$. The coordinates of $\Phi^k(p_k)$ are exactly the coordinates of $(\Phi \circ \gamma)^{(k)}(0) = \Phi^k(\gamma^k(0))$. Moreover the resulting point is independent of the choice of $\gamma \in \mathit{Germ}(p)$ and therefore we can act as if a curve has been chosen when performing actual computations.

Chapter 4

Proofs of Main Results

Now we are ready to prove Theorem 2.1.2. We start at level 1 of the tower and work our way up to level 4. At each level of the tower we classify the number of orbits within each RVT class that appears at that particular level. In this section we show how the various methods and tools from the previous section are used in the classification procedure. Unfortunately we do not have space to present all of the details for the determination of all of orbits within each RVT class at both levels 3 and 4 of the Monster Tower. We will instead present a few instructive examples which will illustrate how the determination of the number of orbits in the remaining classes works.

4.0.1 The classification of points at level 1 and level 2.

Theorem 2.1.4 tells us that all points at the first level of the tower are equivalent, giving that there is a single orbit. For level 2 there are only two possible RVT codes: RR and RV. Again, any point in the class RR is a Cartan point and by Theorem 2.1.4 consists of only one orbit. The class RV consists of a single orbit by Theorem 2.1.5.

4.0.2 The classification of points at level 3.

There is a total of six distinct RVT classes at level three in the Monster Tower. We begin with the class RRR.

The class RRR: Any point within the class RRR is a Cartan point and Theorem 2.1.4 gives that there is only one orbit within this class.

The classes RVR and RRV: From Theorem 2.1.5 we know that any point within the class RVR has a single orbit, which is represented by the point $\gamma^3(0)$ where γ is the curve $\gamma(t) = (t^2, t^3, 0)$. Similarly, the class RRV has a single orbit, which is represented by the point $\tilde{\gamma}^3(0)$ where $\tilde{\gamma}(t) = (t^2, t^5, 0)$.
Before we continue, we need to pause and provide some framework to help us with the classification of the remaining RVT codes.

Setup for classes of the form RVC: We set up coordinates x, y, z, u, v, u_2, v_2 for a point in the class RV as in Section 3.4. Then for $p_2 \in RV$ we have $\Delta_2(p_2) = span\{\frac{\partial}{\partial u}, \frac{\partial}{\partial u_2}, \frac{\partial}{\partial v_2}\}$ where $p_2 = (x, y, z, u, v, u_2, v_2) = (0, 0, 0, 0, 0, 0, 0)$, and for any point $p_3 \in RVC \subset \mathcal{P}^3$ that $p_3 = (p_2, \ell_2) = (p_2, [du|_{\ell_2} : du_2|_{\ell_2} : dv_2|_{\ell_2}])$. Since the point p_2 is in the class RV we see that if $du = 0$ along ℓ_2 then $p_3 \in RVV$. If $du_2 = 0$ with $du \neq 0$ along ℓ_2 then p_3 will be an element of the class RVT, and if $du = 0$ and $du_2 = 0$ along ℓ_2 that $p_3 \in RVL$. With this in mind, we are ready to continue with the classification.

The class RVV: Let $p_3 \in RVV$ and let $\gamma \in Germ(p_3)$. We prolong γ two times and write $\gamma^2(t) = (x(t), y(t), z(t), u(t), v(t), u_2(t), v_2(t))$. We look at the component functions $u(t)$, $u_2(t)$, and $v_2(t)$. Since these component functions are analytic we can set $u(t) = \Sigma_i a_i t^i$, $u_2(t) = \Sigma_j b_j t^j$, and $v_2(t) = \Sigma_k c_k t^k$. We note that the reason for looking only at these terms is because $\delta_2(p_2)$ is spanned by the collection of vectors $\left\{\frac{\partial}{\partial u}, \frac{\partial}{\partial u_2}, \frac{\partial}{\partial v_2}\right\}$. Now, since $\gamma^2(t)$ needs to be tangent to the vertical hyperplane in Δ_3 then $\frac{d}{dt}\gamma^2|_{t=0}$ must be a proper vertical direction in Δ_3; that is $\frac{d}{dt}\gamma^2|_{t=0}$ is not an L direction. Since Δ_3 is coframed by du, du_2, and dv_2, we must have that $du = 0$ and $du_2 \neq 0$ along $\frac{d}{dt}\gamma^2|_{t=0}$. This imposes the condition for the functions $u(t)$ and $u_2(t)$ that $a_1 = 0$ and $b_1 \neq 0$, but the coefficient c_1 in $v_2(t)$ may or may not be zero. Also it must be true that $a_2 \neq 0$ or else the curve γ will not be in the set $Germ(p_3)$. We first look at the case when $c_1 \neq 0$.

- *Case* 1, $c_1 \neq 0$*:* From looking at the one-forms that determine Δ_2, we see that in order for the curve γ^3 to be integral to this distribution, the component functions for γ^3 must satisfy the following relations:

$$\dot{y}(t) = u(t)\dot{x}(t), \dot{z}(t) = v(t)\dot{x}(t)$$

$$\dot{x}(t) = u_2(t)\dot{u}(t), \dot{v}(t) = v_2(t)\dot{u}(t)$$

We start with the expressions for $\dot{x}(t)$ and $\dot{v}(t)$ and see, based upon what we know about $u(t)$, $u_2(t)$, and $v_2(t)$, that $x(t) = \frac{2a_2b_1}{3}t^3 + \dots$ and $v(t) = \frac{2a_2c_1}{3}t^3 + \dots$. We can then use this information to help us find $y(t)$ and $z(t)$. This gives us $y(t) = \frac{2a_2^2b_1}{5}t^5 + \dots$ and $z(t) = \frac{4a_2^2b_1c_1}{3}t^7 + \dots$. Now, we know what the first nonvanishing coefficients are for the curve $\gamma(t) = (x(t), y(t), z(t))$ and we want to determine the simplest curve that γ must be equivalent to. In order to do this we will first look at the semigroup for the curve γ. In this case the semigroup is given by $S = \{3, [4], 5, 6, 7, \cdots\}$.

This means that every term, t^i for $i \geq 7$, can be eliminated from the above power series expansion for the component functions $x(t)$, $y(t)$, and $z(t)$ by a change of variables. With this in mind, after we rescale the leading coefficients for each of the components of γ, we end up with

$$\gamma(t) = (x(t), y(t), z(t)) \sim (\tilde{x}(t), \tilde{y}(t), \tilde{z}(t)) = (t^3 + \alpha t^4, t^5, t^7).$$

We now want to see if we can eliminate the α term, if it is nonzero. To do this we will use a combination of reparametrization techniques along with semigroup arguments. Use the reparametrization $t = T(1 - \frac{\alpha}{3}T)$ and we get that $\tilde{x}(T) = T^3(1 - \frac{\alpha}{3}T)^3 + T^4(1 - \frac{\alpha}{3}T)^4 + \dots = T^3 + O(T^5)$. This gives us that $(\tilde{x}(T), \tilde{y}(T), \tilde{z}(T)) = (T^3 + O(T^5), T^5 + O(T^6), T^7 + O(T^8))$. At the same time we can use the semigroup to eliminate all of the terms of degree 5 or higher. As a result, these arguments show that $(\tilde{x}(T), \tilde{y}(T), \tilde{z}(T)) \sim (T^3, T^5, T^7)$. This means that our original γ is equivalent to the curve (t^3, t^5, t^7).

- *Case* 2, $c_1 = 0$*:* By repeating an argument similar to the above one, we will end up with $\gamma(t) = (x(t), y(t), z(t)) = (\frac{2a_2b_1}{3}t^3 + \dots, \frac{2a_2^2b_1}{5}t^5 + \dots, \frac{a_2^2b_1c_2}{8}t^8 + \dots)$. Note that c_2 may or may not be equal to zero. This gives that the semigroup for the curve γ is $S = \{3, [4], 5, 6, [7], 8 \cdots\}$ and that our curve γ is such that

$$\gamma(t) = (x(t), y(t), z(t)) \sim (\tilde{x}(t), \tilde{y}(t), \tilde{z}(t)) = (t^3 + \alpha_1 t^4 + \alpha_2 t^7, t^5 + \beta t^7, 0)$$

Again, we want to know if we can eliminate the α_i and β terms. First we focus on the α_i terms in $\tilde{x}(t)$. We use the reparametrization given by $t = T(1 - \frac{\alpha_1}{3}T)$ to give us $\tilde{x}(T) = T^3 + \alpha_2' T^7 + O(T^8)$. Then to eliminate the α_2' term we use the reparametrization given by $T = S(1 - \frac{\alpha_2'}{3}S^4)$ to give $\tilde{x}(S) = S^3 + O(S^8)$. We now

turn our attention to the $\tilde{y}$ function. Because of our two reparametrizations we get that $\tilde{y}$ is of the form $\tilde{y}(S) = S^5 + \beta' S^7$. To get rid of the β' term we simply use the rescaling given by $S \mapsto \frac{1}{\sqrt{|\beta'|}} S$ and then use the scaling diffeomorphism given by $(x, y, z) \mapsto (|\beta'|^{\frac{3}{2}} x, |\beta'|^{\frac{5}{2}} y, z)$ to give us that γ is equivalent to either $(t^3, t^5 + t^7, 0)$ or $(t^3, t^5 - t^7, 0)$. Note that the above calculations were done under the assumption that $\beta \neq 0$. If $\beta = 0$ then we see, using similar calculations as above, that we get the normal form $(t^3, t^5, 0)$. This means that there is a total of 4 possible normal forms that represent the points within the class RVV. It is tempting, at first glance, to believe that these curves are all inequivalent. However, it can be shown that the 3 curves $(t^3, t^5 + t^7, 0)$, $(t^3, t^5 - t^7, 0)$, and $(t^3, t^5, 0)$ are actually equivalent. It is not very difficult to show this equivalence, but it does amount to rather messy calculation. *As a result, the techniques used to show this equivalence are outlined in Section 5.3 of the appendix.*

This means that the possible normal forms are: $\gamma_1(t) = (t^3, t^5, t^7)$ and $\gamma_2(t) = (t^3, t^5, 0)$. We will show that these two curves are inequivalent. One possibility is to look at the semigroups that each of these curves generate. The curve γ_1 has the semigroup $S_1 = \{3, [4], 5, 6, 7, \cdots\}$, while the curve γ_2 has the semigroup $S_2 = \{3, [4], 5, 6, [7], 8, \cdots\}$. Since the semigroup of a curve is an invariant of the curve and the two curves generate different semigroups the two curves must be inequivalent. In [CM12] there was another technique used to check and see whether or not these two curves are equivalent. We will now present this alternative of showing that the two curves γ_1 and γ_2 are inequivalent.

One can see that the curve $(t^3, t^5, 0)$ is a planar curve and in order for the curve γ_1 to be equivalent to the curve γ_2 we must be able to find a way to turn γ_1 into a planar curve. More precisely, we need to find a change of variables and/or a reparametrization which will make the third component function of γ_1 zero. If it were true that γ_1 is RL equivalent a planar curve, then γ_1 must lie in an embedded surface in $\mathbb{R}^3$ (or embedded surface germ), say M. This means there exists a local defining function at each point on the manifold M. Let the local defining function near the origin be the real analytic function $f : \mathbb{R}^3 \to \mathbb{R}$. Since γ_1 is on M, then $f(\gamma_1(t)) = 0$ for all t near zero. However, when one looks at the individual terms in the Taylor series expansion of f composed with γ_1 there will be nonzero terms which will show up and give that $f(\gamma_1(t)) \neq 0$ for all t near zero, which creates a contradiction. This tells us that γ_1 cannot be equivalent

to any planar curve near $t = 0$. As a result, there is a total of two inequivalent normal forms for the class RVV: (t^3, t^5, t^7) and $(t^3, t^5, 0)$. When we prolong γ_1 and γ_2 to the third level in the tower we end up with $\gamma_1^3(0) = \gamma_2^3(0)$, which means that there is only one orbit within the class RVV.

The remaining classes RVT and RVL are proved in an almost identical manner using the above ideas and techniques. As a result, we will omit the proofs and leave them to the reader.

With this in mind, we are now ready to move on to the fourth level of the tower. We initially tried to tackle the problem of classifying the orbits at the fourth level by using the curve approach from the third level. Unfortunately, the curve approach became a bit too unwieldy to determine what the normal forms were for the various RVT classes. The problem was simply this: when we looked at the semigroup for a particular curve in a number of the RVT classes at the fourth level, there were too many *gaps* corresponding semigroup. The first occurring class, according to codimension, in which this occurred was the class $RVVV$. This turns the equivalence problem of curve germs computationally hard.

Example 4.0.1 (The semigroups for the class $RVVV$) *Let $p_4 \in RVVV$, and for $\gamma \in Germ(p_4)$ let $\gamma^3(t) = (x(t), y(t), z(t), u(t), v(t), u_2(t), v_2(t), u_3(t), v_3(t))$ with $u = \frac{dy}{dx}$, $v = \frac{dz}{dx}$, $u_2 = \frac{dx}{du}$, $v_2 = \frac{dv}{du}$, $u_3 = \frac{du}{du_2}$, $v_3 = \frac{dv_2}{du_2}$. Since $\gamma^4(0) = p_4$ we must have that $\gamma^3(t)$ is tangent to the vertical hyperplane within Δ_3, which is coframed by $\{du_2, du_3, dv_3\}$. One can see that $du_2 = 0$ along $\frac{d}{dt}\gamma^3|_{t=0}$. Then, looking at the relevant component functions at the fourth level, we set $u_2(t) = \Sigma_i a_i t^i$, $u_3(t) = \Sigma_j b_j t^j$, $v_3(t) = \Sigma_k c_k t^k$ where we must have $a_1 = 0$, $a_2 \neq 0$, $b_1 \neq 0$, and c_1 may or may not be equal to zero. When we go from the fourth level back down to level zero we end up with $\gamma(t) = (t^5 + O(t^{11}), t^8 + O(t^{11}), O(t^{11}))$. If $c_1 \neq 0$, then we get $\gamma_1(t) = (t^5 + O(t^{12}), t^8 + O(t^{12}), t^{11} + O(t^{12}))$ and the semigroup for this curve is $S = \{5, [6], [7], 8, [9], 10, 11, [12], 13, [14], 15, 16, [17], 18 \cdots\}$. If $c_1 \neq 0$, then we get $\gamma_2(t) = (t^5 + O(t^{12}), t^8 + O(t^{12}), O(t^{12}))$ and the semigroup for this curve is $S = \{5, [6], [7], 8, [9], 10, [11], [12], 13, [14], 15, 16, [17], 18, [19], 20, 21, [22], 23 \cdots\}$. This shows there is a larger number of gaps in our semigroups and meant that we could not eliminate the various terms as easily in the various component functions of γ_1 and γ_2. As a result, it became impractical to work strictly using the curve approach. This meant that we had to look at a different approach to the classification problem. These*

types of issues are why we needed to develop a new approach and lead us to work with the isotropy method.

4.0.3 The classification of points at level 4.

In classifying the points within the fourth level of the Monster Tower we worked almost exclusively with the isotropy method. While this method proved to be very effective in determining the number of orbits, we unfortunately do not present all of the calculations using this technique. This is because the calculations can be lengthy and because of how many different possible RVT codes there are at level 4. So we will present the proof for the classification of the class $RVVV$ as an example of how the isotropy method works.

The class RVVV. Before we get started, we will summarize the main idea of the following calculation. Our goal is to determine the number of orbits within the class $RVVV$. Let $p_4 \in RVVV \subset \mathcal{P}^4$ and start with the projection of p_4 to level zero, $\pi_{4,0}(p_4) = p_0$. Since all of the points at level zero are equivalent, then one is free to choose any representative for p_0. For simplicity, it is easiest to choose it to be the point $p_0 = \mathbf{0}$ and fix coordinates there. Next, we look at all of the points at the first level, which project to p_0. Since all of these points at level 1 are equivalent it means that there is a single orbit in the first level and we are again able to choose any point in $\mathcal{P}^1$ as our representive so long as it projects to the point p_0. We will pick $p_1 = (0, 0, 0, [1 : 0 : 0]) = (0, 0, 0, 0, 0)$ with $u = \frac{dy}{dx}$ and $v = \frac{dz}{dx}$, and we will look at all of the diffeomorphisms Φ that fix the point p_0 and satisfying $\Phi_*([1 : 0 : 0]) = [1 : 0 : 0]$. Note, by an abuse of notation, that when we write "$\Phi_*([1 : 0 : 0]) = [1 : 0 : 0]$" we mean the pushforward of Φ, at the point p_0, which fixes the line $span\{\frac{\partial}{\partial x}\}$ in $\Delta_0(p_0)$. This condition will place some restrictions on the component functions of the diffeomorphism germs Φ in $Diff_0(3)$ when we evaluate at the the point p_0 and tell us what $\Phi^1 = (\Phi, \Phi_*)$ will look like at the point p_1. We call this group of diffeomorphisms G_1. We can then move on to the second level and look at the class RV. Any $p_2 \in RV$ is of the form $p_2 = (p_1, \ell_1)$ with ℓ_1 contained in the vertical hyperplane inside of $\Delta_1(p_1)$. Now, apply the pushforwards of the Φ^1's in G_1 to the vertical hyperplane and see if these symmetries will act transitively on the critical hyperplane. If they do act transitively then there is a single orbit within the class RV. If not, then there exists more than one orbit within the class RV. We then count the number of different equivalence classes

there are within this hyperplane and that number tells us how many orbits there are within that class. Again, we want to point out that there could be an infinite number of equivalence classes. Note that because of Theorem 2.1.5, we should expect to only see one orbit within this class. Once this is done, we can just iterate the above process to classify the number of orbits within the class RVV at the third level and then within the class $RVVV$ at the fourth level.

- *Level 0:* Let G_0 $(= \mathit{Diff}_0(3))$ be the group of all diffeomorphism germs that fix the origin.

- *Level 1:* We know that all the points in $\mathcal{P}^1$ are equivalent, thus there is only a single orbit. So we pick a representative element from the single orbit of $\mathcal{P}^1$. We will take our representative to be $p_1 = (0,0,0,0,0) = (0,0,0,[1:0:0]) = (x,y,z,[dx:dy:dz])$ and take G_1 to be the set of all $\Phi \in G_0$ such that Φ^1 will take the lines tangent to the x-axis back to the x-axis, meaning $\Phi_*([1:0:0]) = [1:0:0]$.

  Then for $\Phi \in G_1$ and $\Phi(x,y,z) = (\phi^1(x,y,z), \phi^2(x,y,z), \phi^3(x,y,z))$ we must have

$$\Phi_* = \begin{pmatrix} \phi^1_x & \phi^1_y & \phi^1_z \\ \phi^2_x & \phi^2_y & \phi^2_z \\ \phi^3_x & \phi^3_y & \phi^3_z \end{pmatrix} = \begin{pmatrix} \phi^1_x & \phi^1_y & \phi^1_z \\ 0 & \phi^2_y & \phi^2_z \\ 0 & \phi^3_y & \phi^3_z \end{pmatrix}$$

  when we evalutate at $(x,y,z) = (0,0,0)$.

  Here is the *Taylor triangle* representing the different coefficients in the Taylor series of a diffeomorphism in G_i. The three digits represent the number of partial derivatives with respect to either x, y, or z. For example, $(1,2,0) = \frac{\partial^3}{\partial x \partial^2 y}$. The vertical column denotes the coefficient order. We start with the Taylor triangle for ϕ^2:

$n=0$:			~~(0,0,0)~~			
$n=1$:		~~(1,0,0)~~	(0,1,0)	(0,0,1)		
$n=2$:	(2,0,0)	(1,1,0)	(1,0,1)	(0,2,0)	(0,1,1)	(0,0,2)

We have crossed out $(1,0,0)$ since $\frac{\partial \phi^2}{\partial x}(\mathbf{0}) = 0$. Next is the Taylor triangle for ϕ^3:

$n=0$:			~~(0,0,0)~~			
$n=1$:		~~(1,0,0)~~	(0,1,0)	(0,0,1)		
$n=2$:	(2,0,0)	(1,1,0)	(1,0,1)	(0,2,0)	(0,1,1)	(0,0,2)

This describes some properties of the elements $\Phi \in G_1$.

We now try to figure out what Φ^1, for $\Phi \in G_1$, will look like in KR-coordinates. First, we look at a line $\ell \subset \Delta_0$ and write $\ell = span\{a\frac{\partial}{\partial x} + b\frac{\partial}{\partial y} + c\frac{\partial}{\partial z}\}$ with $a, b, c \in \mathbb{R}$ and $a \neq 0$.

Applying the pushforward of Φ to the line ℓ we get

$$\begin{aligned}
\Phi_*(\ell) &= span\left\{(a\phi^1_x + b\phi^1_y + c\phi^1_z)\frac{\partial}{\partial x} + (a\phi^2_x + b\phi^2_y + c\phi^2_z)\frac{\partial}{\partial y} + (a\phi^3_x + b\phi^3_y + c\phi^3_z)\frac{\partial}{\partial z}\right\} \\
&= span\left\{(\phi^1_x + u\phi^1_y + v\phi^1_z)\frac{\partial}{\partial x} + (\phi^2_x + u\phi^2_y + v\phi^2_z)\frac{\partial}{\partial y} + (\phi^3_x + u\phi^3_y + v\phi^3_z)\frac{\partial}{\partial z}\right\} \\
&= span\left\{a_1\frac{\partial}{\partial x} + a_2\frac{\partial}{\partial y} + a_3\frac{\partial}{\partial z}\right\}
\end{aligned}$$

where in the second line we divided by a and wrote $u = \frac{b}{a}$ and $v = \frac{c}{a}$. Now, since Δ_1 is given by

$$\begin{aligned}
dy - udx &= 0 \\
dz - vdx &= 0.
\end{aligned}$$

Since $[dx : dy : dz] = [1 : \frac{dy}{dx} : \frac{dz}{dx}]$ we have for $\Phi \in G_1$ we write Φ^1 in local coordinates as $\Phi^1(x, y, z, u, v) = (\phi^1, \phi^2, \phi^3, \tilde{u}, \tilde{v})$ where

$$\begin{aligned}
\tilde{u} &= \frac{a_2}{a_1} = \frac{\phi^2_x + u\phi^2_y + v\phi^2_z}{\phi^1_x + u\phi^1_y + v\phi^1_z} \\
\tilde{v} &= \frac{a_3}{a_1} = \frac{\phi^3_x + u\phi^3_y + v\phi^3_z}{\phi^1_x + u\phi^1_y + v\phi^1_z}.
\end{aligned}$$

- *Level* 2*:* At level 2 we are looking at the class RV which consists of a single orbit by Theorem 2.1.5. This means that we can pick any point in the class RV as our representative. We will pick our point to be $p_2 = (p_1, \ell_1)$ with $\ell_1 \subset \Delta_1(p_1)$ equal to the vertical line $\ell_1 = [dx : du : dv] = [0 : 1 : 0]$. Now, we will let G_2 be the set of symmetries from G_1 that fix the vertical line $\ell_1 = [0 : 1 : 0]$ in $\Delta_1(p_1)$, those satisfying $\Phi^1_*([0 : 1 : 0]) = [0 : 1 : 0]$ for all $\Phi \in G_2$. This implies $\Phi^1_*([dx|_{\ell_1} : du|_{\ell_1} : dv|_{\ell_1}]) = \Phi^1_*([0 : 1 : 0]) = [0 : 1 : 0] = [d\phi^1|_{\ell_1} : d\tilde{u}|_{|\ell_1} : d\tilde{v}|_{|\ell_1}]$. When we fix this direction it might yield some new information about the component functions of the elements of G_2. In particular, we need to set $d\phi^1|_{\ell_1} = 0$ and $d\tilde{v}|_{\ell_1} = 0$.

  • Looking at the restriction $d\phi^1|_{\ell_1} = 0$.

  One has $d\phi^1 = \phi^1_x dx + \phi^1_y dy + \phi^1_z dz$ and when we set $d\phi^1|_{\ell_1} = 0$ we can see that we will not gain any new information about the component functions for $\Phi \in G_2$. This is because the covectors dx, dy, and dz will be zero along the line ℓ_1.

  • Looking at the restriction $d\tilde{v}|_{\ell_1} = 0$

  Can see that $d\tilde{v} = d(\frac{a_3}{a_1}) = \frac{da_3}{a_1} - \frac{(da_1)a_3}{a_1^2}$ and notice when we evaluate at $(x, y, z, u, v) = (0, 0, 0, 0, 0)$, we have $a_3 = 0$, and since we are setting $d\tilde{v}|_{\ell_1} = 0$ then $da_3|_{\ell_1}$ must be equal to zero. We calculate that

$$da_3 = \phi^3_{xx} dx + \phi^3_{xy} dy + \phi^3_{xz} dz + \phi^3_y du + u(d\phi^3_y) + \phi^3_z dv + v(d\phi^3_z)$$

  and when we evaluate we get

$$da_3|_{\ell_1} = \phi^3_y(\mathbf{0}) du|_{\ell_1} = 0.$$

  But $du|_{\ell_1} \neq 0$, so $\phi^3_y(\mathbf{0}) = 0$.

  This gives us the updated Taylor triangle for ϕ^3:

$n = 0$:			~~(0,0,0)~~			
$n = 1$:		~~(1,0,0)~~	~~(0,1,0)~~	(0,0,1)		
$n = 2$:	(2,0,0)	(1,1,0)	(1,0,1)	(0,2,0)	(0,1,1)	(0,0,2)

We have determined some of the properties of elements in G_2 and now we will see what these elements look like locally. We look at a point p_1' near the point p_1 and at $\Phi_*^1(\ell)$ for $\ell \subset \Delta_1(p_1')$, near the vertical hyperplane in $\Delta_1(p_1')$, which is of the form $\ell = span\{aX^{(1)} + b\frac{\partial}{\partial u} + c\frac{\partial}{\partial v}\}$ with $a, b, c \in \mathbb{R}$ and $b \neq 0$ with $X^{(1)} = u\frac{\partial}{\partial y} + v\frac{\partial}{\partial z} + \frac{\partial}{\partial x}$. Let $\mathbf{w} = aX^{(1)} + b\frac{\partial}{\partial u} + c\frac{\partial}{\partial v}$ and we apply Φ_*^1 to $\mathbf{w}$ to get

$$\Phi_*^1(\mathbf{w}) = \begin{pmatrix} \phi_x^1 & \phi_y^1 & \phi_z^1 & 0 & 0 \\ \phi_x^2 & \phi_y^2 & \phi_z^2 & 0 & 0 \\ \phi_x^3 & \phi_y^3 & \phi_z^3 & 0 & 0 \\ \frac{\partial \tilde{u}}{\partial x} & \frac{\partial \tilde{u}}{\partial y} & \frac{\partial \tilde{u}}{\partial z} & \frac{\partial \tilde{u}}{\partial u} & \frac{\partial \tilde{u}}{\partial v} \\ \frac{\partial \tilde{v}}{\partial x} & \frac{\partial \tilde{v}}{\partial y} & \frac{\partial \tilde{v}}{\partial z} & \frac{\partial \tilde{v}}{\partial u} & \frac{\partial \tilde{v}}{\partial v} \end{pmatrix} \begin{pmatrix} a \\ au \\ av \\ b \\ c \end{pmatrix}$$

$$\begin{aligned} = \quad & (a\phi_x^1 + au\phi_y^1 + av\phi_z^1)\frac{\partial}{\partial x} \\ + \quad & (a\frac{\partial \tilde{u}}{\partial x} + au\frac{\partial \tilde{u}}{\partial y} + av\frac{\partial \tilde{u}}{\partial z} + b\frac{\partial \tilde{u}}{\partial u} + c\frac{\partial \tilde{u}}{\partial v})\frac{\partial}{\partial u} \\ + \quad & (a\frac{\partial \tilde{v}}{\partial x} + au\frac{\partial \tilde{v}}{\partial y} + av\frac{\partial \tilde{v}}{\partial z} + b\frac{\partial \tilde{v}}{\partial u} + c\frac{\partial \tilde{v}}{\partial v})\frac{\partial}{\partial v} \end{aligned}$$

This means that when we look at Φ_*^1 applied to the line ℓ we get

$$\begin{aligned} \Phi_*^1(\ell) \quad = \quad & span\{(a\phi_x^1 + au\phi_y^1 + av\phi_z^1)\frac{\partial}{\partial x} \\ + \quad & (a\frac{\partial \tilde{u}}{\partial x} + au\frac{\partial \tilde{u}}{\partial y} + av\frac{\partial \tilde{u}}{\partial z} + b\frac{\partial \tilde{u}}{\partial u} + c\frac{\partial \tilde{u}}{\partial v})\frac{\partial}{\partial u} \\ + \quad & (a\frac{\partial \tilde{v}}{\partial x} + au\frac{\partial \tilde{v}}{\partial y} + av\frac{\partial \tilde{v}}{\partial z} + b\frac{\partial \tilde{v}}{\partial u} + c\frac{\partial \tilde{v}}{\partial v})\frac{\partial}{\partial v}\} \end{aligned}$$

$$\begin{aligned} = \quad & span\{(u_2\phi_x^1 + uu_2\phi_y^1 + vu_2\phi_z^1)\frac{\partial}{\partial x} \\ + \quad & (u_2\frac{\partial \tilde{u}}{\partial x} + uu_2\frac{\partial \tilde{u}}{\partial y} + vu_2\frac{\partial \tilde{u}}{\partial z} + \frac{\partial \tilde{u}}{\partial u} + v_2\frac{\partial \tilde{u}}{\partial v})\frac{\partial}{\partial u} \\ + \quad & (u_2\frac{\partial \tilde{v}}{\partial x} + uu_2\frac{\partial \tilde{v}}{\partial y} + vu_2\frac{\partial \tilde{v}}{\partial z} + \frac{\partial \tilde{v}}{\partial u} + v_2\frac{\partial \tilde{v}}{v})\frac{\partial}{\partial v}\} \end{aligned}$$

$= span\{b_1\frac{\partial}{\partial x} + b_2\frac{\partial}{\partial u} + b_3\frac{\partial}{\partial v}\}$. Notice that we have only paid attention to the x, u, and v coordinates since Δ_1 is framed by dx, du, and dv. Since $u_2 = \frac{dx}{du}$ and $v_2 = \frac{dv}{du}$ we get

$$\tilde{u}_2 = \frac{b_1}{b_2} = \frac{u_2\phi_x^1 + uu_2\phi_y^1 + vu_2\phi_z^1}{u_2\frac{\partial\tilde{u}}{\partial x} + uu_2\frac{\partial\tilde{u}}{\partial y} + vu_2\frac{\partial\tilde{u}}{\partial z} + \frac{\partial\tilde{u}}{\partial u} + v_2\frac{\partial\tilde{u}}{\partial v}}$$

$$\tilde{v}_2 = \frac{b_3}{b_2} = \frac{u_2\frac{\partial\tilde{v}}{\partial x} + uu_2\frac{\partial\tilde{v}}{\partial y} + vu_2\frac{\partial\tilde{v}}{\partial z} + \frac{\partial\tilde{v}}{\partial u} + v_2\frac{\partial\tilde{v}}{\partial v}}{u_2\frac{\partial\tilde{u}}{\partial x} + uu_2\frac{\partial\tilde{u}}{\partial y} + vu_2\frac{\partial\tilde{u}}{\partial z} + \frac{\partial\tilde{u}}{\partial u} + v_2\frac{\partial\tilde{u}}{\partial v}}$$

The above equations now tell us what the new component functions $\tilde{u}_2$ and $\tilde{v}_2$ are for Φ^2 in a neighborhood of p_2.

- *Level* 3*:* At level 3 we are looking at the class RVV. We know from our work on the third level that there will be only one orbit within this class. This means that we can pick any point in the class RVV as our representative. We will pick the point $p_3 = (p_2, \ell_2)$ with $\ell_2 \subset \Delta_2$ equal to the vertical line $\ell_2 = [du : du_2 : dv_2] = [0 : 1 : 0]$. Now, we will let G_3 be the set of symmetries from G_2 that fix the vertical line $\ell_2 = [0 : 1 : 0]$ in Δ_2, meaning we want $\Phi_*^2([0 : 1 : 0]) = [0 : 1 : 0] = [d\tilde{u}|_{\ell_3} : d\tilde{u}_2|_{\ell_3} : d\tilde{v}_2|_{\ell_3}]$ for all $\Phi \in G_3$. Since we are taking $du|_{\ell_3}0$ and $dv_2|_{\ell_3} = 0$, with $du_2|_{\ell_3} \neq 0$ we need to look at $d\tilde{u}|_{\ell_3} = 0$ and $d\tilde{v}_2|_{\ell_3} = 0$ to see if these relations will give us more information about the component functions of Φ.

  • Looking at the restriction $d\tilde{u}|_{\ell_3} = 0$

  Looking at $d\tilde{u} = d(\frac{a_2}{a_1}) = \frac{da_2}{a_1} - \frac{a_2 da_1}{a_1^2}$ and since $a_2(p_2) = 0$, we must have $da_2|_{\ell_3} = 0$. When we evaluate this expression one finds

  $da_2|_{\ell_3} = \phi_{xx}^2 dx|_{\ell_3} + \phi_{xy}^2 dy|_{\ell_3} + \phi_{xz}^2 dz|_{\ell_3} + \phi_y^2 du|_{\ell_3} + \phi_z^2 dv|_{\ell_3} = 0$. Since all of the differentials are going to be equal to zero when we evaluate them along the line ℓ_3 then we do not gain any new information about the ϕ^i's.

  • Looking at the restriction $d\tilde{v}_2|_{\ell_3} = 0$

  $d\tilde{v}_2 = d(\frac{b_3}{b_2}) = \frac{db_3}{b_2} - \frac{b_3 db_2}{b_2^2}$. Evaluating we find $b_3(p_2) = 0$ since $\frac{\partial\tilde{v}}{\partial u}(p_2) = \phi_y^3(\mathbf{0}) = 0$,

which implies that we only need to look at $\frac{db_3}{b_2}$. We compute

$$\begin{aligned} db_3 &= d(u_2\frac{\partial\tilde{v}}{\partial x} + u_2u\frac{\partial\tilde{v}}{\partial z} + \frac{\partial\tilde{v}}{\partial u} + v_2\frac{\partial\tilde{v}}{\partial v}) \\ &= \frac{\partial\tilde{v}}{\partial x}du_2 + u_2(d\frac{\partial\tilde{v}}{\partial x}) + u\frac{\partial\tilde{v}}{\partial y}du_2 \\ &+ u_2\frac{\partial\tilde{v}}{\partial y}du + u_2u(d\frac{\partial\tilde{v}}{\partial y}) + v\frac{\partial\tilde{v}}{\partial z}du_2 \\ &+ u_2\frac{\partial\tilde{v}}{\partial z}dv + u_2v(d\frac{\partial\tilde{v}}{\partial z}) + \frac{\partial\tilde{v}}{\partial u\partial x}dx \\ &+ \frac{\partial\tilde{v}}{\partial u\partial y}dy + \frac{\partial\tilde{u}}{\partial u\partial z}dz + \frac{\partial\tilde{v}}{\partial v}dv_2 + v_2(d\frac{\partial\tilde{v}}{\partial v}). \end{aligned}$$

Evaluating we get $db_3|_{\ell_3} = \frac{\partial\tilde{v}}{\partial x}(p_3)du_2|_{\ell_3} = 0$, and since $du_2|_{\ell_3} \neq 0$ this forces $\frac{\partial\tilde{v}}{\partial x}(p_3) = 0$. We have $\frac{\partial\tilde{v}}{\partial x}(p_3) = \frac{\phi^3_{xx}(\mathbf{0})}{\phi^1_x(\mathbf{0})} - \frac{\phi^1_{xx}(\mathbf{0})\phi^3_x(\mathbf{0})}{\phi^1_x(\mathbf{0})}$ and $\phi^3_x(\mathbf{0}) = 0$, which give $\frac{\partial\tilde{v}}{\partial x}(p_3) = \frac{\phi^3_{xx}(\mathbf{0})}{\phi^1_x(\mathbf{0})} = 0$ which forces $\phi^3_{xx}(\mathbf{0}) = 0$. This gives us information about Φ^3 along with the updated Taylor triangle for ϕ^3:

$n=0$:			~~(0,0,0)~~			
$n=1$:		~~(1,0,0)~~	~~(0,1,0)~~	(0,0,1)		
$n=2$:	~~(2,0,0)~~	(1,1,0)	(1,0,1)	(0,2,0)	(0,1,1)	(0,0,2)

Now, our goal is to look at how the Φ^3_*'s act on the distribution $\Delta_3(p_3)$ in order to determine the number of orbits within the class $RVVV$. In order to do so we will need to figure out what the local component functions, call them $\tilde{u}_3$ and $\tilde{v}_3$, are for Φ^3, with $\Phi \in G_3$. To do this we will again look at Φ^2_* applied to a line ℓ that is near the vertical hyperplane in Δ_2.

Set $\ell = span\{aX^{(2)} + b\frac{\partial}{\partial u_2} + c\frac{\partial}{\partial v_2}\}$ for $a, b, c \in \mathbb{R}$ and $b \neq 0$ where $X^{(2)} = u_2(u\frac{\partial}{\partial y} + v\frac{\partial}{\partial z} + \frac{\partial}{\partial x}) + \frac{\partial}{\partial u} + v_2\frac{\partial}{\partial v}$. Let $\mathbf{w} = aX^{(2)} + b\frac{\partial}{\partial u_2} + c\frac{\partial}{\partial v_2}$ and we compute

$$\Phi^2_*(\mathbf{w}) = \begin{pmatrix} \phi^1_x & \phi^1_y & \phi^1_z & 0 & 0 & 0 & 0 \\ \phi^2_x & \phi^2_y & \phi^2_z & 0 & 0 & 0 & 0 \\ \phi^3_x & \phi^3_y & \phi^3_z & 0 & 0 & 0 & 0 \\ \frac{\partial \tilde{u}}{\partial x} & \frac{\partial \tilde{u}}{\partial y} & \frac{\partial \tilde{u}}{\partial z} & \frac{\partial \tilde{u}}{\partial u} & \frac{\partial \tilde{u}}{\partial v} & 0 & 0 \\ \frac{\partial \tilde{v}}{\partial x} & \frac{\partial \tilde{v}}{\partial y} & \frac{\partial \tilde{v}}{\partial z} & \frac{\partial \tilde{v}}{\partial u} & \frac{\partial \tilde{v}}{\partial v} & 0 & 0 \\ \frac{\partial \tilde{u}_2}{\partial x} & \frac{\partial \tilde{u}_2}{\partial y} & \frac{\partial \tilde{u}_2}{\partial z} & \frac{\partial \tilde{u}_2}{\partial u} & \frac{\partial \tilde{u}_2}{\partial v} & \frac{\partial \tilde{u}_2}{\partial u_2} & \frac{\partial \tilde{u}_2}{\partial v_2} \\ \frac{\partial \tilde{v}_2}{\partial x} & \frac{\partial \tilde{v}_2}{\partial y} & \frac{\partial \tilde{v}_2}{\partial z} & \frac{\partial \tilde{v}_2}{\partial u} & \frac{\partial \tilde{v}_2}{\partial v} & \frac{\partial \tilde{v}_2}{\partial u_2} & \frac{\partial \tilde{v}_2}{\partial v_2} \end{pmatrix} \begin{pmatrix} au_2 \\ auu_2 \\ avu_2 \\ a \\ av_2 \\ b \\ c \end{pmatrix}$$

Then for Φ^2_* applied to the line ℓ we end up with it being equal to

$$\begin{aligned} &span\{(au_2\frac{\partial \tilde{u}}{\partial x} + auu_2\frac{\partial \tilde{u}}{\partial y} + avu_2\frac{\partial \tilde{u}}{\partial z} + a\frac{\partial \tilde{u}}{\partial u} + av_2\frac{\partial \tilde{u}}{\partial v})\frac{\partial}{\partial u} \\ &+ (au_2\frac{\partial \tilde{u}_2}{\partial x} + auu_2\frac{\partial \tilde{u}_2}{\partial y} + avu_2\frac{\partial \tilde{u}_2}{\partial z} + a\frac{\partial \tilde{u}_2}{\partial u} + av_2\frac{\partial \tilde{u}_2}{\partial v} + b\frac{\partial \tilde{u}_2}{\partial u_2} + c\frac{\partial \tilde{u}_2}{\partial v_2})\frac{\partial}{\partial u_2} \\ &+ (au_2\frac{\partial \tilde{v}_2}{\partial x} + auu_2\frac{\partial \tilde{v}_2}{\partial y} + avu_2\frac{\partial \tilde{v}_2}{\partial z} + a\frac{\partial \tilde{v}_2}{\partial u} + av_2\frac{\partial \tilde{v}_2}{\partial v} + b\frac{\partial \tilde{v}_2}{\partial u_2} + c\frac{\partial \tilde{v}_2}{\partial v_2})\frac{\partial}{\partial v_2}\} \\ &= span\{(u_3u_2\frac{\partial \tilde{u}}{\partial x} + u_3uu_2\frac{\partial \tilde{u}}{\partial y} + u_3vu_2\frac{\partial \tilde{u}}{\partial z} + u_3\frac{\partial \tilde{u}}{\partial u} + u_3v_2\frac{\partial \tilde{u}}{\partial v})\frac{\partial}{\partial u} \\ &+ (u_3u_2\frac{\partial \tilde{u}_2}{\partial x} + u_3uu_2\frac{\partial \tilde{u}_2}{\partial y} + u_3vu_2\frac{\partial \tilde{u}_2}{\partial z} + u_3\frac{\partial \tilde{u}_2}{\partial u} + u_3v_2\frac{\partial \tilde{u}_2}{\partial v} + \frac{\partial \tilde{u}_2}{\partial u_2} + v_3\frac{\partial \tilde{u}_2}{\partial v_2})\frac{\partial}{\partial u_2} \\ &+ u_3u_2\frac{\partial \tilde{v}_2}{\partial x} + u_3uu_2\frac{\partial \tilde{v}_2}{\partial y} + u_3vu_2\frac{\partial \tilde{v}_2}{\partial z} + u_3\frac{\partial \tilde{v}_2}{\partial u} + u_3v_2\frac{\partial \tilde{v}_2}{\partial v} + \frac{\partial \tilde{v}_2}{\partial u_2} + v_3\frac{\partial \tilde{v}_2}{\partial v_2})\frac{\partial}{\partial v_2}\} \\ &= span\{c_1\frac{\partial}{\partial u} + c_2\frac{\partial}{\partial u_2} + c_3\frac{\partial}{\partial v_2}\}, \end{aligned}$$

because our local coordinates are given by $[du : du_2 : dv_2] = [\frac{du}{du_2} : 1 : \frac{dv_2}{du_2}] = [u_3 : 1 : v_3]$ we end up with

$$\tilde{u}_3 = \frac{c_1}{c_2} = \frac{u_3u_2\frac{\partial \tilde{u}}{\partial x} + u_3uu_2\frac{\partial \tilde{u}}{\partial y} + u_3vu_2\frac{\partial \tilde{u}}{\partial z} + u_3\frac{\partial \tilde{u}}{\partial u} + u_3v_2\frac{\partial \tilde{u}}{\partial v}}{u_3u_2\frac{\partial \tilde{u}_2}{\partial x} + u_3uu_2\frac{\partial \tilde{u}_2}{\partial y} + u_3vu_2\frac{\partial \tilde{u}_2}{\partial z} + u_3\frac{\partial \tilde{u}_2}{\partial u} + u_3v_2\frac{\partial \tilde{u}_2}{\partial v} + \frac{\partial \tilde{u}_2}{\partial u_2} + v_3\frac{\partial \tilde{u}_2}{\partial v_2}}$$

$$\tilde{v}_3 = \frac{c_3}{c_2} = \frac{u_3u_2\frac{\partial \tilde{v}_2}{\partial x} + u_3uu_2\frac{\partial \tilde{v}_2}{\partial y} + u_3vu_2\ \frac{\partial \tilde{v}_2}{\partial z} + u_3\frac{\partial \tilde{v}_2}{\partial u} + u_3v_2\frac{\partial \tilde{v}_2}{\partial v} + \frac{\partial \tilde{v}_2}{\partial u_2} + v_3\frac{\partial \tilde{v}_2}{\partial v_2}}{u_3u_2\frac{\partial \tilde{u}_2}{\partial x} + u_3uu_2\frac{\partial \tilde{u}_2}{\partial y} + u_3vu_2\frac{\partial \tilde{u}_2}{\partial z} + u_3\frac{\partial \tilde{u}_2}{\partial u} + u_3v_2\frac{\partial \tilde{u}_2}{\partial v} + \frac{\partial \tilde{u}_2}{\partial u_2} + v_3\frac{\partial \tilde{u}_2}{\partial v_2}}.$$

- *Level* 4*:* Now that we know what the component functions are for Φ^3, with $\Phi \in G_3$, we are ready to apply its pushforward to the distribution Δ_3 at p_3 and figure out how many orbits there are for the class $RVVV$. We let $\ell = span\{b\frac{\partial}{\partial u_3} + c\frac{\partial}{\partial v_3}\}$,

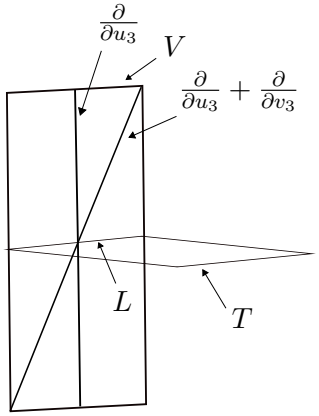

Figure 4.1: Orbits within the class $RVVV$.

with $b, c \in \mathbb{R}$ and $b \neq 0$, be a vector in the vertical hyperplane of $\Delta_3(p_3)$ and we see that

$$\Phi^3_*(\ell) = span\left\{(b\frac{\partial \tilde{u}_3}{\partial u_3}(p_3) + c\frac{\partial \tilde{u}_3}{\partial v_3}(p_3))\frac{\partial}{\partial u_3} + (b\frac{\partial \tilde{v}_3}{\partial u_3}(p_3) + c\frac{\partial \tilde{v}_3}{\partial v_3}(p_3))\frac{\partial}{\partial v_3}\right\}.$$

This means that we need to compute $\frac{\partial \tilde{u}_3}{\partial u_3}(p_3)$, $\frac{\partial \tilde{u}_3}{\partial v_3}(p_3)$, $\frac{\partial \tilde{v}_3}{\partial u_3}(p_3)$, and $\frac{\partial \tilde{v}_3}{\partial v_3}(p_3)$ where $p_3 = (x, y, z, u, v, u_2, v_2, u_3, v_3) = (0, 0, 0, 0, 0, 0, 0, 0, 0)$. This will amount to a somewhat long process, so we will just state what the above terms are equal to *and leave the computations for the appendix.* After evaluating we will see that $\Phi^3_*(\ell) = span\left\{(b\frac{(\phi^2_y(\mathbf{0}))^2}{(\phi^1_x(\mathbf{0}))^3})\frac{\partial}{\partial u_3} + (c\frac{\phi^3_z(\mathbf{0})}{(\phi^1_x(\mathbf{0}))^2})\frac{\partial}{\partial v_3}\right\}$. This means that for $\ell = span\{\frac{\partial}{\partial u_3}\}$ $(c = 0)$ we get $\Phi^3_*(\ell) = span\left\{\frac{(\phi^2_y(\mathbf{0}))^2}{(\phi^1_x(\mathbf{0}))^3}\frac{\partial}{\partial u_3}\right\}$ to give one orbit. This orbit is characterized by all vectors of the form $b'\frac{\partial}{\partial u_3}$ with $b' \neq 0$. Then, for $\ell = span\{\frac{\partial}{\partial u_3} + \frac{\partial}{\partial v_3}\}$ we see that $\Phi^3_*(\ell) = span\left\{(\frac{(\phi^2_y(\mathbf{0}))^2}{(\phi^1_x(\mathbf{0}))^3})\frac{\partial}{\partial u_3} + (\frac{\phi^3_z(\mathbf{0})}{(\phi^1_x(\mathbf{0}))^2})\frac{\partial}{\partial v_3}\right\}$, and notice that $\phi^1_x(\mathbf{0}) \neq 0$, $\phi^2_y(\mathbf{0}) \neq 0$, and $\phi^3_z(\mathbf{0}) \neq 0$. However, we can choose $\phi^1_x(\mathbf{0})$, $\phi^2_y(\mathbf{0})$, and $\phi^3_z(\mathbf{0})$ to be equal to anything else other than zero. Then since our distribution $\Delta_3(p_3)$ is coframed by du_2, du_3, dv_3 and with $\ell' \equiv \Phi^3_*(\ell)$ we get

$$[du_2|_{\ell'}, du_3|_{\ell'}, dv_3|_{\ell'}] = [0, \frac{(\phi^2_y(\mathbf{0}))^2}{(\phi^1_x(\mathbf{0}))^3}, \frac{\phi^3_z(\mathbf{0})}{(\phi^1_x(\mathbf{0}))^2}] = [0, 1, \frac{\phi^1_x(\mathbf{0})\phi^3_z(\mathbf{0})}{(\phi^2_y(\mathbf{0}))^2}]$$

to give another, separate orbit. In the present case, for ℓ to be a vertical direction, it must be of the form $\ell = span\{b\frac{\partial}{\partial u_3} + c\frac{\partial}{\partial v_3}\}$ with $b \neq 0$. This means that there is a total of 2 orbits for the class $RVVV$, as depicted in Figure 4.1.

The classification of the other RVT classes at level 4 are done in a very similar manner.

4.0.4 The Proof of Theorem 2.1.7

Proof Let $R\cdots R\omega$ the RVT class that has s more R's added to the beginning of the class ω. We begin by constructing a bijection between the equivalence classes of curves that represent points in ω and $R\cdots R\omega$. Let γ be a curve germ that realizes a point in ω. Then we can apply a RL- transformation to γ to find its symbol, say $[n, m, p]$, where p could be zero. Now, notice that if alter the symbol of γ to be $[n, m+sn, p+sn]$ (or $[n, m+sn, 0]$ if $p = 0$), then the resulting curve will represent a point in the RVT class $R\cdots R\omega$. This is because when we look at the Cartan prolongation in KR-coordinates of the curve $(t^n, t^{m+sn}, t^{p+sn})+O(t^{p+sn})$ the x-coordinate will divide the y and z coordinates, as well as the u_i and v_i fiber coordinates for $i = 1, \cdots, s$, an extra s times. We can define a mapping which sends curves with symbol $[n, m, p] \mapsto [n, m+ns, p+ns]$ and hence sends equivalence classes of curves with RVT code ω to equivalence classes of curves with RVT code $R\cdots R\omega$. Now, take $\tilde{\gamma}$ to be any curve germ that has RVT code $R\cdots R\omega$ and the symbol of $\tilde{\gamma}$ is $[n', m', p']$, where, again, p' could be zero. Since $\tilde{\gamma}$ is RL-equivalent to a curve germ of the form $\sigma(t) = (t^{n'}, t^{m'}, t^{p'}) + O(t^{p'})$ we notice when we prolong σ that the X-coordinate must divide both the y and z coordinates and the fiber coordinates u_i and v_i for $i \leq k$. This means we can rewrite the symbol of $\tilde{\gamma}$ as $[n', m + sn', p + sn']$ (or as $[n', m + sn', 0]$ when $p = 0$) and that any curve germ with symbol $[n', m, p]$ will have RVT code ω and as a result establishes a bijection between equivalence classes of curve germs with RVT codes ω and $R\cdots R\omega$. Now, take $p_i \in \omega$ for $i = 1, \cdots, k$ be points that are representatives for each of the k orbits in ω and γ_i to be curve germs from $Germ(p_i)$ for $i = 1, \cdots, k$. Then the image of these curves by the above bijection are inequivalent curve germs, say $\tilde{\gamma}_i$, which realize inequivalent points $\tilde{p}_i$ for $i = 1, \cdots, k$ in $R\cdots R\omega$. As a result, these points $\tilde{p}_i$ for $i = 1, \cdots k$ represent each of the distinct orbits within $R\cdots R\omega$. □

4.1 The Moduli Question

When trying to classify points within the Monster Tower one can run into a situation when there exists an continuums worth of inequivalent orbits within a given RVT class. Montgomery and Zhitomirksii pointed this out in [MZ10] with the $\mathbb{R}^2$ Monster Tower. In particular, they were able to characterize which RVT classes had

moduli by using their singular curves approach and showed that in certain RVT class that there exists a family of inequivalent curves which are parametrized by at least one real variable.

Incidents of when moduli occur within the $\mathbb{R}^2$ Monster Tower can be found in [MZ10], specifically in Chapter 5.7. One interesting phenomenon is that moduli can occur somewhat unexpectedly within various RVT classes. For example, the RVT class $RRVTR^q$ for $q = 0, \cdots, 4$ will contain a single orbit represented by the normal form $(t^5, t^{12}+t^{13})$. However, for $q = 5, 6$ this RVT class jumps from there being a single orbit to an infinite number of orbits given by the curve normal forms $(t^5, t^{12} + t^{13} + at^{16})$, and for $q \geq 7$ the normal forms are given by $(t^5, t^{12} + t^{13} + at^{16} + bt^{18})$. The letters a and b are parameters that can take any real number and the curves are inequivalent for different values of a and b. Hence, once q is larger than 4 the RVT class goes from containing a single orbit to not just a countably infinite number of orbits, but a whole continuums worth of inequivalent points.

When classifying the $\mathbb{R}^3$ Monster Tower we were interested in trying to see when moduli first appeared within the tower. While this thesis only contains the complete classification up to level 4 of the tower, a great deal of the classification of the fifth level of the tower has been done using the isotropy method. Unfortunately, even with the aid of Theorem 2.1.7 the task of trying to classify the orbits by hand became too unwieldy. One of the main reasons is because there are over 60 distinct RVT classes (recall that there are only 23 RVT classes at level 4). A majority of the RVT classes have been classified at level 5 and it appears that moduli will not appear within the fifth level of the tower. Based on our calculations, there are two RVT class of interest within the fifth level where moduli could possibly occur: the class $RVTTT$ or $RVTTR$. The reasoning for this is because the class $RVTT$ has 4 distinct orbits within the fourth level, ended up having a number of restrictions on the values that the component functions of the symmetries that fixed the various orbits in level 3 of the tower, and hence the most time consuming to calculate. For this reason, this class has yet to be calculated by the author during the time this was written. Based upon these calculations there is strong evidence to suggest that the sixth level of the tower will contain moduli. Some RVT classes of interest are: $RVTTTT$, $RVTTTR$, and $RVTRVR$.

The first instance of moduli within the Monster Tower has been discovered by Mormul and Pelletier in [MP10]. By using their knowledge of the existence of moduli

for 1-flags they were able to produce an example of where moduli exist for 2-flags. In Mormul's singularity class coding system, moduli occur within the class 1.2.1.2.1.2.1, which is a collection of points within the seventh level of the Monster Tower. In Section 5.7.2 we show which RVT classes make up the singularity class 1.2.1.2.1.2.1.

Based on the above we believe that there is the following number of orbits within the first 7 levels of the $\mathbb{R}^3$ Monster Tower

Level 1:	Level 2:	Level 3:	Level 4:	Level 5:	Level 6:	Level 7
1	2	7	34	$77 \geq$	∞ ?	∞

One interesting question to ask is whether it is possible to find some geometric reasoning, or even better, find some sort of invariant that tells us when moduli occur within the $\mathbb{R}^3$ Monster Tower?

Chapter 5

Appendix

5.1 Definition of a Goursat n-flag.

In this section we present the definition of a Goursat n-flag of length k, or what is also referred to as a Special n-flag of length k. We follow the definition presented in [SY09].

Let $n \geq 2$, k a non-negative integer and D a distribution of rank $n+1$. Assume further that the ambient manifold Z has dimension $(n+1)+kn$.

Our distribution D will be defined locally by the vanishing of the one forms ω_i for $i = 1, \cdots, s$, which are pointwise linearly independent as covectors.

The *Cauchy characteristic system* of D is the linear subbundle defined by the linear constraints

$$Ch(D)(p) = \{X \in D(p) | X \lrcorner d\omega_i = 0 \mod \omega_i, \forall i \in \{1, \cdots, s\}\}.$$

We say that a nonholonomic distribution D admits a *special n-flag of length k* if it has integrable subbundle F of $\partial^{k-1}D$ of corank 1 and that satisfies the following sandwich diagram:

$$\begin{array}{ccccccccccc}
 & & D & \subset & \partial D & \cdots & \subset & \partial^{k-2}D & \subset & \partial^{k-1}D & \subset & \partial^k D = TZ \\
 & & \cup & & \cup & & & \cup & & \cup & & \\
Ch(D) & \subset & Ch(\partial D) & \subset & Ch(\partial^2 D) & \cdots & \subset & Ch(\partial^{k-1}D) & \subset & F & &
\end{array}$$

where ∂D is called the *derived system of* D, and geometrically $\partial D = D + [D, D]$. Proceeding recursively, $\partial^i D = \partial(\partial^{i-1} D)$ and we can verify that $\text{rank}(\partial^i D) = \text{rank}(\partial^{i-1} D) + n$ for $i = 1, \cdots, k$. In our language, $F = \ker(d\pi_{k,0})$ for $\pi_{k,0} : \mathcal{P}^k \to \mathbb{R}^3$ ([SY09]).

Example 5.1.1 *Take* $\mathbb{R}^3$ *with distribution given by the contact form* $dy - zdx = 0$ *is a Goursat* 1*-flag of length* 1*.*

One can also find a variety of examples in [MZ01], where they explicitly calculate the sandwich diagram for various Goursat 1-flags.

5.2 Derivation of the Kinematic Equations for the Car with n Trailers

In this portion of the appendix we present a derivation for the kinematic equation for the car with n trailers. Our follows the one given by F. Pelletier and M. Slayman in [PS12].

We begin the construction in $\mathbb{R}^2$ where we have one car towing n trailers. Let M_0 denote the car and $M_1, \cdots, M_n$ denote the n trailers that are being towed by the car. Also assume that there is a fixed constant length between each of the trailers. In this system we impose the nonholonomic constraint that the wheels are rolling without sliding. The configuration space is $\mathbb{R}^2 \times (S^1)^{n+1}$, where the (x, y) coordinate in $\mathbb{R}^2$ is the position of the car and $(n+1)$ angle coordinates. This is a system with two degrees of freedom. The two inputs are the tangential velocity v_n and the angular velocity ω_n of the car. This represents the driver of the car having control over the accelerator and the steering wheel. Pick a reference point of a M_{n-r} to the midpoint m_r between the wheels and denote its coordinates by (x_r, y_r). The angle coordinate θ_r is the angle between the hitch of M_{n-r} that connects it to the trailer in front of it M_{n+1-r} and the positive X-Axis. The following equations describe the connections between pair of trailers and car.

$$x_r - x_{r-1} = cos(\theta_{r-1})$$
$$y_r - y_{r-1} = sin(\theta_{r-1})$$

Any point in the configuration space can be written as $q = (x_0, y_0, \theta_0, \theta_1, \cdots, \theta_n)$ where:

• (x_0, y_0) are the coordinates of the last trailer M_n in the system.

• θ_n is the orientation of the car with respect to the positive X-Axis.

• θ_r, for $r = 0, \cdots, n-1$, is the orientation of the $(n-r)$-th trailer with respect to the positive X-Axis. Since we are assuming that the wheels are rolling without sliding, then this imposes the following nonholonomic constraint:

$$\dot{x}_r sin(\theta_r) - \dot{y}_r cos(\theta_r) = 0.$$

Let us now represent each of the points m_r, for $r = 0, \cdots, n$, as points within the complex plane $\mathbb{C}$. We now write $m_r = x_r + iy_r$ and the constraint that connects two consecutive trailers is given by:

$$m_r = m_{r-1} + e^{i\theta_{r-1}} \text{ for } r \neq 0. \tag{5.2.1}$$

and results in the equation

$$m_r = m_0 + \sum_{l=0}^{r-1} e^{\theta_l}. \tag{5.2.2}$$

The kinematic constraint for M_{n-r} is

$$\dot{m}_r = \lambda_r e^{i\theta_r} \tag{5.2.3}$$

and can be rewritten as $Im(e^{-i\theta_r}\dot{m}_r) = 0$. Using equations 5.2.1, 5.2.2, 5.2.3 yields the kinematic contraints

$$-\dot{x}_0 sin(\theta_r) + \dot{y}_r cos(\theta_r) + \sum_{j=0}^{r-1} cos(\theta_j - \theta_r) = 0 \text{ for } r = 0, \cdots, n \tag{5.2.4}$$

Then combine equation 5.2.2 with the derivative of the equation

$$|m_{r+1} - m_r|^2 = 1$$

to get the equation

$$\lambda_r = \lambda_{r+1}(cos(\theta_{r+1}) - cos(\theta_r))$$

and we get the relation

$$\lambda_r = \lambda_n cos(\theta_n - \theta_{n-1}) \cdots cos(\theta_{r+1} - \theta_r)$$

and combining the above equations along with the fact that $\lambda_n = v_n$, the tangential velocity of the car M_0, we get

$$\dot{m}_r = v_n(\prod_{j=r+1}^{n} cos(\theta_j) - cos(\theta_{j-1}))e^{i\theta_r}$$

Then, by using the above formulas we end up with the kinematic relations

$$\begin{aligned}
\dot{x}_0 &= v_0 cos(\theta_0) \\
\dot{y}_0 &= v_0 sin(\theta_0) \\
\dot{\theta}_0 &= v_1 sin(\theta_1 - \theta_0) \\
&\vdots \\
\dot{\theta}_r &= v_{r+1} sin(\theta_{r+1} - \theta_r) \\
&\vdots \\
\dot{\theta}_{n-1} &= v_n sin(\theta_n - \theta_{n-1}) \\
\dot{\theta}_n &= \omega_n
\end{aligned}$$

in the above each tangential velocity v_r is related to the input velocity v_n, which is given by the formula $v_r = \prod_{j=r+1}^{n} cos(\theta_j - \theta_{j-1}) v_n$. The motion of this dynamical system is characterized by the equation:

$$\dot{q} = \omega_n X_1^n(q) + v_n X_2^n(q)$$

with
$$\begin{cases}
X_1^n &= \frac{\partial}{\partial \theta_n} \\
X_2^n &= cos(\theta_0) f_0^n \frac{\partial}{\partial x} + sin(\theta_0) f_0^n \frac{\partial}{\partial y} \\
&\quad + sin(\theta_1 - \theta_0) f_1^n \frac{\partial}{\partial \theta_0} + \cdots + sin(\theta_n - \theta_{n-1}) \frac{\partial}{\partial \theta_{n-1}}
\end{cases}$$

and $f_i^n = \prod_{j=i+1}^{n} cos(\theta_j - \theta_{j-1})$.

We want to point out that the rank-2 distribution generated by $\{X_1^n, X_2^n\}$ is a Goursat 1-flag and is one of the motivating reasons for the interest in studying Goursat Multi-Flags. F. Jean in [Jea96] was particularly interested in understanding the connection between the various trailer configurations and the degree of nonholonomy of this rank-2 distribution generated by X_1^n and X_2^n.

Definition 5.2.1 (Degree of Nonholonomy) *Let D be a distribution associated with a control system. Define $D_1 = D$ and $D_i = D_{i-1} + [D_1, D_{i-1}]$, where $[D_1, D_{i-1}] = span\{[X, Y] \,|\, X \in D_1,\ Y \in D_{i-1}\}$. Then the degree of nonholonomy is the smallest integer n such that the rank of D_n is equal to the rank of D_{n+1}.*

5.3 A technique to eliminate terms in the short parameterization of a curve germ.

The following technique that we will discuss is outlined in [Zar06] on pg. 23. Let C be a planar curve germ. A *short parametrization* of C is a parametrization of the form

$$C = \begin{cases} \tilde{x} = t^n \\ \tilde{y} = t^m + \Sigma_{i=1}^{q} a'_{\nu_i} t^{\nu_i} \end{cases}$$

where the $\nu_1 < \nu_2 < \cdots < \nu_q$ are integers that belong to the set $\{m+1, \cdots, c\}$ which do not belong to the semigroup of the curve C. In [Zar06] there is a result, Proposition 2.1, which says that if C is any planar analytic curve germ, then there exists a branch $\tilde{C}$ with the above short parametrization and $\tilde{C}$ is RL-equivalent to C.
We look at a particular case of the short parametrization where we define ρ to be an integer, less than or equal to $q+1$, and $a_{\nu_i} = 0$ for $i < \rho$, and $a_{\nu_p} = b$. This gives a short parametrization of the following form

$$C = \begin{cases} x = t^n \\ y = t^m + bt^{\nu_\rho} + \Sigma_{i=\rho+1}^{q} a_{\nu_i} t^{\nu_i} \quad b \neq 0 \text{ if } \rho \neq q+1 \end{cases}$$

Suppose that $\nu_\rho + n \in n\mathbb{Z}_+ + m\mathbb{Z}_+$. Now, notice that $\nu_\rho + n \in m\mathbb{Z}_+$ because ν_ρ is not in the semigroup of C. Let $j \in \mathbb{Z}_+$ be such that $\nu_\rho + n = (j+1)m$; notice that $j \geq 1$ since $\nu_\rho > m$. Then set $a = \frac{bn}{m}$ and
$x' = t^n + at^{jm}+$(terms of degree $> jm$). Let $\tau^n = t^n + at^{jm}+$ (terms of degree $> jm$). From this expression one can show that $t = \tau - \frac{a}{n}\tau^{jm-n+1}+$ (terms of degree $> jm - n + 1$), and when we substitute this into the original expression above for C that

$$C = \begin{cases} x' = \tau^n \\ y = \tau^m + (\text{terms of degree} > \nu_\rho) \end{cases}$$

We can now apply Proposition 2.1 to the above expression for C and see that C admits the parametrization

$$C = \begin{cases} x' = \tau^n \\ y' = \tau^m + \Sigma_{i=\rho+1}^{q} a'_{\nu_i} \tau^{\nu_i} \end{cases}$$

We can now apply the above technique to the two curves $(t^3, t^5+t^7, 0)$ and $(t^3, t^5-t^7, 0)$ in order to eliminate the t^7 in both of these curve germs. This means that these two curves will end up being equivalent to the curve $(t^3, t^5, 0)$.

5.4 Kumpera-Ruiz Coordinates

While we presented the Kumpera-Ruiz coordinates through an example in Section 3.4, we have also included the general method for determining the KR coordinates at any given level of the $\mathbb{R}^n$ Monster Tower for completeness. The following material that will be presented first appeared in [CM12]. We want to note that KR coordinates for the planar $\mathbb{R}^2$ Monster were described in detail in [MZ10]. They can also be found in [LJ06]. Generalizations from $n = 2$ to $n > 2$ were presented in [Mor04] and called EKR coordinates. We will proceed level by level.

Level 0: Take any coordinates $(x_1, \ldots, x_n)$ on n-space. They need not be linear.

Level 1: A point in $\mathcal{P}^1(n-1)$ is a point p at level 0 and a tangent line ℓ to that point. Then $[dx_1 : \ldots : dx_n]$ are homogeneous coordinates for Δ_0, the tangent space to the n-space at p, with the corresponding homogeneous coordinates of ℓ being $[dx_1(v) : \ldots : dx_n(v)]$ where v is any nonzero vector spanning ℓ. For at least one index i we have $dx_i(v) \neq 0$. Select such an index, i_0, and divide by dx_{i_0} we get $n-1$ fiber affine coordinates which we write $u_j^1 = dx_j(v)/dx_{i_0}(v)$, $j \neq i$. In this way a point of $\mathcal{P}^1(n-1)$ is covered by $n-1$ charts. Δ_1 is locally defined in one of these charts by solving for dx_j in terms of the u_j^1 and the selected dx_i. That is, to say Δ_1 is defined by the n_1 Pfaffian equations $dx_j - u_j^1 dx_{i_0} = 0$.

In order to induct in an organized manner, it is better to insist that the indices j of u^1_j run through a fixed subset of $\{1, \cdots, n\}$ of cardinality $n-1$, rather than letting this set vary with the selected i_0. We will take this fixed subset to be $\{2, \cdots, n\}$. We do this by relabeling indices using the unique monotone bijection

$$\sigma(j; i_0) : \{1, \cdots, n\} \setminus \{i_0\} \to \{2, \cdots, n\}.$$

Thus, if $i_0 = 1$ which is to say, if $dx_1 \neq 0$, then we continue with our same labelling:

$$u^1_j = dx^j/dx^1, j = 1, \cdots, n, \text{ if } dx_1 \neq 0.$$

In this way,

$$u^i_{j+1} = dx_j/dx_{i_0}, j < i_0$$

while

$$u^i_j = dx_j/dx_{i_0}, j > i_0.$$

Inductive step. level k to level $k+1$: Suppose that p is at level $k+1$ with $p = (p_k, \ell_k)$. Suppose we have covered $\mathcal{P}^k(n-1)$ with KR coordinates charts and that the coordinates of a chart containing p_k consists of $n + k(n-1)$ functions:

$$(x_1, \cdots, x_n, u^1_2, \cdots, u^1_n, \cdots, u^k_2, \cdots, u^k_n).$$

Suppose that these coordinates are such that (1) the last set of $n-1$, namely $u^k_2, \cdots, u^k_n$ are fiber-affine coordinates for the fiber $\mathcal{P}^k(n-1) \to \mathcal{P}^{k-1}(n-1)$, and that (2) a basis for the dual space $\Delta^*_k(p)$ is given by $df^k, du^k_2, \cdots, du^k_n$ (restricted to $\Delta_k(p)$), where f^k is a distinguished coordinate, taken from amongst the previous level $k-1$ KR coordinates

$$f^k \in \{x_1, \cdots, x_n, u^1_2, \cdots, u^1_n, \cdots, u^{k-1}_2, \cdots, u^{k-1}_n\}.$$

The coordinate f^k will be called the *uniformizing coordinate* at level k and plays the role of an independent variable in jet terms.

We can use our dual basis to represent lines in $\Delta_k(p)$ via homogeneous coordinates and so represent ℓ as $[df^k(v) : du^k_2 : \ldots : du^k_n(v)]$ where v spans ℓ. Constructing level $k+1$ coordinates is a matter of deciding which linear coordinate to divide by, df^k, or one of the du^k_i. The labeling of the resulting coordinates proceeds quite like in the base of the induction, $k = 1$, with f^k now playing the role of x_1 from the $k = 1$ step. We proceed on a case-by-case basis, depending on whether or not the line ℓ is vertical. Since the u^k_i are fiber coordinates, we see that ℓ is vertical if and only if $df^k(v) = 0$.

Case 1: ℓ is *not* vertical. Then $df^k(v) \neq 0$. Dividing we get new fiber affine coordinates

$$u_j^{k+1} = du_j^k(v)/df^k(v), j = 2, \cdots, n$$

and we set

$$f^{k+1} = f^k,$$

which means we continue to use the previous uniformizing coordinate as the new one.

Case 2: ℓ is vertical. Then $df^k(v) = 0$. Choose the 1st i such that $du_i^k(v) \neq 0$ and call this i_0. Set

$$f^{k+1} = u_{i_0}^k$$

thus defining a new uniformizing coordinate. The new fiber affine coordinates are

$$u_2^{k+1} = df^k(v)/df^{k+1}(v) = df^k/du_{i_0}^k$$

while for the subscripts $r > 2$ of u_r^{k+1} we have

$$u_{\sigma(j;i_0)}^{k+1} = du_j^k(v)/df^{k+1}(v), j > 1$$

where, as in the $k = 1$ case, $j \mapsto \sigma(j; i_0)$ is the unique order preserving map $\{1, 2, \cdots, n-1\} \setminus \{i_0\} \to \{2, \cdots, n-1\}$. Specifically

$$u_{j+1}^{k+1} = du_j^k(v)/df^{k+1} = du_j^k(v)/du_{i_0}^k,\ 2 \leq j < i_0.$$

while

$$u_j^{k+1} = du_j^k(v)/df^{k+1} = du_j^k(v)/du_{i_0}^k,\ j > i_0.$$

In the new coordinates the distribution Δ_{k+1} is described by intersecting the pull-back $\pi_{k+1,k}^*\Delta_k$ of the level k distribution with the hyperplane distributions defined by the vanishing of the one-forms obtained by rewriting the defining equations for the u_j^{k+1} as Pfaffian systems. Thus, for example, in the case of ℓ not vertical, these are

$$du_j^k - u_j^{k+1}df^k = 0.$$

In all cases, a basis for $\Delta_{k+1}^*(p)$ is df^{k+1} together with the $du_i^{k+1}, i = 2, \cdots, n$. The new coordinates at level $k+1$ satisfy (i) and (ii) of the beginning of this inductive step, with the index shifted now from k to $k+1$, so induction holds and we can continue up to the next level.

Meaning of the 'uniformizing' coordinate

Theorem 5.4.1 *Let $p \in \mathcal{P}^k(n-1)$ at level k. Fix KR coordinates about p with f^k the uniformizing coordinate at that level k. Then any $\gamma \in Germ(p)$ can be parameterized so that along γ^k we have $f^k(t) = t$.*

Proof. Since γ^k is regular, its one step projection γ^{k-1} is an immersed curve by Proposition 5.4.2 below. So write $v = d\gamma^{k-1}/dt|_{t=0} \neq 0$. Because $\gamma^k = (\gamma^{k-1})^1$ we have that γ^{k-1} is tangent to the line ℓ which comprises p; thus $p = (p_{k-1}, \ell)$ with $\ell = \text{span}(v)$. Now the uniformizing coordinate f^k for level k is chosen according to the condition that $df^k|_\ell \neq 0$. Thus, $df^k/dt|_{t=0} = df^k(v) \neq 0$ relative to any good parameterization $t \mapsto \gamma^k(t)$ of γ^k. We can now reparameterize so that $df^k/dt = 1$ and so $f^k = t$ along γ^k (and along γ^{k-1}).

Proposition 5.4.2 *Let σ be a regular integral curve germ at level k. Let σ^1 denote its one step prolongation and $\sigma_1 = \pi_{k,k-1} \circ \sigma$ its one step projection at level $k-1$.*
Then

(a) $\sigma^1(t)$ is a regular integral curve germ at level $k+1$ passing through a regular point.

(b) σ_1 is an embedded integral curve, not necessarily regular.

(c) If $\sigma(0)$ is a regular point, then σ_1 is a regular integral curve germ.

5.5 Cartan Prolongation applied to curve germs.

In this section we want to present some of the basics of prolonging curve germs. We will not give a presentation on how to do this in the general case, but instead provide a few useful examples. The main motivation for this section is to help show the interested reader how to write the curve locally in KR coordinates. The other purpose of this section is to show how one can read off the RVT code that is associated to the given curve germ.

Example 5.5.1 (The $(t^2, t^3, 0)$ case) *Recall that a parametrized curve $\gamma(t) = (t^2, t^3, 0)$ belongs to the class A_{2k}, for $k = 1$. From Table 2.1 we know that it represents a curve in the RVT class RV. We want to prolong γ in a neighborhood of the its singularity at the origin. We take $[dx : dy : dz]$ to be our coframing for the tangent bundle $\Delta_0 = T\mathbb{R}^3$.*

The first prolongation is given by

$$\begin{aligned}\gamma^{(1)}(t) &= (t^2, t^3, 0, [dx : dy : dz]) \\ &= (t^2, t^3, 0, [2t : 3t^2 : 0]) \\ &= (t^2, t^3, 0, [1 : \frac{3}{2}t : 0]) \\ &= (t^2, t^3, 0\frac{3}{2}t, 0)\end{aligned}$$

Again, since we want to look at when $t = 0$, that the only thing we can do is to divide by the dx term and then take the limit as $t \to 0$. This gives us fiber coordinates $u = \frac{dy}{dx}$ and $v = \frac{dz}{dx}$ and that our distribution Δ_1 on $\mathcal{P}^1$ is locally defined to be

$$dy - udx = 0$$
$$dz - vdx = 0$$

Since every direction at the first level is equivalent, the RVT code for the curve γ begins with the letter R.

We now want to prolong $\gamma^{(1)}(t)$ to the second level of the tower. However, this time it is not entirely obvious what the coframing should be for Δ_1 near $\gamma^{(1)}(0)$. From looking at the equation for Δ_1 above, one can see that the distribution is locally spanned by the vector fields $X^{(1)} = \frac{\partial}{\partial x} + u\frac{\partial}{\partial y} + v\frac{\partial}{\partial z}$, $\frac{\partial}{\partial u}$, and $\frac{\partial}{\partial v}$. As a result, we need to take our coframing to be $[dx : du : dv]$, where we use dx to capture information about the vector field $X^{(1)}$ coming from one level below. The 1-form dx is used because it is possible to have $u = 0$ and/or $v = 0$. We also need to include the two fiber coordinates, which is why du and dv are used. This gives

$$\begin{aligned}\gamma^{(2)}(t) &= (t^2, t^3, 0\frac{3}{2}t, 0, [dx : du : dv]) \\ &= (t^2, t^3, 0\frac{3}{2}t, 0, [2t : \frac{3}{2} : 0]) \\ &= (t^2, t^3, 0\frac{3}{2}t, 0, [\frac{4}{3}t : 1 : 0]) \\ &= (t^2, t^3, 0\frac{3}{2}t, 0, \frac{4}{3}t, 0)\end{aligned}$$

Here we picked our fiber coordinates to be $u_2 = \frac{dx}{du}$ and $v_2 = \frac{dv}{du}$ since we are interested in when $t \to 0$ and we want to end up with a tangible finite number in the expression for $\gamma^{(2)}(0)$. Notice as well that the du term is $\frac{3}{2}$, but the dx one is $2t$. This tells us that $\frac{d\gamma^{(1)}}{dt}|_{t=0}$ will be tangent to the fiber space and hence be a vector in the vertical space.

As a result, we add the letter V to the RVT code for γ and that the RVT code for γ is just RV. If we prolong $\gamma^{(2)}$ to any higher level of the Monster Tower ten we will just end up placing the letters R onto the RVT code.

Example 5.5.2 (The case (t^2, t^4, t^5)) *The curve $\gamma(t) = (t^2, t^4, t^5)$ will have RVT code RVT. Just as in the above, the first prolongation is given by*

$$\begin{aligned}\gamma^{(1)}(t) &= (t^3, t^4, t^5, [dx : dy : dz]) \\ &= (t^3, t^4, t^5, [3t^2 : 4t^3 : 5t^4]) \\ &= (t^3, t^4, t^5, \frac{4}{3}t, \frac{5}{3}t^2)\end{aligned}$$

to give $u = \frac{dy}{dx}$, $v = \frac{dz}{dx}$, the first letter in the RVT code is R, and Δ_1 is locally given by

$$dy - udx = 0$$

$$dz - vdz = 0$$

Then for the second prolongation we have

$$\begin{aligned}\gamma^{(2)}(t) &= (t^3, t^4, t^5, \frac{4}{3}t, \frac{5}{3}t^2, [dx : du : dv]) \\ &= (t^3, t^4, t^5, \frac{4}{3}t, \frac{5}{3}t^2, [3t^2 : \frac{4}{3} : \frac{10}{3}t]) \\ &= (t^3, t^4, t^5, \frac{4}{3}t, \frac{5}{3}t^2, \frac{9}{4}t^2, \frac{5}{2}t)\end{aligned}$$

to give $u_2 = \frac{dx}{du}$, $v_2 = \frac{dv}{du}$ and since $\frac{d\gamma^{(2)}}{dt}|_{t=0}$ is tangent to the fiber space we add the letter V to the code.

The distribution Δ_2 is given by

$$dx - u_2 du = 0$$

$$dv - v_2 dv = 0$$

With this in mind, the third prolongation is given by

$$\begin{aligned}\gamma^{(3)}(t) &= (t^3, t^4, t^5, \frac{4}{3}t, \frac{5}{3}t^2, \frac{9}{4}t^2, \frac{5}{2}t, [du : du_2 : dv_2]) \\ &= (t^3, t^4, t^5, \frac{4}{3}t, \frac{5}{3}t^2, \frac{9}{4}t^2, \frac{5}{2}t, [\frac{4}{3} : \frac{9}{2}t : \frac{10}{4}]) \\ &= (t^3, t^4, t^5, \frac{4}{3}t, \frac{5}{3}t^2, \frac{9}{4}t^2, \frac{5}{2}t, \frac{27}{8}t, \frac{15}{8})\end{aligned}$$

This gives $u_3 = \frac{du_2}{du}$, $v_3 = \frac{dv_2}{du}$ and we notice that the du_2 term will be zero when $t = 0$ and imply that $\frac{d\gamma^{(2)}}{dt}|_{t=0}$ is tangent to the tangency hyperplane. Hence, we add the letter T to the RVT code of γ.

5.6 Computations for the class $RVVV$.

In this section we work out the computations for the functions $\frac{\partial \tilde{u}_3}{\partial u_3}$, $\frac{\partial \tilde{u}_3}{\partial v_3}$, $\frac{\partial \tilde{v}_3}{\partial u_3}$, $\frac{\partial \tilde{v}_3}{\partial v_3}$ evaluated at $p_3 = (x, y, z, u, v, u_2, v_2, u_3, v_3) = (0, 0, 0, 0, 0, 0, 0, 0, 0)$, which we omitted in Section 5.

(i) Computation of $\frac{\partial \tilde{u}_3}{\partial u_3}$.

Starting with $\tilde{u}_3 = \frac{c_1}{c_2}$, one computes

$$\frac{\partial \tilde{u}_3}{\partial u_3} = \frac{u_2 \frac{\partial \tilde{u}}{\partial x} + u u_2 \frac{\partial \tilde{u}}{\partial y} + \frac{\partial \tilde{u}}{\partial u} + v_2 \frac{\partial \tilde{u}}{\partial v}}{c_2} - \frac{\frac{\partial c_2}{\partial u_3} c_1}{c_2^2}$$

and

$$\frac{\partial \tilde{u}_3}{\partial u_3}(p_3) = \frac{\frac{\partial \tilde{u}}{\partial u}(p_3)}{\frac{\partial \tilde{u}_2}{\partial u_2}(p_3)},$$

since $c_1(p_3) = 0$. We recall that $\frac{\partial \tilde{u}}{\partial u}(p_3) = \frac{\phi_y^2(\mathbf{0})}{\phi_x^1(\mathbf{0})}$, $\frac{\partial \tilde{u}_2}{\partial u_2}(p_3) = \frac{\phi_x^1(\mathbf{0})}{\frac{\partial \tilde{u}}{\partial u}(p_3)}$ to give

$$\frac{\partial \tilde{u}_3}{\partial u_3}(p_3) = \frac{(\phi_y^2(\mathbf{0}))^2}{(\phi_x^1(\mathbf{0}))^3}.$$

(ii) Computation of $\frac{\partial \tilde{u}_3}{\partial v_3}$.

Since $\tilde{u}_3 = \frac{c_1}{c_2}$, then

$$\frac{\partial \tilde{u}_3}{\partial v_3}(p_3) = \frac{\frac{\partial c_1}{\partial v_3}(p_3)}{c_2(p_3)} - \frac{\frac{\partial c_2}{\partial v_3}(p_3) c_1(p_3)}{c_2^2(p_3)} = 0,$$

because c_1 is not a function of v_3 and $c_1(p_3) = 0$.

(iii) Computation of $\frac{\partial \tilde{v}_3}{\partial u_3}$.

Have that $\tilde{v}_3 = \frac{c_3}{c_2}$, then

$$\frac{\partial \tilde{v}_3}{\partial u_3} = \frac{u_2 \frac{\partial \tilde{v}_2}{\partial x} + ... + \frac{\partial \tilde{v}_2}{\partial u} + v_2 \frac{\partial \tilde{v}_2}{\partial v}}{c_2} - \frac{(u_2 \frac{\partial \tilde{u}_2}{\partial x} + ... + \frac{\partial \tilde{u}_2}{\partial u} + ... + v_2 \frac{\partial \tilde{u}_2}{\partial v}) c_1}{c_2^2}$$

$$\frac{\partial \tilde{v}_3}{\partial u_3}(p_3) = \frac{\frac{\partial \tilde{v}_2}{\partial u}(p_3)}{\frac{\partial \tilde{u}_2}{\partial u_2}(p_3)} - \frac{\frac{\partial \tilde{u}_2}{\partial u}(p_3) \frac{\partial \tilde{v}_2}{\partial u_2}(p_3)}{(\frac{\partial \tilde{u}_2}{\partial u_2}(p_3))^2}$$

We will need to figure out what $\frac{\partial \tilde{u}_2}{\partial u_2}$, $\frac{\partial \tilde{v}_2}{\partial u_2}$, and $\frac{\partial \tilde{v}_2}{\partial u}$ are when we evaluate at p_3.

(a) $\frac{\partial \tilde{v}_2}{\partial u_2}$

Recall from work at level 3 that

$$\frac{\partial \tilde{v}_2}{\partial u_2}(p_3) = \frac{\frac{\partial \tilde{v}}{\partial x}(p_3)}{\frac{\partial \tilde{u}}{\partial u}(p_3)} = 0$$

since $\frac{\partial \tilde{v}}{\partial x}(p_3) = \frac{\phi^3_{xx}(\mathbf{0})}{\phi^1_x(\mathbf{0})}$ and have $\phi^1_{xx}(\mathbf{0}) = 0$ to give us $\frac{\partial \tilde{v}_2}{\partial u_2}(p_3) = 0$.

This gives the reduced expression

$$\frac{\partial \tilde{v}_3}{\partial u_3}(p_3) = \frac{\frac{\partial \tilde{v}_2}{\partial u}(p_3)}{\frac{\partial \tilde{u}_2}{\partial u_2}(p_3)}.$$

(b) $\frac{\partial \tilde{v}_2}{\partial u}$

Recall that $\tilde{v}_2 = \frac{b_3}{b_2}$, then we find

$$\frac{\partial \tilde{v}_2}{\partial u} = \frac{u_2 \frac{\partial^2 \tilde{v}}{\partial x \partial u} + u_2 \frac{\partial \tilde{v}}{\partial y} + ... + \frac{\partial \tilde{v}}{\partial^2 u} + v_2 \frac{\partial^2 \tilde{v}}{\partial v \partial u}}{b_2} - \frac{(u_2 \frac{\partial^2 \tilde{u}}{\partial x \partial u} + ... + \frac{\partial^2 \tilde{u}}{\partial^2 u} + v_2 \frac{\partial^2 \tilde{u}}{\partial v \partial u}) b_3}{b_2^2}$$

$$\frac{\partial^2 \tilde{v}_2}{\partial u}(p_3) = \frac{\frac{\partial^2 \tilde{v}}{\partial^2 u}(p_3)}{\frac{\partial \tilde{u}}{\partial u}(p_3)} - \frac{\frac{\partial^2 \tilde{u}}{\partial^2 u}(p_3) \frac{\partial \tilde{v}}{\partial u}(p_3)}{(\frac{\partial \tilde{u}}{\partial u}(p_3))^2}$$

since $b_2(p_3) = \frac{\partial \tilde{u}}{\partial u}(p_3)$ and $b_3(p_3) = \frac{\partial \tilde{v}}{\partial u}(p_3)$. In order to find $\frac{\partial \tilde{v}_2}{\partial u}(p_3)$ we will need to determine $\frac{\partial \tilde{v}}{\partial u}(p_3)$, $\frac{\partial^2 \tilde{v}}{\partial^2 u}(p_3)$, and $\frac{\partial^2 \tilde{u}}{\partial^2 u}(p_3)$.

(c) $\frac{\partial \tilde{v}}{\partial u}$

Recall that $\tilde{v} = \frac{a_3}{a_1}$ and that $\frac{\partial \tilde{v}}{\partial u} = \frac{\phi^3_y}{a_1} - \frac{\phi^1_y a_3}{a_1^2}$, then

$$\frac{\partial \tilde{v}}{\partial u}(p_3) = \frac{\phi^3_y(\mathbf{0})}{\phi^1_x(\mathbf{0})} - \frac{\phi^1_y(\mathbf{0})\phi^3_x(\mathbf{0})}{(\phi^1_x(\mathbf{0}))^2} = 0$$

since $\phi^3_y(\mathbf{0}) = 0$ and $\phi^3_x(\mathbf{0}) = 0$.

(d) $\frac{\partial^2 \tilde{v}}{\partial^2 u}$

From the above we have $\frac{\partial \tilde{v}}{\partial u} = \frac{\phi^3_y}{a_1} - \frac{\phi^1_y a_3}{a_1^2}$, then

$$\frac{\partial^2 \tilde{v}}{\partial^2 u}(p_3) = \frac{0}{a_1(p_3)} - \frac{\phi^3_y(\mathbf{0})\phi^1_y(\mathbf{0})}{a_1^2(p_3)} - \frac{\phi^1_y(\mathbf{0})\phi^3_y(\mathbf{0})}{a_1^2(p_3)} + \frac{(\phi^1_y(\mathbf{0}))^2 \phi^3_x(\mathbf{0})}{a_1^3(p_3)} = 0$$

since $\phi^3_y(\mathbf{0}) = 0$ and $\phi^3_x(\mathbf{0}) = 0$.

We do not need to determine what $\frac{\partial^2 \tilde{u}}{\partial^2 u}(p_4)$ is, since $\frac{\partial \tilde{v}}{\partial u}$ and $\frac{\partial^2 \tilde{v}}{\partial^2 u}$ will be zero at p_3 and give $\frac{\partial \tilde{v}_3}{\partial u_3}(p_3) = 0$.

(iv) Computation of $\frac{\partial \tilde{v}_3}{\partial v_3}$.

Recall that $\tilde{v}_3 = \frac{c_3}{c_2}$, then

$$\frac{\partial \tilde{v}_3}{\partial v_3} = \frac{\frac{\partial \tilde{v}_2}{\partial v_2}}{c_2} - \frac{\frac{\partial \tilde{u}_2}{\partial v_2} c_3}{c_2^2}$$

$$\frac{\partial \tilde{v}_3}{\partial v_3}(p_3) = \frac{\frac{\partial \tilde{v}_2}{\partial v_2}(p_3)}{\frac{\partial \tilde{u}_2}{\partial u_2}(p_3)} - \frac{\frac{\partial \tilde{u}_2}{\partial v_2}(p_3)\frac{\partial \tilde{v}_2}{\partial u_2}(p_3)}{(\frac{\partial \tilde{u}_2}{\partial u_2}(p_3))^2}.$$

This means we need to look at $\frac{\partial \tilde{v}_2}{\partial v_2}$, $\frac{\partial \tilde{u}_2}{\partial v_2}$, $\frac{\partial \tilde{v}_2}{\partial u_2}$, and $\frac{\partial \tilde{u}_2}{\partial u_2}$ evaluated at p_3.

(a) $\frac{\partial \tilde{v}_2}{\partial v_2}$.

We recall from an earlier calculation that

$$\frac{\partial \tilde{v}_2}{\partial v_2}(p_3) = \frac{\frac{\partial \tilde{v}}{\partial v}(p_3)}{\frac{\partial \tilde{u}}{\partial u}(p_3)} = \frac{\phi_z^3(\mathbf{0})}{\phi_y^2(\mathbf{0})}.$$

(b) $\frac{\partial \tilde{u}_2}{\partial v_2}$.

It is not hard to see that $\frac{\partial \tilde{u}_2}{\partial v_2}(p_3) = 0$.

(c) $\frac{\partial \tilde{u}_2}{\partial u_2}$.

Recall $\tilde{u}_2 = \frac{b_1}{b_2}$ and that

$$\frac{\partial \tilde{u}_2}{\partial u_2} = \frac{\phi_x^1 + u\phi_y^1 + v\phi_z^1}{b_2} - \frac{(\frac{\partial \tilde{u}}{\partial x} + u\frac{\partial \tilde{u}}{\partial y} + v\frac{\partial \tilde{u}}{\partial z})b_1}{b_2^2},$$

then

$$\frac{\partial \tilde{u}_2}{\partial u_2}(p_3) = \frac{\phi_x^1(\mathbf{0})}{\frac{\partial \tilde{u}}{\partial u}(p_3)} = \frac{(\phi_x^1(\mathbf{0}))^2}{\phi_y^2(\mathbf{0})}.$$

With the above in mind we have $\frac{\partial \tilde{v}_3}{\partial v_3}(p_3) = \frac{\phi_z^3(\mathbf{0})}{(\phi_x^1(\mathbf{0}))^2}$.

Then the above calculations give

$$\begin{aligned}\Phi_*^3(\ell) &= span\left\{(b\frac{\partial \tilde{u}_3}{\partial u_3}(p_3) + c\frac{\partial \tilde{u}_3}{\partial v_3}(p_3))\frac{\partial}{\partial u_3} + (b\frac{\partial \tilde{v}_3}{\partial u_3}(p_3) + c\frac{\partial \tilde{v}_3}{\partial v_3}(p_3))\frac{\partial}{\partial v_3}\right\} \\ &= span\left\{(b\frac{(\phi_y^2(\mathbf{0}))^2}{(\phi_x^1(\mathbf{0}))^3})\frac{\partial}{\partial u_3} + c\frac{\phi_z^3(\mathbf{0})}{(\phi_x^1(\mathbf{0}))^2}\frac{\partial}{\partial v_3}\right\}\end{aligned}$$

for $\ell = span\{b\frac{\partial}{\partial u_3} + c\frac{\partial}{\partial v_3}\}$ with $b, c \in \mathbb{R}$ and $b \neq 0$.

5.7 Relationship between Mormul's Coding and the RVT Coding System

In [Mor09] Mormul constructed a system for coding system for labeling singularity classes of points in the $\mathbb{R}^3$ Monster Tower. Mormul's codes are words in the letters $\mathbf{1}, \mathbf{2}, \mathbf{3}$. We have presented a coding system in this thesis whose codes are words in the letters R, C, and a refined code with whose codes are words in letters R, V, T, L with various decorations. A natural question to ask is the following:

> *How is Mormul's coding system related to the one constructed by A. Castro and R. Montgomery?*

We have found no simple precise correspondence, however we will establish here a tight relation between the two codings which will hold on classes of low codimension, which means that the corresponding codes consist primarily of 1's or of R's. It is also worth pointing out that at the time this thesis was written that F. Pelletier and M. Slayman had been able to establish a dictionary between Mormul's coding system and RVT code for words of length at most 4 ([PS12]).

Extended Kumpera-Ruiz System.

We begin by explaining Mormul's *Extended Kumpera-Ruiz* coding system. Consider data consisting of a rank-3 distribution germ framed by local vector fields (Z_1, Z_2, Z_3) and endowed with local coordinates $u_1, ..., u_s$. Mormul defined three operations on this data, which he labels $\mathbf{1}, \mathbf{2}, \mathbf{3}$, whose output is new data of the same type, on a space of two dimensions more. The three operations correspond to the three standard affine charts of $\mathbb{P}^2$. The new coordinates are written $u_1, \cdots, u_s, x_l, y_l$. This new framing is written $(Z_1^{(1)}, Z_2^{(1)}, Z_3^{(1)})$. In all three cases $Z_2^{(1)} = \frac{\partial}{\partial x_l}$ and $Z_3^{(1)} = \frac{\partial}{\partial y_l}$. $Z_1^{(1)}$ alone depends on which operation is used, and is defined by

$$Z_1^{(1)} = \begin{cases} Z_1 + (b_l + x_l)Z_2 + (c_l + y_l)Z_3 & \text{when } \mathbf{k = 1} \\ x_l Z_1 + Z_2 + (c_l + y_l)Z_3 & \text{when } \mathbf{k = 2} \\ x_l Z_1 + y_l Z_2 + Z_3 & \text{when } \mathbf{k = 3} \end{cases}$$

The b_l's and c_l's are constants that may or may not be equal to zero, the details of which we leave to Mormul's paper.

Mormul initiates his procedure as we do, with the base data of $\mathbb{R}^3$. He uses coordinates (t, x, y), distribution the whole tangent bundle, and framing the coordinate framing $(\frac{\partial}{\partial t}, \frac{\partial}{\partial x}, \frac{\partial}{\partial y})$. He repeatedly applies one of his 3 operations $\mathbf{k}$ to produce a sequence of new rank 3 distributions, labeling the distributions (or data) according to the order of application of the operations.

Mormul calls the resulting words $\mathbf{j_1 j_2 \cdots j_k}$ or their associated singularity classes of distributions "EKRs" (for "Extended Kumper-Ruiz"). These words obey two spelling rules. The first asserts that the first letter is $\mathbf{1}$. The second rule Mormul calls the "least upwards jump" rule and it asserts that if $\mathbf{j_{l+1}} > \mathbf{max}(\mathbf{j_1}, \cdots, \mathbf{j_l})$, then $\mathbf{j_{1+l}} = \mathbf{1} + \mathbf{max}(\mathbf{j_1}, \cdots, \mathbf{j_l})$ for $l = 1, 2, ..., r-1$. For example, the word $\mathbf{1.3}$ is not allowed, but the word $\mathbf{1.2.1.3}$ is allowed since the number $\mathbf{2}$ has been introduced.

Singularity Class Coding.

Mormul shows that his coding is intrinsic by constructing another coding, called *Singularity Class* coding, which is manifestly invariant, being based on the sandwich lemma of ([MZ01]) and establishing the equality of this codings with the EKR coding.

$\mathbf{1.1 \ldots 1} = RR \ldots R$.

The class of Cartan points correspond to Mormul's code $\mathbf{1.1 \ldots 1}$ and to our code $RR \ldots R$.

$\mathbf{1 \ldots 1.2} = R \ldots RC$.

We begin with $\mathbf{1.2} = RC$. Start with $\mathbf{1}$ and its associated framing $Z_1^{(1)} = \frac{\partial}{\partial x} + u_1^1 \frac{\partial}{\partial y} + u_2^1 \frac{\partial}{\partial z}$, $Z_2^{(1)} = \frac{\partial}{\partial u_1^1}$, $Z_3^{(1)} = \frac{\partial}{\partial u_2^1}$. The Pfaffian equations annihilating this framing are:

$$dy - u_1^1 dx = 0$$
$$dz - u_2^1 dx = 0$$

which are identical to the equations defining Δ_1 locally. Now apply operation 2 to get the framing $Z_1^{(2)} = u_1^2 Z_1^{(1)} + \frac{\partial}{\partial u_1^1} + u_2^2 \frac{\partial}{\partial u_2^1}$, $Z_2^{(2)} = \frac{\partial}{\partial u_1^2}$, $Z_3^{(2)} = \frac{\partial}{\partial u_2^2}$ which represents those germs with code $\mathbf{1.2}$.

We compare with our code RC. Let $p_2 \in \mathcal{P}^2$ be written $p_2 = (p_1, \ell)$ with $\ell \subset \Delta_1(p_1)$. Then $\Delta_2(p_2) = d\pi^{-1}_{(p_1,\ell)}(\ell)$. A basis for $\Delta_1^*(p_1)$ is dx, du_1^1, du_2^1. The line ℓ has homogeneous coordinates $[dx, du_1^1, du_2^1]$. Let us assume that $p_2 \in RC$ which is to say that the line ℓ is vertical. Then $dx = 0$ along ℓ. We may assume, without loss of generality, that $du_1^1 \neq 0$ along ℓ. Then we divide by du_1^1 to get affine coordinates in a neighborhood of ℓ: $[dx : du_1^1 : du_2^1] = [\frac{dx}{du_1^1} : 1 : \frac{du_2^1}{du_1^1}]$. The affine coordinates are $u_1^2 = \frac{dx}{du_1^1}$ and $u_2^2 = \frac{du_2^1}{du_1^1}$.

Now, we return to our old frame $Z_1^{(1)}, Z_2^{(1)}, Z_3^{(1)}$ for Δ_1 derived above. We can also write $\ell = span\{aZ_1^{(1)} + bZ_2^{(1)} + CZ_3^{(1)}\}$ in which case $[a : b : c] = [dx : du_1^1 : du_2^1]$. Thus $\ell = span\{aZ_1 + b\frac{\partial}{\partial u_1^1} + c\frac{\partial}{\partial u_2^1}\} = span\{\frac{a}{b}Z_1^{(1)} + \frac{\partial}{\partial u_1^1} + \frac{c}{b}\frac{\partial}{\partial u_2^1}\} = span\{u_1^2 Z_1^{(1)} + \frac{\partial}{\partial u_1^1} + u_2^2\frac{\partial}{\partial u_2^1}\}$. A moment's thought now shows that we can indeed let the fiber coordinates vary, thus varying ℓ and that Δ_2 in a neighborhood of p_2 is spanned by three vector fields having exactly the expression given by $Z_1^{(2)}$, $Z_2^{(2)}$, $Z_3^{(2)}$ as given above. This shows that $\mathbf{1.2} = RC$. A nearly identical argument shows that $\mathbf{1} \ldots \mathbf{1.2} = \mathbf{R} \ldots \mathbf{RC}$.

For future use, the Pfaffian equations defining Δ_2 near p_2 are :

$$dy - u_1^1 dx = 0$$
$$dz - u_2^1 dx = 0$$
$$dx - u_1^2 du_1^1 = 0$$
$$du_2^1 - u_2^2 du_1^1 = 0$$

5.7.1 $\mathbf{1.2.1} = RVR \cup RVT$

Apply the operation **1** to the previous frame to obtain the frame
$Z_1^{(3)} = Z_1^{(2)} + u_1^3\frac{\partial}{\partial u_1^2} + u_2^3\frac{\partial}{\partial u_2^2}$, $Z_2^{(3)} = \frac{\partial}{\partial u_1^3}$, $Z_3^{(3)} = \frac{\partial}{\partial u_2^3}$
representing germs in the class **1.2.1**.

We compare this framing with one for Δ_3 in a neighborhood of points whose code is either RVR or RVT. Let $p_3 = (p_2, \ell) \in \mathcal{P}^3$ be in the class RVR or RVT. From above, we see that $\Delta_2^*(p_2)$ has basis du_1^1, du_1^2, du_2^2 and so homogenous fiber coordinates for ℓ are $[du_1^1 : du_1^2 : du_2^2]$. Since the RVT code of p_3 does not end with a V or an L we must have that $du_1^1 \neq 0$ along ℓ so we divide by du_1^1 to get the affine coordinates

$u_1^3 = \frac{du_1^2}{du_1^1}$, $u_2^3 = \frac{du_2^2}{du_1^1}$. In either case, we get that Δ_3, in a neighborhood of p_3, is given by

$$dy - u_1^1 dx = 0$$
$$dz - u_2^1 dx = 0$$
$$dx - u_1^2 du_1^1 = 0$$
$$du_2^1 - u_2^2 du_1^1 = 0$$
$$du_1^2 - u_1^3 du_1^1 = 0$$
$$du_2^2 - u_2^3 du_1^1 = 0$$

Using the previous expression for $Z_1^{(2)}$ we see that in a neighborhood of our p_3 the distribution is framed by $Z_1^{(2)} + u_1^3 \frac{\partial}{\partial u_1^2} + u_2^3 \frac{\partial}{\partial u_2^2}$, $\frac{\partial}{\partial u_1^3}$, $\frac{\partial}{\partial u_2^3}$ corresponding exactly to the expression for the framing $Z_1^{(3)}, Z_2^{(3)}, Z_3^{(3)}$ above. This shows us that the class **1.2.1** is the union of the two classes RVR and RVT.

5.7.2 1.2.1.2.1.2.1

The singularity class 1.2.1.2.1.2.1 will be of importance in the next section when discussing moduli within the $\mathbb{R}^3$ Monster Tower. Recall from the above that **1.2** $= RV$ and **1.2.1** $= RVR \cup RVT$. If we use the same reasoning as in the case of **1.2** we can show that

$$\textbf{1.2.1.2} = RVRV \cup RVTV$$

and we can then apply the same reasoning as we used in the case of **1.2.1** to show that

$$\textbf{1.2.1.2.1} = RVRVR \cup RVRVT \cup RVTVR \cup RVTVT.$$

When we iterate these arguments one more time we end up with the following:

$$\textbf{1.2.1.2.1.2} = RVRVRV \cup RVRVTV \cup RVTVRV \cup RVTVTV \text{ and}$$

$$\begin{aligned}\textbf{1.2.1.2.1.2.1} = {} & RVRVRVR \cup RVRVRVT \cup RVRVTVR \cup RVRVTVT \cup RVTVRVR \\ & \cup RVTVRVT \cup RVTVTVR \cup RVTVTVT\end{aligned}$$

5.7.3 1.2.3 $= RVL$

Recall the above expressions for the frame corresponding to **1.2**. Apply operation 3 to this frame to get the frame

$$Z_1^{(3)} = u_1^3 Z_1^{(2)} + u_2^3 \frac{\partial}{\partial u_1^2} + \frac{\partial}{\partial u_2^2}, Z_2^{(3)} = \frac{\partial}{\partial u_1^3}, Z_3^{(3)} = \frac{\partial}{\partial u_2^3}$$

realizing the normal form for the germs in Mormul's class **1.2.3**.

We compare this frame with a frame constructed for Δ_2 near a point $p_3 = (p_2, \ell)$ with RVT code RVL. The linear coordinates on Δ_2 near a point of type RV are du_1^1, du_1^2, du_2^2 so homogeneous coordinates are $[du_1^1, du_1^2, du_2^2]$. Since ℓ is an L direction we must have $du_1^1 = 0$ and $du_1^2 = 0$ along ℓ. (Recall that $du_1^1 = 0$ corresponds to vertical lines and $du_1^2 = 0$ corresponds to tangency lines.). This means that we must divide by du_2^2 to get the fiber affine coordinates in a neighborhood of p_3: $u_1^3 = \frac{du_1^1}{du_2^2}$, $u_2^3 = \frac{du_1^2}{du_2^2}$. Expressing points $\tilde{\ell}$ near ℓ as $span\{aZ_1^{(2)} + b\frac{\partial}{\partial u_1^2} + c\frac{\partial}{\partial u_2^2}\}$ we see that $span\{aZ_1^{(2)} + b\frac{\partial}{\partial u_1^2} + c\frac{\partial}{\partial u_2^2}\} = span\{\frac{a}{c}Z_1^{(2)} + \frac{b}{c}\frac{\partial}{\partial u_1^2} + \frac{\partial}{\partial u_2^2}\} = span\{u_1^3 Z_1^{(2)} + u_2^3\frac{\partial}{\partial u_1^2} + \frac{\partial}{\partial u_2^2}\}$. The expression inside the span is precisely the vector field Z_1^3 of Mormul's **1.2.3** frame above, with the two vertical vector fields corresponding to Mormul's Z_2^3 and Z_3^3. The coordinate expressions of the two frames agree, showing that **1.2.3** $= RVL$. A nearly identical computation shows that $R \ldots RVL = \mathbf{1}. \ldots . \mathbf{1.2.3}$.

Part II

Action Selectors and the Fixed Point Set of a Hamiltonian Diffeomorphism

Chapter 6

Introduction

In this part of the thesis we switch topics and focus on symplectic geometry. We will be working primarily within the area of Floer homology and cohomology, which was formulated by Andreas Floer in [Flo89(2)] and [Flo89(3)]. Floer theory is a version of infinite dimensional Morse Theory. We will begin by briefly describing the basics of Morse theory in order to establish this connection to Floer theory.

Morse theory is a homology theory that allows one to calculate the homology of a manifold M by using Morse functions, meaning functions that have nondegenerate critical points. Take $f : M \to \mathbb{R}$ to be a Morse function and we take each of the critical points p of f and assign to them an integer known as the index. The index of a critical point p is the number of negative eigenvalues in the Hessian of f at p. Using the index allows us to create the Morse chain complex $C_*(f) = \oplus_{k=0}^{n} C_k(f)$, where each $C_k(f)$ is the free abelian group generated by the critical points of index k. Next define a boundary operator $\partial_k : C_k(f) \to C_{k-1}(f)$ that comes from counting the negative gradient flow lines of f, along with their orientation, that originate from p and terminate at each of the critical points of index $k-1$. This allows us to define the Morse homology groups to be $HM_k(f;\mathbb{Z}) = ker(\partial_k)/im(\partial_{k+1})$, which is isomorphic to the singular homology groups $H_k(M;\mathbb{Z})$.

During the early 1980's symplectic geometers were interested in trying to extend the concepts of Morse theory to symplectic manifolds. Using Morse theory as motivation, they wanted to try and formulate a similar relationship between the one-periodic orbits of a Hamiltonian vector field and the homology of a symplectic manifold (M, ω). Conley and Zehnder were some of the first who tried to tackle this problem in

the $M = \mathbb{R}^{2n}$ setting ([CZ84]). They looked at a functional defined on the loop space of M given by

$$f(x(t)) = \int_0^1 (\frac{1}{2} < \dot{x}, Jx > -H_t(x(t)))dt,$$

where J is the standard symplectic structure on $\mathbb{R}^{2n}$ and H_t is a Hamiltonian that is one-periodic in time. Taking the first variation of this functional yields

$$\delta f(x) \cdot \xi = \int_0^1 < -J\dot{x} - \nabla H_t(x), \xi > dt \quad \text{for } \xi \in T_{x(t)}M$$

This means that the critical points of f will be one-periodic solutions to the Hamiltonian vector field X_H. However, while the second variation of f at an isolated one-periodic solution $x(t)$ gives rise to a bilinear form it can be shown that it will have an infinite number of both positive and negative eigenvalues. As a result of this, one can't really study the stable and unstable manifolds and give the same topological decomposition on M like in Morse theory. Conley and Zehnder though tried to work around this issue. They developed a version of the Morse index for the functional f at the one-periodic solutions of the Hamiltonian vector field generated by H_t. They also used a result due to Amann and Zehnder ([AZ80]) which allowed them to relate the critical loops of f to critical points of another functional that is defined on a finite dimensional space of trigonometric polynomials of fixed order. More specifically, the critical points of the functional defined on the finite dimensional space are in one to one correspondence with the critical points of f. By making this link to finite dimensional manifolds they wanted to try and look at a the gradient flow lines of the functional on this finite dimensional space. In order to do this, Conley and Zehnder established a connection between their Morse-type of index and then applied it to what they called the Morse decomposition of a topological space. This allowed them to develop a theory that connected their Morse-type of index to gradient-like flows on topological spaces and, hence, enabled them to take the first steps towards the generalization of Morse theory on symplectic manifolds.

By the late 1980's Floer was able to concretely establish the connection between the one-periodic solutions of Hamiltonian diffeomorphisms and the topology of a symplectic manifold. Floer homology is defined in a somewhat similar fashion, but this time we will assume that we are working with a symplectic manifold (M, ω). In the Floer setting, we begin with a time dependent Hamiltonian $H_t : M \to \mathbb{R}$, which is also one-period in time, and take $\bar{\mathcal{P}}(H)$ to be the set of contractible one-periodic capped

solutions to X_H, the Hamiltonian vector field generated by H. We replace the function f from the Morse case with the *action functional* given by

$$\mathcal{A}_H(\bar{x}) = -\int_u \omega + \int_0^1 H_t(x(t))dt$$

for capped loops $\bar{x} = (x, u)$, where x is the loop and u is the disc that is attached along the boundary of x. The critical points of $\mathcal{A}_H$ are the equivalence classes of capped loops $\bar{x}$ which are one-periodic solutions to the equation $\dot{x}(t) = X_H(t, x(t))$. Let g be a metric which is compatible with the symplectic form ω, meaning $\omega(X, JY) = g(X, Y)$ for all $X, Y \in TM$ and J is the almost complex structure on M. Then we can define a metric on the set of contractible one-periodic solutions to X_H given by $\tilde{g}(\xi, \zeta) = \int_0^1 g_{x(t)}(\xi_{x(t)}, \zeta_{x(t)})dt$, for any vector fields ξ, ζ along the one-periodic solution $x(t)$. By taking the gradient of $\mathcal{A}_H$ with respect to the metric $\tilde{g}$ we have

$$grad(\mathcal{A}_H(x(t))) = J(x(t))\dot{x}(t) - \nabla H_t(x(t))$$

Just like in Morse theory, one is interested in trying to find a solution to the equation $\frac{dx}{ds} = -grad(\mathcal{A}_H(\bar{x})$. However, as is pointed out in [HZ11], it isn't possible to find a Banach manifold on which the vector field $grad(\mathcal{A}_H(\bar{x}))$ is defined. This leads us to looking instead at functions $u : \mathbb{R} \times S^1 \to M$ which are solutions to the Floer equation

$$\frac{\partial u}{\partial s} + J(u)\frac{\partial u}{\partial t} + \nabla H_t(u) = 0.$$

Then one uses the function $\mu_{CZ} : \bar{\mathcal{P}}(H) \to \mathbb{Z}$, called the Conley-Zehnder index ([SZ92]), to create the Floer chain complex. Take $CF_k(H)$ to be free abelian group generated by the one-periodic contractible loops of X_H that have Conley-Zehnder index equal to k. The boundary map $\partial_k : CF_k(H) \to CF_{k-1}(H)$, at least in the $\mathbb{F} = \mathbb{Z}_2$ case, counts the number of flow lines from one-periodic loops $\bar{x}$ with $\mu_{CZ}(\bar{x}) = k$ to one-periodic loops $\bar{y}$ with $\mu_{CZ}(\bar{y}) = k - 1$. For a more general field $\mathbb{F}$, the boundary map is a little bit more involved to describe, see [FH93]. We then end up with the Floer homology groups $HF_k(H) = ker(\partial_k)/im(\partial_{k+1})$. From looking at the way the Floer homology is defined one can see the similarities between the Morse and Floer homology and how Floer theory is an extension of the Morse setting.

In the following sections for this part of the thesis we use Floer theory in order to study the relationship between action selectors and the fixed point set for a Hamiltonian diffeomorphism defined on a closed monotone symplectic manifold. In

particular, we are interested in understanding the size of the fixed point set for a time dependent Hamiltonian whose action selectors satisfy a specific condition. We use the Arnold Conjecture as a starting point for the statement of the main results. The *Arnold Conjecture* states that every Hamiltonian diffeomorphism ϕ_H of a compact symplectic manifold (M, ω) possesses at least as many fixed points as a function $f : M \to \mathbb{R}$ possesses critical points. The weaker form of this conjecture asserts that the number of fixed points for ϕ_H is bounded below by the cuplength of the manifold plus one, i.e. $\#Fix(\phi_H) \geq CL(M)+1$. The $\mathbb{F}$-*cuplength of* M, denoted $CL(M)$, of a topological space M is the maximal integer k such that there exists classes $\alpha_1, \cdots, \alpha_k$ in the cohomology ring $H^{*>0}(M; \mathbb{F})$ satisfying

$$\alpha_1 \cup \cdots \cup \alpha_k \neq 0.$$

While the Arnold Conjecture is still an open problem in the case when M is a general rational, weakly monotone manifold, it has been proven in the symplectically aspherical case ([Flo89(1)], [Hof88]). Suppose for the moment that M is symplectically aspherical. As is well known, one can use the basic properties and results concerning action selectors to prove the Arnold Conjecture when the Hamiltonian diffeomorphism has isolated fixed point, see e.g. [GG09]. This is accomplished by using the spectrality properties of action selectors, meaning $c^\alpha(H) \in \mathcal{S}(H)$ where $\alpha \in H^*(M)$, H is a Hamiltonian, $c^\alpha(H)$ denoting our action selector, and $\mathcal{S}(H)$ the action spectrum. Using this fact, one is able to establish the following bound on the size of $\mathcal{S}(H)$:

$$\#\mathcal{S}(H) \geq CL(M) + 1,$$

which in turn implies $\#Fix(\phi_H) \geq CL(M) + 1$. Now, when H instead satisfies the condition $\#\mathcal{S}(H) < CL(M) + 1$, it necessarily implies that the fixed point set for ϕ_H can't be isolated. As a result, this presents us with the following question: "How large" is the set $Fix(\phi_H)$ when $\#\mathcal{S}(H) < CL(M) + 1$?
This leads us to one of the main results.

Theorem 6.0.1 *Suppose that (M, ω) is a symplectic manifold, which is closed and symplectically aspherical and H is a time dependent Hamiltonian with the property $\#\mathcal{S}(H) < CL(M) + 1$. Let F denote the set of fixed points for the Hamiltonian diffeomorphism ϕ_H. Then $H^j(F) \neq 0$ for some $1 \leq j \leq 2n$.*

Remark 6.0.2 *Because we are assuming that M is symplectically aspherical, this allows us to keep track of the various orbits. Hence, when M is not symplectially aspherical then since the cappings are nontrivial this presents the problem of determining what the geometrically distinct orbits are for H.*

Theorem 6.0.1 will actually become an almost immediate corollary once the following result has been shown.

Theorem 6.0.3 *Let (M, ω) be a closed, monotone symplectic manifold, H be a time dependent Hamiltonian that is one-periodic in time and define F to be the fixed point set for the Hamiltonian diffeomorphism ϕ_H. Also assume that there exists cohomology elements $\alpha \in HQ^*(M)$, with $\alpha \neq 0$ and $HQ^*(M)$ the quantum cohomology of M, $\beta \in H^k(M)$ with $k > 0$, and satisfying the condition $c^{\alpha * \beta}(H) = c^{\alpha}(H)$. Then $H^k(F) \neq 0$ for $k = deg(\beta)$.*

Remark 6.0.4 *It is worth noting that Theorem 6.0.3 also holds in the negative monotone case as well.*

We would like to point out the similarity of Theorem 6.0.3 to a result due to Viterbo. In [Vit97] he deals with the Morse theoretic analogue of action selectors known as *critical value selectors* defined by the equation

$$c_{LS}^{\alpha}(f) = inf\{a \in \mathbb{R} | \alpha \neq 0 \, \text{in} \, H^*(M^a)\},$$

where $M^a = \{x \in M | f(x) \leq a\}$ and $f : M \to \mathbb{R}$ is at least C^1. Viterbo looks at the connection between the critical points of the function f and the the critical value selectors. He establishes that when M is a Hilbert manifold, f a C^1-function on M satisfying the Palais-Smale condition, and for any $\alpha, \beta \in H^*(M)$ with cup-product $\alpha \cup \beta \neq 0$ in $H^*(M^a)$, then $c_{LS}^{\alpha \cup \beta}(f) \leq c_{LS}^{\alpha}(f)$. When $c_{LS}^{\alpha \cup \beta}(f) = c_{LS}^{\alpha}(f)$, F_a the set of critical points of f at level $a = c_{LS}^{\alpha}(f)$; then β is nonzero on $H^*(F_a)$. As a result, $dim(F_a) \geq deg(\beta)$ and hence F_a is uncountable when $deg(\beta) \neq 0$.

Based on this result by Viterbo it is suspected that Theorem 6.0.3 should hold for a more general element β in the cohomology ring $HQ_-^*(M) = H^{*<2n}(M) \otimes \Lambda$. In future work we hope to extend Theorem 6.0.3 for $\beta \in HQ_-^*(M)$ and possibly when the manifold is weakly monotone as well.

Chapter 7

Preliminaries

This chapter will outline the necessary background from symplectic geometry needed to understand the above results.

7.1 Symplectic Manifolds

Throughout this part of the thesis we will assume that (M, ω) is a closed symplectic manifold, i.e. M is compact and $\partial M = \emptyset$. The manifold M is *monotone* if $[\omega]|_{\pi_2(M)} = \lambda c_1(M)|_{\pi_2(M)}$ for some non-negative constant λ. A *negative monotone* manifold satisfies the same condition, but with $\lambda \leq 0$. The manifold M is *rational* if $< [\omega], \pi_2(M) >= \lambda_0 \mathbb{Z}$, where $\lambda_0 \geq 0$. When $< c_1(M), \pi_2(M) >$ is a discrete subgroup of $\mathbb{R}$, then we call the positive generator N of this subgroup the *minimal Chern number*. When M has the property $[\omega]|_{\pi_2(M)} = 0 = c_1(M)|_{\pi_2(M)}$, then M is called *symplectically aspherical*.

In this thesis we will be working with time dependent Hamiltonians H. More specifically, we are going to be dealing with Hamiltonians which are one-periodic in time, meaning $H : S^1 \times M \to \mathbb{R}$ with $S^1 = \mathbb{R}/\mathbb{Z}$ and $H_t(\cdot) = H(t, \cdot)$ for $t \in S^1$. Let X_H denote the time dependent vector field that H generates, where X_H satisfies $i_{X_H}\omega = -dH$. Let ϕ_H^t denote the time dependent flow for the vector field X_H.

In this thesis we are interested in studying the time-one map of ϕ_H^t. We call the map $\phi_H := \phi_H^1$ a *Hamiltonian diffeomorphism*.

Let K and H be time dependent Hamiltonians, then we define $(K\#H)_t :=$

$K_t + H_t \circ (\phi_K^t)^{-1}$. The flow for the time dependent vector field generated by the Hamiltonian $K\#H$ is the composition $\phi_K^t \circ \phi_H^t$. As an aside, the composition $K\#H$ may not necessarily be one-periodic in time. If, however, $H_0 = 0 = H_1$, then the composition is one-periodic. One is able to impose this condition on H by reparametrizing H as a function of time without changing its time-one map. This allows us to treat $K\#H$ as a one-periodic Hamiltonian.

7.2 Filtered Floer Homology and Filtered Floer Cohomology

7.2.1 Capped periodic orbits and filtered Floer homology

In this section we begin by introducing the basics of Floer homology. We plan on only presenting the basic elements of Floer homology. For a more in depth discussion and for more on the specific details we refer the reader to [MS04], [HZ11], [BH05].

We start by looking at the contractible loops $x : S^1 \to M$. Since x is contractible we can attach a disk along the the boundary of the loop, which produces a new mapping $u : D^2 \to M$ with $u|_{S^1}(t) = x(t)$. We call the map u a *capping* of the loop x and use the notation $\bar{x}$ to represent the pair (x, u). Let u_1 and u_2 be two cappings for the loop x. The two cappings are equivalent if the integrals of ω and $c_1(M)$ over the sphere formed by the connected sum $u_1\#(-u_2)$ is equal to zero. In the symplectically aspherical case all cappings of a fixed loop x are equivalent. Let $\mathcal{P}(H)$ be the set of contractible one-periodic solutions to X_H and $\bar{\mathcal{P}}(H)$ be the set of contractible capped one-periodic solutions to X_H.

The cappings of these loops allows us to define the *action functional* $\mathcal{A}_H$ for a time dependent Hamiltonian H. For a capped loop $\bar{x} = (x, u)$ we define

$$\mathcal{A}_H(\bar{x}) = -\int_u \omega + \int_0^1 H_t(x(t))dt.$$

The critical points for the action functional are the equivalence classes of capped loops $\bar{x}$ which are one-periodic solutions to the equation $\dot{x}(t) = X_H(t, x(t))$. The set of critical values for the action functional is called the *action spectrum* of H and is denoted by $\mathcal{S}(H)$. The action spectrum is a set of measure zero. In addition, when the manifold M is rational, $\mathcal{S}(H)$ is a closed set and implies it is a nowhere dense set ([HZ11]).

Following the terminology used in [SZ92], we will call a capped one-periodic orbit $\bar{x}$ of H *non-degenerate* if the pushforward $d\phi_H : T_{x(0)}M \to T_{x(0)}M$ has no eigenvalues equal to one. When all of the one-periodic orbits of H are non-degenerate, then we say H is *non-degenerate*. Note that the condition of degeneracy does not depend on the capping of the loop $x(t)$.

Whenever we are working with a non-degenerate Hamiltonian H we will end up with a finite number of elements in the set $\bar{\mathcal{P}}(H)$. By fixing a field $\mathbb{F}$ (i.e. $\mathbb{Z}_2, \mathbb{Q}, \mathbb{C}$) we can use the Conley-Zehnder index, denoted μ_{CZ}, to impose a grading on the vector space that is generated by the elements in the set $\bar{\mathcal{P}}(H)$ over $\mathbb{F}$. Define $CF_k^{(-\infty,b)}(H)$, for $b \in (-\infty, \infty]$ and b not an element in the set $\mathcal{S}(H)$, to be the vector space of sums given by

$$\sum_{\bar{x} \in \bar{\mathcal{P}}(H)} a_{\bar{x}} \bar{x},$$

with $a_{\bar{x}} \in \mathbb{F}$, $\mu_{CZ}(\bar{x}) = k$, $\mathcal{A}_H(\bar{x}) < b$, and the number of terms in the sum with $a_{\bar{x}} \neq 0$ is semi-finite, meaning for every $c \in \mathbb{R}$ the number of terms with $a_{\bar{x}} \neq 0$ and $\mathcal{A}_H(\bar{x}) > c$ is finite. There is a linear boundary operator $\partial : CF_k^{(-\infty,b)}(H) \to CF_{k-1}^{(-\infty,b)}(H)$, where for $\bar{x} \in \bar{\mathcal{P}}(H)$ with $\mu_{CZ}(\bar{x}) = k$ is defined to be

$$\partial \bar{x} = \sum_{\mu_{CZ}(\bar{y}) = k-1} n(\bar{x}, \bar{y}) \bar{y}$$

and $\partial^2 = 0$. When $\mathbb{F} = \mathbb{Z}_2$ the number $n(\bar{x}, \bar{y})$ counts the number of components in the 1-dimensional moduli space $\mathcal{M}(\bar{x}, \bar{y})$ *mod* 2. For a more general field $\mathbb{F}$, the number $n(\bar{x}, \bar{y})$ is a bit more involved to describe and we refer the reader to [FH93]. One can further define $CF_k^{(a,b)}(H) := CF_k^{(-\infty,b)}(H)/CF_k^{(-\infty,a)}(H)$, for $-\infty \leq a < b \leq \infty$ not in $\mathcal{S}(H)$. The above construction results in what is known as the *filtered Floer homology* of H and is denoted by $HF_*^{(a,b)}(H)$. Note when $(a, b) = (-\infty, \infty)$ we end up with the standard Floer homology $HF_*(H)$.

Since the results of this part of the thesis deal with Hamiltonians that are degenerate, it is worth pointing out that filtered Floer homology can be defined in the degenerate case. Take H to be a Hamiltonian on M with $a, b \notin \mathcal{S}(H)$ and M to be a rational manifold. By virtue of the fact that we can always find a non-degenerate Hamiltonian $\tilde{H}$ from an arbitrarily small perturbation of H it allows us to define

$$HF_*^{(a,b)}(H) = HF_*^{(a,b)}(\tilde{H}).$$

7.2.2 Filtered Floer cohomology

Now that the basics of Floer homology have been presented it then becomes a fairly straightforward process to explain the setup for the Floer cohomology.

We again take H to be a non-degenerate Hamiltonian and R to be a fixed commutative ring. Define the cochain complex $CF^*(H)$ to be the set of functions $\alpha : \bar{\mathcal{P}}(H) \to R$ that satisfy the finiteness condition $\#\{\bar{x} \in \bar{\mathcal{P}}(H) \,|\, \alpha(\bar{x}) \neq 0, \mathcal{A}_H(\bar{x}) \leq c\} < \infty$ for every real number c. Define the *filtered Floer chain complex* by $CF^k_{(-\infty,b)}(H)$ for $b \in (-\infty, \infty]$ and b not in $\mathcal{S}(H)$ to be the vector space of formal sums

$$\sum_{\bar{x} \in \bar{\mathcal{P}}(H)} \alpha_{\bar{x}} \alpha,$$

where $\mu_{CZ}(\bar{x}) = k$ and $\alpha(\bar{x}) \neq 0$. Also, using the same numbers $n(\bar{x}, \bar{y})$ from the Floer chain complex determines a linear coboundary operator $\delta : CF^k_{(-\infty,b)}(H) \to CF^{k+1}_{(-\infty,b)}(H)$, given by

$$\delta\alpha(\bar{x}) = \sum_{\mu_{CZ}(\bar{y})=k+1} n(\bar{x}, \bar{y})\alpha(\bar{y}),$$

where $\bar{x} \in \bar{\mathcal{P}}(H)$, $\mu_{CZ}(\bar{x}) = k$, and satisfies $\delta^2 = 0$. We define $CF^k_{(a,b)}(H) := CF^k_{(-\infty,b)}(H)/CF^k_{(-\infty,a)}(H)$, for $-\infty \leq a < b \leq \infty$ which are not elements of $\mathcal{S}(H)$. This results in giving us the *filtered Floer cohomology* of H and is denoted by $HF^*_{(a,b)}(H)$.

Just like the case of Floer homology, we can also define the filtered Floer cohomology for a degenerate Hamiltonian H by choosing a non-degenerate Hamiltonian $\tilde{H}$ that is close to H and setting

$$H^*_{(a,b)}(H) = H^*_{(a,b)}(\tilde{H}).$$

7.3 Quantum Cohomology

The *quantum cohomology* is obtained by tensoring the cohomology ring $H^*(M)$ with the Novikov ring Λ over a field $\mathbb{F}$, i.e.

$$HQ^*(M) = H^*(M) \otimes_{\mathbb{F}} \Lambda.$$

Let $\alpha \in H^*(M)$ and $A \in \Lambda$, then the degree of the generator $\alpha \otimes e^A$ is given by $deg(\alpha \otimes e^A) = deg(\alpha) + I_{c_1}(A)$. This leads to a grading on $HQ^*(M)$ where the cohomology

classes of degree k are elements in the direct sum

$$QH^k(M) = \oplus_{i=0}^{k} H^i(M) \otimes_{\mathbb{F}} \Lambda^{k-i}.$$

One can also take $\Lambda = \mathbb{Z}[q, q^{-1}]$, which is the ring of Laurent polynomials.[1] This is done by sending the element $e^A \mapsto q^{c_1(A)/N}$, where N is the minimal Chern number, and q is a variable of degree $2N$. This results in the isomorphism $QH^k(M) \cong QH^{k+2N}(M)$ for all k when we multiply the quantum cohomology elements by q.

There is also a product structure defined on the quantum cohomology: let $\alpha \in HQ^k(M)$, $\beta \in HQ^l(M)$, then the *quantum cup product* of α with β is given by

$$\alpha * \beta = \sum_A (\alpha * \beta)_A q^{c_1(A)/N},$$

where $deg(\alpha * \beta) = deg(\alpha) + deg(\beta)$ and each of the cohomology classes $(\alpha * \beta)_A \in H^{k+l-2c_1(A)}(M)$ are defined by the Gromov-Witten invariants $GW^M_{A,3}$. The invariants $GW^M_{A,3}$ satisfy

$$\int_c (\alpha * \beta)_A = \int_M (\alpha * \beta)_A \cup \eta = GW^M_{A,3}(a, b, c),$$

where $c \in H_{k+l-2c_1(A)}(M)$, $a = PD(\alpha)$, $b = PD(\beta)$, $c = PD(\eta)$ and $deg(a) + deg(b) + deg(c) = 4n - 2c_1(A)$.[2] When this degree condition is not met, then $GW^M_{A,3}(a, b, c) = 0$. Also, when $c_1(A) = 0$ then $(\alpha * \beta)_A$ reduces to the cup product $\alpha \cup \beta$. One can also find a detailed presentation of Gromov-Witten invariants in [MS04].

7.4 The Classical Ljusternik-Schirelman Theory: Critical Value Selectors and Action Selectors

In order to prove Theorems 6.0.1 and 6.0.3 we will use tools from the Ljusternik-Schnirelmann theory known as critical value selectors and action selectors. The action selectors, also known as spectral invariants in the literature, are the Floer theoretic version of critical value selectors.

7.4.1 Critical Value Selectors

Definition 7.4.1 (Critical Value Selectors)

[1] Note that instead of $\mathbb{Z}$ one can replace it with any commutative ring R with unit.

[2] Here, and in throughout, the notation "PD" stands for the Poincaré dual.

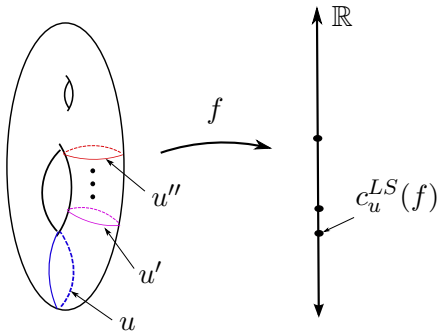

Figure 7.1: Critical value selector.

Let M be a n-dimensional manifold and $f \in C^\infty(M)$. For any $u \in H_*(M)$ we define the critical value selector by the formula

$$\begin{aligned} c_u^{LS}(f) &= inf\{a \in \mathbb{R} | u \in im(i^a)\} \\ &= inf\{a \in \mathbb{R} | j^a(u) = 0\}, \end{aligned}$$

where $i^a : H_*(\{x \in M | f(x) \leq a\}) \to H_*(M)$ and $j^a : H_*(M) \to H_*(M, \{x \in M | f(x) \leq a\})$ are the natural "inclusion" and "quotient" maps respectively.

One can think of the critical value selectors geometrically in terms of minimax principles. Take a nonzero homology class $u \in H_*(M)$, then one can think of $c_u^{LS}(f)$ to be the maximum value f takes on the any representative cycle $u' \in [u]$ that has been "pushed down" as far as possible within the manifold M, see Figure 1. So, when f is a Morse function then we can write

$$c_u^{LS}(f) = min \ \ max_{[u]=u'}\{f(x) \,|\, x \in u'\}.$$

The following is a listing of some useful properties concerning critical value selectors.

- By definition, $c_0^{LS}(f) = -\infty$. When $f \equiv$ const then $c_u^{LS}(f) \equiv$ const as well, and for any nonzero $\lambda \in \mathbb{F}$, $c_{\lambda u}^{LS}(f) = c_u^{LS}(f)$. For any function f we have

$$c_1^{LS}(f) = min(f) \leq c_u^{LS}(f) \leq max(f) = c_{[M]}^{LS}(f).$$

- Continuity: $c_u^{LS}(f)$ is Lipschitz with respect to the C^0-topology.

- Triangle Inequality: $c^{LS}_{u\cap w}(f+g) \leq c^{LS}_u(g) + c^{LS}_w(g)$.
- Criticality or minimax principle: $c^{LS}_u(f)$ is a critical value of f.
- $c^{LS}_{u\cap w}(f) \leq c^{LS}_u(f)$, also, if $w \neq [M]$ and the critical points of f are isolated, we have strict inequality $c^{LS}_{u\cup w}(f) < c^{LS}_u(f)$.

7.4.2 The Hamiltonian Ljusternik–Schnirelman theory: action selectors

In this section we present the definition and outline the fundamental properties pertaining to action selectors on cohomology. The action selectors are defined in a somewhat similar manner, where one big difference is the function $f : M \to \mathbb{R}$ is replaced by the action functional $\mathcal{A}_H$ for some Hamiltonian H. There are numerous sources on the subject of spectral invariants. Some of the first instances concerning the theory can be found in [HZ11], [Vit92]. A thorough treatment of the symplecticially aspherical case can be found in [Sch00]. Other known sources can be found in [EP03], [EP09], [Gin05], [GG09], [MS04]. We will be primarily following the definitions and results found in [Oh05].

Definition 7.4.2 (Action Selectors on Cohomology) *For any nonzero element $\alpha \in HQ^*(M) \cong HF^*(H)$ we define the action selector on cohomology by the formula*

$$\begin{aligned} c^\alpha(H) &= inf\{a \in \mathbb{R} - \mathcal{S}(H) | PD(\alpha) \in im(i^a_*)\} \\ &= inf\{a \in \mathbb{R} - \mathcal{S}(H) | j^a_*(PD(\alpha)) = 0\}, \end{aligned}$$

where $i^a_* : HF^{(-\infty,a)}_*(H) \to HF_*(H)$ and $j^a_* : HF_*(H) \to HF^{(a,\infty)}_*(H)$ are the "inclusion" and "quotient" maps respectively.

When H is a non-degenerate Hamiltonian we can write

$$c^\alpha(H) = \inf_{[\sigma]=a} \mathcal{A}_H(\sigma),$$

where $a = PD(\alpha)$ and $\mathcal{A}_H(\sigma) = max\{\mathcal{A}_H(\bar{x}) | \sigma_{\bar{x}} \neq 0\}$ for $\sigma = \sum \sigma_{\bar{x}} \bar{x} \in CF_*(H)$. Just like critical value selectors, one can formulate a geometrical interpretation of the actions selectors, where they take the various capped one-periodic orbits representing a particular cohomology class and push the "energy" down as far as possible.

From the above definitions we point out some of their useful properties.

- Projective invariance: $c^{\lambda\alpha}(H) = c^{\alpha}(H)$ for any $\lambda \in \mathbb{Q}$, $\lambda \neq 0$.
- Symplectic invariance: $c^{\alpha}(\phi^* H) = c^{\alpha}(H)$ for any symplectic diffeomorphism ϕ.
- Lipschitz continuous: c^{α} is Lispschitz continuous in the C^0-topology on the space of Hamiltonians H. In particular, $|c^{\alpha}(H) - c^{\alpha}(K)| \leq \|H - K\|$, where $\|\cdot\|$ is the Hofer norm.
- Triangle inequality: $c^{\alpha * \beta}(H \# K) \leq c^{\alpha}(H) + c^{\beta}(K)$.
- Hamiltonian shift: $c^{\alpha}(H + a(t)) = c^{\alpha}(H) + \int_0^1 a(t)dt$, where $a : S^1 \to \mathbb{R}$.
- Homotopy invariance: Let H and K be two Hamiltonians which are homotopic to each other, then we have $c^{\alpha}(H) = c^{\alpha}(K)$, for all $\alpha \in QH^*(H)$.
- Spectrality: When M is a rational manifold and H is a one-periodic Hamiltonian on M, then $c^{\alpha}(H) \in \mathcal{S}(H)$.

Let $\widetilde{\mathcal{H}am}(M, \omega)$ be the universal covering space for the group of Hamiltonian diffeomorphisms $\mathcal{H}am(M, \omega)$. It is worth mentioning that one can also look at the action selectors c^{α} as functions from $\widetilde{\mathcal{H}am}(M, \omega)$ to the reals ([Oh05]).

Remark 7.4.1 *We also point out that one can define the action selectors on the homology of M for any Hamiltonian H. In the non-degenerate case one can define the action selector on the elements $u \in HQ_*(M)$ by $c_u(H) = \inf_{[\sigma]=u} \mathcal{A}_H(\sigma)$ for $\sigma = \sum a_{\bar{x}} \bar{x} \in CF_*(M)$. The action selectors on homology also satisfy similar properties for to the ones on cohomology. The details of which are outlined in [GG09] and [Oh05]. There is one property in particular which interests us: $c_u(H) = c_u^{LS}(H)$ for $u \in H_*(M)$ and for H an autonomous and C^2-small Hamiltonian. Also, based on the definitions for action selectors on cohomology and homology we see they share the relationship $c^{\alpha}(H) = c_{PD(\alpha)}(H)$. Putting these two facts together we end up with $c^{\alpha}(H) = c^{LS}_{PD(\alpha)}(H)$ when H is autonomous and C^2-small.*

7.5 Alexander-Spanier Cohomology

Our last preliminary that needs to be introduced is a version of cohomology due to J.M. Alexander and E.H. Spanier. We will be primarily following the exposition given in [HZ11], [Mas91], [Spa81].

Begin by fixing a subspace $A \subset M$ and define $\mathcal{O}_A$ to be the set of all open neighborhoods of the subset A. One is then able to define an ordered structure on this set in the following manner: for $U, V \in \mathcal{O}_A$ we say $U \leq V$ if and only if $V \subseteq U$. We call $(\mathcal{O}_A, \leq)$ the *directed system of neighborhoods for the set A*.

Now let $\mathcal{C}$ to be the category of all subspaces of the manifold M and the category $\mathcal{A}$ to be an algebraic category, which, for our purposes, will either be the category of abelian groups, the category of commutative rings, or the category of modules over a fixed ring. Define a continuous functor $H : \mathcal{C} \to \mathcal{A}$ that takes continuous maps $f : V \to U$, for $U, V \in \mathcal{C}$ and maps it to a homomorphism $H(f) : H(U) \to H(V)$. If $U \leq V$ we can define the inclusion map $i_{VU} : H(U) \to H(V)$. From any directed system $\mathcal{O}_A$ we define $D_A := \bigoplus_{U \in \mathcal{O}_A} H(U)$ and the homomorphism $j_U : H(U) \to D_A$ as the inclusion map into the U-th component of D_A. Next take K_A to be the subring that is generated by elements of the form $j_U(\alpha_U) - j_V i_{VU}(\alpha_U)$ for $U \leq V$, $\alpha_U \in H(U)$. We denote the quotient of D_A by K_A by $dir\ \lim_{U \in \mathcal{O}_A} H(U) := D_A / K_A$, which we call the *direct limit of A*.

We define $\bar{H}^*(A; \mathbb{Z}) := dir\ \lim_{U \in \mathcal{O}_A} H^*(U; \mathbb{Z})$ to be the *Alexander-Spanier cohomology* for the subspace $A \subseteq M$. $H^*(U; \mathbb{Z})$ is the usual singular cohomology. The restriction maps from $H^k(U; \mathbb{Z})$ to $H^k(A; \mathbb{Z})$ end up defining a natural homomorphism from $\bar{H}^k(A; \mathbb{Z})$ to $H^k(A; \mathbb{Z})$. When this homomorphism is an isomorphism that holds for all k and any coefficient group, then we say the subspace A is *taut in M*. The following result gives us a useful list of criteria for when A will be taut in the manifold M.

Theorem 7.5.1 *In each of the following four cases the subspace A is taut in M:*

- *A is compact and M is Hausdorff.*
- *A is closed and M is paracompact Hausdorff.*
- *A is arbitrary and every open subset of M is paracompact Hausdorff.*
- *A is a retract of some open subset of M.*

7.6 Proofs of Theorems 6.0.1 and 6.0.3

We are now in a position to present the proofs for Theorems 6.0.1 and 6.0.3. We will begin by showing the monotone case result and then present the aspherical one.

Proof [Proof of Theorem 6.0.3]

We start by looking at the fixed points of ϕ_H which have associated action equal to $c^\alpha(H) = a$ and call this set F_a. Let $\delta > 0$ be small and define $F_{(a-\delta,a+\delta)}$ to be the set of all fixed points of ϕ_H that have their associated action in the interval $(a-\delta, a+\delta)$. We then take U_δ to be a neighborhood of the set $F_{(a-\delta,a+\delta)}$. We want to show $H^k(U_\delta) \neq 0$ for some $1 \leq k \leq 2n$ and for δ close to 0.

Suppose not and that $H^k(U_\delta) = 0$ for all $0 < k \leq 2n$ in order to arrive at a contradiction. Let $h : M \to \mathbb{R}$ be a C^2-small function on M where h is identically equal to zero on the neighborhood U_δ and outside of this set it is strictly negative. Let $\eta \in H^k(M)$, where $deg(\eta) > 0$. We can approximate the function h by a sequence of Morse functions that are at least C^2-small, call them h_n, such that $h_n \to h$ as $n \to \infty$ in the C^0-topology and for a fixed $x \in F_a$ we have $h_n(x) = 0$ only at this single point and strictly negative everywhere else. By making use of the fact that $c^{LS}_{PD(\eta)}(h_n) < 0$ for all $\eta \in H^k(M)$, with $k > 0$, and since c^η is Lipschitz in the C^0-topology we have $c^\eta(h) < -\delta_h < 0$ for all $\eta \in H^k(M)$ with $k > 0$ and δ_h is a positive constant depending on the function h. It is worth noting that we cannot say the same thing about $PD(\alpha)$ because it is possible that $PD(\alpha) = [M]$, which implies $c^\alpha(h) = c^{LS}_{[M]}(h) = max(h) = 0$.

Define $r : S^1 \to \mathbb{R}$ to be a nonnegative, C^2-small function, equal to zero outside of a small neighborhood of zero in S^1. Set $f_t = r(t)h$. This means that the Hamiltonian flow of f will be a reparametrization of the flow of h through time $\epsilon = \int_0^1 r(t)dt$.

Next we look at the family of Hamiltonians $H\#(sf)$ for $s \in [0,1]$. By the construction of f we have $H\#(sf) = H$ on the set U_δ, but outside of the set U_δ it is possible, for values of s close to 1, that $H\#(sf)$ has a 1-periodic orbit, say $\bar{x}$, such that $c^\alpha(H\#(sf)) = \mathcal{A}_{H\#(sf)}(\overline{x}) \neq a$. However, we claim that for small values of s that we can prevent this situation from occurring. In particular, we claim that one can find a nonzero s' in $[0,1]$ such that for all $0 \leq s \leq s'$ the Hamiltonians $H\#(sf)$ may have new 1-periodic orbits such that their action is not in $\mathcal{S}(H)$ and that their values may drift into the interval $(a-\delta, a+\delta)$, but by picking s' small enough these new critical values

for $H\#(s'f)$ cannot drift into the neighborhood $(a-\frac{\delta}{2}, a+\frac{\delta}{2})$. We will show this fact below in Lemma 7.6.1 and suppose for the time being that such an s' exists. Then for all $0 \leq s \leq s'$ we have $\mathcal{S}(H\#(sf)) \cap (a-\frac{\delta}{2}, a+\frac{\delta}{2}) = \mathcal{S}(H) \cap (a-\frac{\delta}{2}, a+\frac{\delta}{2})$.

Now, when h and a are sufficiently C^2- small, ϵh and f have the same periodic orbits, which are the critical point of h, and they have the same action spectrum. This is also true for the functions $\epsilon s'h$ and $s'f$. The same will be true for every function in the linear family $\tilde{f}_l = (1-l)\epsilon s'h + ls'f$, with $l \in [0,1]$, connecting $\epsilon s'h$ and $s'f$. Using the continuity property of c_u, the fact that each $\mathcal{S}(\tilde{f}_l)$ is a set of measure zero, and that $\mathcal{S}(\tilde{f}) = \mathcal{S}(\tilde{f}_l)$ for all l, we conclude that $c_{PD(\beta)}(s'f) = c_{PD(\beta)}(\epsilon s'h) < 0$.

We again use the continuity property of c^α and that the sets $\mathcal{S}(H\#(sf))$ have measure zero for all s to give us $c^\alpha(H\#(s'f)) = c^\alpha(H) = a$. Since $c^{\alpha*\beta}(H) = c^\alpha(H)$ we have $c^{\alpha*\beta}(H\#(s'f)) = c^{\alpha*\beta}(H)$ as well. We then use the following triangle inequality for action selectors to give

$$c^{\alpha*\beta}(H) = c^{\alpha*\beta}(H\#(s'f)) \leq c^\alpha(H) + c^\beta(s'f) = c^\alpha(H) + c_{PD(\beta)}(s'f) < c^\alpha(H)$$

and creates a contradiction to the fact that $c^{\alpha*\beta}(H) = c^\alpha(H)$. This means we must have $H^k(U_\delta) \neq 0$ for $k = deg(\beta)$.

Now let $\mathcal{O}_{F_a}$ be a directed system of neighborhoods for the set F_a. Then Theorem 7.5.1 along with the basic properties outlined in Section 7.5 almost immediately implies $H^k(F) \neq 0$ for $k = deg(\beta)$, which proves Theorem 6.0.3. □

With the above in mind, we are able to prove Theorem 6.0.1.

Proof [Proof of Theorem 6.0.1]

First recall the assumption that M is symplectically aspherical, let $CL(M) = m$ and let $\alpha_1, \cdots, \alpha_m$ be cuplength representative in $H^{*>0}(M)$. Using a result from [GG09] which in the symplectically aspherical case says that for $\alpha, \beta \in H^*(M)$ with $deg(\beta) > 0$ we have $c^{\alpha\cup\beta}(H) \leq c^\alpha(H)$. This gives us the following monotonically decreasing sequence

$$c^{\tilde{\alpha}_m}(H) \leq \cdots \leq c^{\tilde{\alpha}_1}(H) \leq c^{\tilde{\alpha}}(H)$$

with $\tilde{\alpha} = PD([M])$, $\tilde{\alpha}_1 = \alpha_1$, $\tilde{\alpha}_2 = \alpha_2 \cup \tilde{\alpha}_1$, $\cdots$, $\tilde{\alpha}_m = \alpha_m \cup \tilde{\alpha}_{m-1}$. Since each $c^\beta(H) \in \mathcal{S}(H)$ and $\#\mathcal{S}(H) \leq m$ it implies there must be equality somewhere in the above chain of inequalities. So, $c^{\tilde{\alpha}_{i+1}}(H) = c^{\tilde{\alpha}_i}(H)$ for some $1 \leq i \leq m$, or $\tilde{\alpha}_i = PD([M])$. Since $\tilde{\alpha}_{i+1} = \alpha_{i+1} \cup \tilde{\alpha}_i$ we just rename $\alpha_{i+1} = \beta$ and $\tilde{\alpha}_i = \alpha$ for notational convenience. This

means $c^{\alpha\cup\beta}(H) = c^{\alpha}(H)$ and as we have pointed out in Section 7.3 the quantum product in the symplectically aspherical case reduces to the cup product, i.e. $\alpha * \beta = \alpha \cup \beta$, so we can apply Theorem 6.0.3, which immediately gives us our result. □

Lemma 7.6.1 *There exists some nonzero s' in $[0,1]$ such that $\mathcal{S}(H\#(sf))$ does not gain any new critical values within the interval $(a - \frac{\delta}{2}, a + \frac{\delta}{2})$ for all $0 \leq s \leq s'$.*

Proof Suppose not and we cannot find such a number s'. This means we can find a sequence of s_n in $[0,1]$ where $s_n \to 0$ as $n \to \infty$ and that there exists a one-periodic orbit x_n of $X_{H\#(s_n f)}$ such that $\mathcal{A}_{H\#(s_n)f}(\overline{x}_n) = a_n$ with $lim_{n\to\infty} a_n = a$. Now, since $H\#(s_n f) = H$ on the set U_δ, it means the fixed points for $\phi_{H\#(s_n f)}$, with associated action $a_n \in \mathcal{S}(H\#(s_n f))$, can't be elements of the set U_δ.

Our next step is to show we can find a one-periodic orbit x_* for X_H with $\mathcal{A}(\overline{x}_*) = a$ that comes from some subsequence of the x_n's. In order to show this we will use the generalized Arzela Ascoli theorem for metric spaces which says the following: If X_1 is compact Hausdorff space, X_2 is a metric space, $C(X_1, X_2)$ be the set of continuous functions from X_1 to X_2, and let $\{f_n\}$ be a sequence of functions in $C(X_1, X_2)$ that is uniformly bounded and equicontinuous, then there exists a subsequence $\{f_{n_j}\}$ that converges uniformly. We apply this to our capped loops $\bar{x}_n$, taking $X_1 = [0,1]$ and $X_2 = M$. Let d be the distance function that comes from the Riemannian metric g on M. We want to first show that there exists some real number $L > 0$ such that $d(x_n(t), x_n(s)) \leq L|t - s|$ for all n. Note that since the manifold M is compact that there is a uniform bound on the $X_{H\#(s_n f)}$ where $\|X_{H\#(s_n f)}\| \leq L$ for some $L > 0$ and for all n. Since the distance between two points $p, q \in M$ is given by $d(p,q) = \inf_\gamma(L(\gamma))$ for $L(\gamma) = \int_a^b \|\dot{\gamma}(t)\|dt$ we have $d(x_n(t), x_n(s)) \leq \int_s^t \|\dot{x}_n(u)\|du = \int_s^t \|X_{H\#(s_n f)}(x_n)\|du \leq L|t-s|$. This shows that the family of curves $\{x_n\}$ is uniformly Lipschitz, which implies that this family of curves is uniformly bounded and equicontinuous. This means there is a subsequence $\{x_{n_j}\}$ that converges to the curve x_*. The curve x_* is only a continuous loop from $[0,1]$ to M, but we can use the following result which tells us that x_* is actually a smooth solution to X_H.

Proposition 7.6.2 *Assume that the sequence of Hamiltonian vector fields $X_{H_n} \to X_H$ as $n \to \infty$ in the C^0-topology and x_n is a solution to X_{H_n} and $x_n \to x_*$ in the C^0-topology. Then x_* is a solution to X_H.*

This means x_* is a one-periodic solution to X_H. Our next step is to show that $\mathcal{A}(H)(\overline{x}_*) = a$. Let $\epsilon > 0$. Since $\mathcal{A}_{H\#(s_nf)}(\overline{x}_n) = a_n$ we can find some N_1 such that for all $n > N_1$ we get $|a_n - a| < \frac{\epsilon}{3}$. At the same time, the Hamiltonians $H\#(s_nf) \to H$ in the C^1-topology and we can find some N_2 such that for all $n > N_2$ we have $|\mathcal{A}_H(\overline{x}) - \mathcal{A}_{H\#(s_nf)}(\overline{x})| < \frac{\epsilon}{3}$. Lastly, since the x_{n_j} converge uniformly to the one-periodic solution x_* of X_H we can find some N_3 such that for all $n_j > N_3$ we get that $|\mathcal{A}_H(\overline{x}_*) - \mathcal{A}_H(\overline{x}_{n_j})| < \frac{\epsilon}{3}$. Then for $N = max\{N_1, N_2, N_3\}$ we have for $n > N$ that $|\mathcal{A}_H(\overline{x}) - a| \leq |\mathcal{A}_H(\overline{x}_*) - \mathcal{A}_H(\overline{x}_{n_j})| + |\mathcal{A}_H(\overline{x}_{n_j}) - \mathcal{A}_{H\#(s_{n_j}f)}(\overline{x}_{n_j})| + |\mathcal{A}_{H\#(s_{n_j}f)}(\overline{x}_{n_j}) - a| < \epsilon$. Since this is true for every $\epsilon > 0$ it gives $\mathcal{A}_H(\overline{x}_*) = a$.

Our next step is to show that the fixed point $x_*(0) = x_*(1)$ for ϕ_H that has associated action $\mathcal{A}_H(\overline{x}_*) = a$ is a point that is outside of the U_δ. In order to do this we will look at the other fixed points p_{n_j} for $\phi_{H\#(s_{n_j}f)}$ that come from the loops x_{n_j}. In order to simplify the notation we will just relabel the points p_{n_j} to be p_n. Now, since M is a compact metric space we know that it is sequentially compact, meaning any sequence $\{y_n\}$ has a convergent subsequence $\{y_{n_j}\}$, and that the collection of points $\{p_n\}$ has a convergent subsequence $\{p_{n_j}\}$ that converges to the point p. In fact, the limit point p is a fixed point for ϕ_H, which we will show. Let $\epsilon > 0$ and we show that $d(\phi_H(p), p) < \epsilon$. Since $s_nf \to 0$ pointwise as $n \to \infty$ and since ϕ_H is continuous it implies that $\phi_{H\#(s_{n_j}f)} = \phi_H \circ \phi_{s_{n_j}f} \to \phi_H$ pointwise as $j \to \infty$. Then there exists some N_1 such that for all $n_j > N_1$ we have $d(\phi_H(p), \phi_{H\#(s_{n_j}f)}(p)) < \frac{\epsilon}{3}$. We can also find some N_2 such that for all $n_j > N_2$ that $d(\phi_{H\#(s_{n_j}f)}(p), \phi_{H\#(s_{n_j}f)}(p_{n_j})) < \frac{\epsilon}{3}$ and we can find an N_3 such that for all $n_j > N_3$ we get $d(p_{n_j}, p) < \frac{\epsilon}{3}$. For $n_j > N = max\{N_1, N_2, N_3\}$ we end up with $d(\phi_H(p), p) \leq d(\phi_H(p), \phi_{H\#(s_{n_j}f)}(p)) + d(\phi_{H\#(s_{n_j}f)}(p), \phi_{H\#(s_{n_j}f)}(p_{n_j})) + d(p_{n_j}, p) < \epsilon$. So, p is a fixed point for ϕ_H.

Let x be the loop formed by the curve $\phi_H^t(p)$ for $0 \leq t \leq 1$. Since both x_* and x are one-periodic solutions for X_H and they both have the point p on them, then by uniqueness of solutions of O.D.E.'s it forces $x_* = x$. Then, we end up with p being a fixed point of ϕ_H, which is on the curve x, and has the associated action $\mathcal{A}_H(\overline{x}) = a$. However, we have that p is the limit point of the points p_{n_j} and we know that $p_{n_j} \notin U_\delta$ for all n and means that $p \notin U_\delta$, which creates a contradiction. $\square$

Bibliography

[AZ80] H. Amann, E. Zehnder, Nontrivial solutions for a class of non-resonance problems and applications to nonlinear differential equations, *Annali Scuaola sup Pisa Cl. Sc. Serie*, **4** (1980), 539-603.

[Arn99] V.I. Arnol'd, Simple singularities of curves, *Tr. Math. Inst. Steklova*, **226** (1999), 27-35.

[Bäc75] A.V. Bäcklund, Ueber Flächentransformationen, *Math. Ann.*, **9** (1875), 297-320.

[BH05] A. Banyaga, D. Hurtubise, *Lectures on Morse Homology*, Kluwer Texts in the Mathematical Sciences, Springer, 2005.

[BH93] R. Bryant, L. Hsu, Rigidity of integral curves of ranks 2 distributions, *Invent. Math.*, **114** (1993), 435-461.

[CC05] A. Campillo, J. Castellanos, *Curve singularities: an algebraic and geometric approach*, Actualités mathématiques, Hermann, 2005.

[CM12] A. Castro, R. Montgomery, Spatial curve singularities and the Monster/Semple Tower, *Israel Journal of Mathematics*, **192** (2012), 1-47.

[CZ84] C. Conley, E. Zehnder, Morse-type Index Theory for Flows and Periodic Solutions for Hamiltonian Equations, *Comm. on Pure and Applied Mathematics*, **37** (1984), 207-253.

[DZ04] S.V. Duzhin, B.D. Chebotarevsky, *Transformation groups for beginners*, American Mathematical Society, Providence, RI, 2004.

[EP03] M. Entov, L. Polterovich, Calabi quasimorphism and quantum homology, *Int. Math. Res. Not.*, **30** (2003), 1635-1676.

[EP09] M. Entov, L. Polterovich, Rigid subsets of symplectic manifolds, *Compos. Math.*, **145** (2009), 773-826.

[Fav57] J. Favard, *Cours de géométrie différentielle locale*, Cahiers scientifiques, Gauthier-Villars, 1957.

[FH93] A. Floer, H. Hofer, Coherent orientations for periodic orbit problems in symplectic geometry, *Math. Z.*, **212** (1993), 13-38.

[Flo89(1)] A. Floer, Cuplength estimates on Lagrangian intersections, *Comm. Pure Appl. Math.*, **4** (1989), 335-356.

[Flo89(2)] A. Floer, Symplectic fixed points and holomorphic spheres, *Comm. Math. Phys.*, **120** (1989), 575-611.

[Flo89(3)] A. Floer, Witten's complex and infinite-dimensional Morse theory, *J. Differential Geom.*, **30** (1989), 207-221.

[GG09] V. Ginzburg, B. Gürel, Action and index spectra and periodic orbits in Hamiltonian dynamics, *Geometry & Topology*, **13** (2009), 2745-2805.

[Gin05] V. Ginzburg, The Weinstain conjecture and theorems of nearby and almost existence, *Progr. Math.*, **232** (2005), 139-172.

[Hof88] H. Hofer, Ljusternik-Schnirelman-theory for Lagrangian intersections, *Ann. Inst. H. Poincaré Anal. Non Linéaire*, **5** (1988), 465-499.

[HZ11] H. Hofer, E. Zehnder, *Symplectic invariants and Hamitonian dynamics*, Mondern Birkhäuser Classics, Birkhäuser Verlag, Basel, 2011.

[Jea96] F. Jean, The car with n trailers: characterization of the singular configurations, *ESAIM Contrôle Optim. Calc. Var.*, **1** (1996), 241-266.

[KN96] S. Kobayashi, K. Nomizu, *Foundations of differential geometry*, Wiley classics library, Wiley, 1996.

[KR82] A. Kumpera, C. Ruiz, *Sur léquivalence locales des systémes de Pfaff en drapeau*, Ist. Nax, Alta Mat. Francesco Severi, Rome, 1982.

[KR82] A. Kumpera, J.L. Rubin, Multi-flag systems and ordinary differential equations, *Nagoya Math. J.*, **166** (2002), 1-27.

[Lau93] J.P. Laumond, Controllability of a multi body robot, *IEEE Trans. on Robotics and Automation*, **9** (1993), 755-763.

[LJ06] M. Lejeune-Jalabert, Chains of points in the Sempale Tower, *Amer. J. Math.*, **128** (2006), 1283-1311.

[LR11] S.J. Li, W. Respondek, The geometry, controllability, and flatness property of the n-bar system, *International Journal of Control*, **84** (2011), 834-850.

[Mas91] W. Massey, *A basic course in algebraic topology*, Graduate Texts in Mathematics, Springer-Verlag, New York, 1991.

[MS04] D. McDuff, D. Salamon, *J-holomorphic Curves and Symplectic Topology*, Colloquium publications, vol. 52, AMS, Providence, RI, 2004.

[Mor03] P. Mormul, *Goursat distributions not strongly nilpotent in dimensions not exceeding seven*, Lecture Notes in Control and Information Sciences, Springer, Berlin/Heidelberg, 2003.

[Mor04] P. Mormul, Multi-dimensional Cartan prolongation and special k-flags, *Banach Center Publ.*, **65** (2004), 157-178.

[Mor09] P. Mormul, Singularities classes of special 2-flags, *SIGMA*, **5** (2009), x + 22.

[MP10] P. Mormul, F. Pelletier, Special 2-flags in lengths not exceeding four: a study in strong nil potency of distributions, Preprint 2010, arXiv: 1011.1763.

[MZ01] R. Montgomery, M. Zhitomirskii, Geometric approach to Goursat flags, *Ann. Inst. H. Poincaré Anal. Non Linéaire*, **18** (2001), 459-493.

[MZ10] R. Mongomery, M. Zhitomirskii, Points and curves in the Monster Tower, *Mem. Amer. Math. Soc.*, **203** (2010), x + 137.

[MS93] R. Murray, S. Sastry, Nonholonomic motion planning: Steering using sinusoids, *IEEE Trans. on Automation and Control*, **38** (1993), 700-716.

[Oh05] Y.G. Oh, Construction of spectral invariants of Hamiltonian paths on closed symplectic manifolds, *Progr. Math.*, **232** (2005), 525-570.

[Olv93] P. Olver, *Applications of Lie groups to differential equations*, Graduate Texts in Mathematics, Springer-Verlag, New York, 1993.

[Pel11] F. Pelletier, Configuration Spaces of a Kinematic System and Monster Tower of Special Multi-Flags, Preprint 2011, arXiv: 1109.4788v3.

[PS12] F. Pelletier, M. Slayman, Configurations of an articulated arm and singularities of special multi-flags, Preprint 2012, arXiv: 1205.2992v1.

[SZ92] D. Salamon, E. Zehnder, Morst theory for periodic solutions of Hamiltonian systems, *Comm. Pure Appl. Math.*, **45** (1992), 1303-1360.

[Sch00] M. Schwarz, On the action spectrum for closed symplectically aspherical manifolds, *Pacific J. Math.*, **2** (2000), 419-461.

[SY09] K. Shibuya, K. Yamaguchi, Drapeau theorem for differential systems, *Differential Geom. Appl.*, **27** (2009), 793-808.

[Spa81] E. Spanier, *Algebraic topology*, Springer-Verlag, New York, 1981.

[Vit92] C. Viterbo, Symplectic topology as the geometry of generating functions, *Math. Ann.*, **292** (1992), 685-710.

[Vit97] C. Viterbo, Some remarks on Masset products, tied cohomology classes, and the Lusternik-Schnirelman category, *Duke Math. J.*, **86** (1997), 547-564.

[Wal04] C.T.C. Wall, *Singular points of plane curves*, London Mathematical Society student texts, Cambridge University Press, 2004.

[Zar06] O. Zariski, *The moduli problem for plane branches*, University Lecture Series, American Mathematical Society, Providence, RI, 2006.